



# At the edge of the external world: the physiological basis of mind wandering and its impact on attentional resources

**Dissertation**

Zur Erlangung des akademischen Grades

**doctor rerum naturalium (Dr. rer. nat.)**

genehmigt durch die Fakultät für Naturwissenschaften der Otto-von-Guericke-  
Universität Magdeburg

von	M. Sc. Paul Schmid
geb. am	22.02.1996 in Heidelberg
Gutachter:	PD Dr. Stefan Dürschmid Prof. Dr. Niko Busch
eingereicht am	11.06.2025
verteidigt am	04.12.2025

“I think I can confidently predict that anyone reading this article will at some point drift away, hopefully only momentarily, to thoughts of forthcoming rendezvous, anticipated dinners, delightful summer vacations, or clever bits of revenge on political opponents in their psychology departments.”

(Singer, 1975)

---

## **Abstract**

### AT THE EDGE OF THE EXTERNAL WORLD: THE PHYSIOLOGICAL BASIS OF MIND WANDERING AND ITS IMPACT ON ATTENTIONAL RESOURCES

*Doctoral thesis submitted by M.Sc. Paul Rocco Schmid*

During a colleague's presentation, we often catch ourselves thinking about unrelated topics. We might notice that we ran out of milk and mentally make a grocery shopping list. This spontaneous memory retrieval is called mind wandering and comes with costs like decrease of performance and dampened brain responses. These results led to the notion that during mind wandering people are perceptually decoupled. But what is the neurophysiological basis of spontaneous memory retrieval and are we really decoupled from the environment during this process? This thesis focused on information propagation to early visual cortex and on visual attentional processes, like the selection of a target among distractors, to test the perceptual decoupling hypothesis using non-invasive brain recordings. Furthermore, cortical response patterns in the high-frequency activity (HFA; 80 - 150 Hz) were analyzed during mind wandering in healthy human subjects.

The first two studies of this thesis tested whether either the first visual feedforward sweep, or feedback information to the visual cortex is affected by mind wandering. The HFA has so far mainly been studied in primate research, with results suggesting that it reflects both feedforward and feedback information. My studies demonstrated that the HFA in humans reflects feedback information and is reduced during the mind wandering. In contrast, the initial input to the visual cortex remained unaffected.

The subsequent three studies investigated whether the HFA serves as a marker for selective attention and how mind wandering affects the neural correlates of selective attention. My results show that the HFA acts as an indicator for distractor suppression and starts earlier than established neural correlates of selective attention. In addition, I found neural correlates of distractor suppression to be enhanced during mind wandering.

Overall, this thesis established the HFA in non-invasive brain recordings as an important component of visual information processing, representing feedback information and distractor suppression, among others. Furthermore, mind wandering has no influence on the initial visual input, but impairs feedback processes.

---

## **Zusammenfassung**

AM RANDE DER AUSSENWELT: DIE PHYSIOLOGISCHEN GRUNDLAGEN DES MIND WANDERING UND SEINE AUSWIRKUNGEN AUF AUFMERKSAMKEITSRESSOURCEN

*Doktorarbeit eingereicht von M.Sc. Paul Rocco Schmid*

Während des Vortrags eines Kollegen erwischen wir uns oft, wie wir über Themen nachdenken, die nichts mit dem Vortrag zu tun haben. Beispielsweise könnte uns auffallen, dass wir keine Milch mehr zuhause haben und fangen an im Kopf eine Einkaufsliste zu erstellen. Diesen spontanen Gedächtnisabruf nennt man Mind Wandering. Mind Wandering wird häufig von behavioralen Kosten (reduzierter Performance) und reduzierten Gehirnantworten begleitet. Diese Ergebnisse haben zu der Annahme geführt, dass Menschen während Mind Wandering perzeptuell von der Umwelt entkoppelt sind. Aber was sind die neurophysiologischen Grundlagen des spontanen Gedächtnisabrufs und sind wir währenddessen wirklich perzeptuell von der Außenwelt abgekoppelt? Die vorliegende Thesis beschäftigt sich mit der Informationsweiterleitung zum visuellen Cortex und mit visuellen Aufmerksamkeitsprozessen, wie der Auswahl eines Zielstimulus unter Distraktoren, um die Annahmen der perzeptuellen Entkopplungstheorie mithilfe nicht-invasiver Gehirnaufnahmen zu untersuchen. Des Weiteren wurde kortikales Antwortverhalten in Form von hochfrequenter Aktivität (HFA, 80-150 Hz) während Mind Wandering in gesunden Probanden untersucht.

In den ersten beiden Studien dieser Thesis wurde untersucht, ob Mind Wandering die feedforward- oder feedback-Informationsverarbeitung zum visuellen Cortex beeinträchtigt. Die HFA wurde bislang vorwiegend in der Primatenforschung untersucht, wobei angenommen wird, dass sie sowohl feedforward- als auch feedback-Informationen widerspiegelt. Meine Studien zeigen, dass die HFA feedback-Informationen widerspiegelt und während Mind Wandering reduziert ist. Im Gegensatz dazu blieb der initiale Input zum visuellen Cortex unbeeinflusst.

Die drei weiteren Studien untersuchten, ob die HFA als Marker selektiver Aufmerksamkeit dient und welchen Einfluss Mind Wandering auf neuronale Korrelate selektiver Aufmerksamkeit hat. Die Ergebnisse zeigen, dass die HFA die Unterdrückung von Distraktoren widerspiegelt und zeitlich früher auftritt als etablierte neuronale Korrelate selektiver Aufmerksamkeit. Zudem konnte nachgewiesen werden, dass neuronale Mechanismen der Distraktorunterdrückung während Mind Wandering verstärkt sind.

In dieser Thesis wurde die HFA in non-invasiven Gehirnmessungen als eine wichtige Komponente der visuellen Informationsverarbeitung etabliert, die unter anderem feedback-Informationen und Distraktorunterdrückung repräsentiert. Des Weiteren wurde gezeigt, dass Mind Wandering keinen Einfluss auf den initialen visuellen Input hat, feedback-Prozesse jedoch beeinträchtigt.

---

## Table of Contents

Abstract.....	I
Zusammenfassung.....	II
Table of Contents .....	III
1 Theoretical Background .....	1
1.1 Mind Wandering.....	1
1.2 High-frequency Activity .....	3
1.3 Selective Attention .....	5
1.4 Statistical Learning in Visual Search.....	7
2 General Methodology.....	9
2.1 Electroencephalography.....	9
2.2 Magnetencephalography .....	10
2.3 Participants .....	11
2.4 Apparatus.....	11
2.5 Thought Probe Sampling .....	11
2.6 General Preprocessing of Brain Data.....	12
2.7 Hilbert Transform.....	13
2.8 Extracting the Broadband High-Frequency Activity Response .....	14
2.9 Surrogate Data Testing.....	14
3 Working Hypotheses.....	16
4 The HFA as a Feedforward or Feedback Signal .....	18
4.1. Introduction.....	18
4.2. Methods and Material .....	19
4.2.1 Participants.....	19
4.2.2 Paradigm.....	19
4.2.3 Experience Sampling.....	20
4.2.4 Simultaneous EEG and MEG Recordings .....	20
4.2.5 Preprocessing and Artifact Rejection.....	20
4.2.6 Statistical Analysis .....	20

---

4.3 Results .....	24
4.4 Discussion .....	28
5 The HFA in Selective Attention.....	31
5.1 Introduction.....	31
5.2 Methods and Materials .....	32
5.2.1 Participants.....	32
5.2.2 Paradigm.....	32
5.2.3 Experience Sampling.....	34
5.2.4 MEG Recordings.....	34
5.2.5 Preprocessing and Artifact Rejection.....	35
5.2.6 Statistical Analysis .....	35
5.3 Results .....	40
5.4 Discussion .....	49
6 General Discussion.....	53
6.1 Summary of Experimental Results .....	53
6.2 Limitations.....	55
6.3 Future Perspectives .....	57
6.4 General Conclusion .....	58
References.....	60
List of Figures .....	77
Declaration of Honor .....	78

---

## Abbreviations

DMN	Default Mode Network
EEG	Electroencephalography
EOG	Electrooculogram
ERF	Event Related Field
ERP	Event Related Potential
FDR	False-discovery rate
fMRI	Functional magnet resonance imaging
iEEG	Intracranial EEG
HFA	Broadband High-Frequency Activity
LVF	Lower visual field
MEG	Magnetoencephalography
MUA	Multi-unit Activity
MW	Mind Wandering
N <sub>T</sub>	Target Negativity
P <sub>D</sub>	Distractor Positivity
RT	Reaction time
SART	Sustained Attention to Response Task
SQUID	Superconducting quantum interference device
UVF	Upper visual field
va	Visual Angle
WMC	Working memory capacity

## **1 Theoretical Background**

Mind wandering (MW) describes a ubiquitous brain state characterized by self-generated thoughts that arise independently of external stimuli. It is assumed that during MW, we become perceptually decoupled, meaning our attention shifts inward to our internal stream of thoughts and is shielded against the external environment. However, I challenge this perspective, as complete decoupling from external stimuli would lead to significant disruptions in our daily functioning. Following the assumptions of the perceptual decoupling theory, one would expect neural correlates of sensory input, attention and implicit learning to be impaired during episodes of MW. The present thesis deals with the neurophysiological signature of a common everyday experience – MW – and how this brain state impacts different cognitive mechanisms.

I conducted five combined electroencephalography (EEG) / magnetoencephalography (MEG) studies, organized in two chapters, examining the neurophysiological processes underlying sensory input, attentional selection, and implicit learning during MW. Using EEG and MEG recordings, participants engaged in visual tasks designed to elicit event-related brain responses. These brain responses arise from synchronized activity of neuronal populations within specific frequency ranges. Event-related potentials (ERPs) are dominated by lower-frequency activity. Recent research highlights high-frequency activity (HFA, 80–150 Hz) as an important signal. This thesis analyzes both lower- and high-frequency brain activity to test the proposed theoretical framework.

The thesis is structured as follows: Chapter 1 provides detailed information of the state-of-the-art research on the different phenomena and neural responses investigated in this thesis. Chapter 2 outlines the general methods used to record and analyze the neural data. Chapter 3 presents the hypotheses derived from the recent studies on the different mechanisms. Chapter 4 and 5 outline the conducted studies, with each chapter discussing the respective results. Finally, Chapter 6 closes the thesis with a summary and evaluation of the results of all studies and a general discussion of the research question.

### **1.1 Mind Wandering**

While driving on a familiar route, you might find yourself no longer focused on the road but instead replaying a recent conversation or planning your dinner. MW, a spontaneous shift of attention, can occupy 30 to 40% of waking time (Killingsworth & Gilbert, 2010). Since a substantial amount of time is spent thinking about matters unrelated to the current, investigating the underlying neurophysiological mechanisms of MW is crucial for a deeper understanding of overall cognitive processes.

In the 1950's Jerome L. Singer launched a research program on daydreaming. With his ongoing work he laid the foundation for every major aspect of today's MW research (Singer, 1975). Most important, his retrospective thought sampling is the basis of our current investigation of MW (Singer & Antrobus, 1965).

As stated at the beginning of my dissertation, there is no definitive terminology. Terms like spontaneous thoughts, daydreaming, task-unrelated thoughts and MW are often used synonymously, making research more difficult. In this work, I define MW as a brain state that occurs when an individual's thoughts become detached from a task at hand. Thus, I define MW as task-independent thoughts (Preiss et al., 2020).

Over the last decade, many studies have consistently shown activation in the so-called default mode network (DMN) prior to reports of MW (Christoff et al., 2009; Mittner et al., 2016). The DMN is an anatomical network which consists of the posterior cingulate cortex, middle frontal gyrus, angular gyrus, medial prefrontal cortex, and precuneus (Broyd et al., 2009). Furthermore, the DMN is associated with semantic memory, episodic memory, and future planning – cognitive processes that are critical during MW (Spreng et al., 2009). Lesion-studies investigating the relationship between ventromedial prefrontal cortex, as well as hippocampus and MW underpin these findings (Bertossi et al., 2016; He et al., 2021). These results suggest, that activations within brain regions of the DMN are crucial in the formation of MW.

On a behavioral level, numerous studies suggested that MW is associated with behavioral costs. Behavioral target detection is decreased in a wide range of tasks tackling specific domains like sustained attention to response (SART) and visual detection, but also everyday tasks like reading and driving (Cheyne et al., 2009; Smallwood & Schooler, 2014; Smilek et al., 2010; Yanko & Spalek, 2014). The SART represents a modification of a traditional go-/no-go task used to measure sustained attention (Robertson et al., 1997). In traditional go-/no-go tasks, participants are sequentially presented with frequent no-go stimuli and infrequent go stimuli to which they have to withhold or commit a button press, respectively. Sustained attention is here assessed by the measurement of omission errors on rare go trials. However, in the SART participants are presented with frequent go stimuli and asked to withhold a button press during rare no-go trials and sustained attention is assessed by measuring commission error on rare no-go trials. Whether the SART actually measures sustained attention or variation of motor control during MW is debated (see for example Head & Helton, 2013; Helton, 2009; Helton et al., 2009). Hence, the SART does not allow to ascribe a loss of performance to perceptual limitations during MW (Seli, Jonker, et al., 2013).

The perceptual decoupling theory posits that behavioral impairments arise from attentional shifts away from external stimuli, leading to a diminished sensory representation (Schooler et al., 2011). This theory is supported by reports of reduced EEG responses to perceptual input during episodes of MW (Braboszcz & Delorme, 2011; Kam et al., 2011; Xu et al., 2018). However, amplitude reductions in ERPs – especially late ones (Braboszcz & Delorme, 2011; Kam et al., 2011; Xu et al., 2018) – do not demonstrate that sensory information is not propagated to sensory cortices during MW. Hence, whether sensory input is fully restricted during MW remains a matter of debate. Moreover, a recent study reported an increase in the N2pc component, an ERP component associated with selective attention, during episodes of MW, clearly contradicting the perceptual decoupling theory (Wienke et al., 2021). At the same time, activity in the high-frequency range, which is thought to mediate feedforward and feedback processing, was found to be reduced during these episodes (Wienke et al., 2021). High-frequency activity has the potential to accurately show changes in neuronal activity, making it a prominent candidate to analyze differences in neuronal activity between episodes of MW and focused attention.

### **1.2 High-frequency Activity**

In the brain, populations of neurons can synchronize their firing patterns in a rhythmic fashion and thus oscillate (Buzsáki & Draguhn, 2004). These oscillations in the human brain have been categorized into multiple frequency bands: delta (0.5 – 4 Hz), theta (4 – 8 Hz), alpha (8 – 12 Hz), beta (12 – 35 Hz) and gamma (> 35 Hz) (Abhang et al., 2016). Broadband high-frequency activity (HFA; 80 to 150 Hz) has emerged as a crucial analytic signal in intracranial recordings (Bartoli et al., 2019; Leonard et al., 2024; Ray et al., 2008; Wienke et al., 2021). While the HFA was often discussed as neural activity in the high-gamma range, recent research focused on the HFA reflecting multi-unit activity (MUA) (Bartoli et al., 2019; Ray et al., 2008). MUA describes an aggregated signal reflecting local spiking activity of multiple neurons (Henze et al., 2000) and is thus different from oscillatory cell ensemble activity. This indicates that the HFA does not represent oscillatory activity.

Recent studies, primarily in the auditory domain, found that HFA correlates with the firing rate of neuronal populations, reflecting the physical properties of external stimuli (Binder et al., 1994; Brugge et al., 2008; Peelle et al., 2004), suggesting it represents local neuronal population dynamics (Ray et al., 2008). In the visual domain a recent study found the HFA onset response to be modulated by differences in visual stimuli (Bartoli et al., 2019) supporting its role in input to visual cortex. Intracranial recordings of epilepsy patients (Bartoli et al., 2019; Gerber et al., 2017; Golan et al., 2017.; Vishne et al., 2023) revealed a rapid response modulation following stimulus onset, with a peak response before 200 ms and a slowly decreasing flank. However, recent findings show that the HFA can also be reliably detected using non-invasive magnetoencephalographic

(MEG) recordings in healthy humans with a temporal profile in response to visual stimuli closely resembling the HFA described in intracranial recordings (Wienke et al., 2021; see **Figure 1**). Since the HFA stems from highly synchronized synaptic events, it has the potential to accurately reveal the onset, magnitude, and duration of changes in neuronal activity during cognitive tasks (Lachaux et al., 2012).

Recent investigations in macaque monkeys revealed a bimodal distribution of the HFA response to visual stimulation across deep and superficial layers of the visual cortex (Leszczyński et al., 2020). The HFA recorded in deep layers correlated with MUA, while the HFA in superficial layers did not show such a relationship. Importantly, the superficial HFA contributed strongest to HFA surface recordings (Leszczyński et al., 2020). These results indicate that the HFA at least contains substantial corticocortical feedback projections.

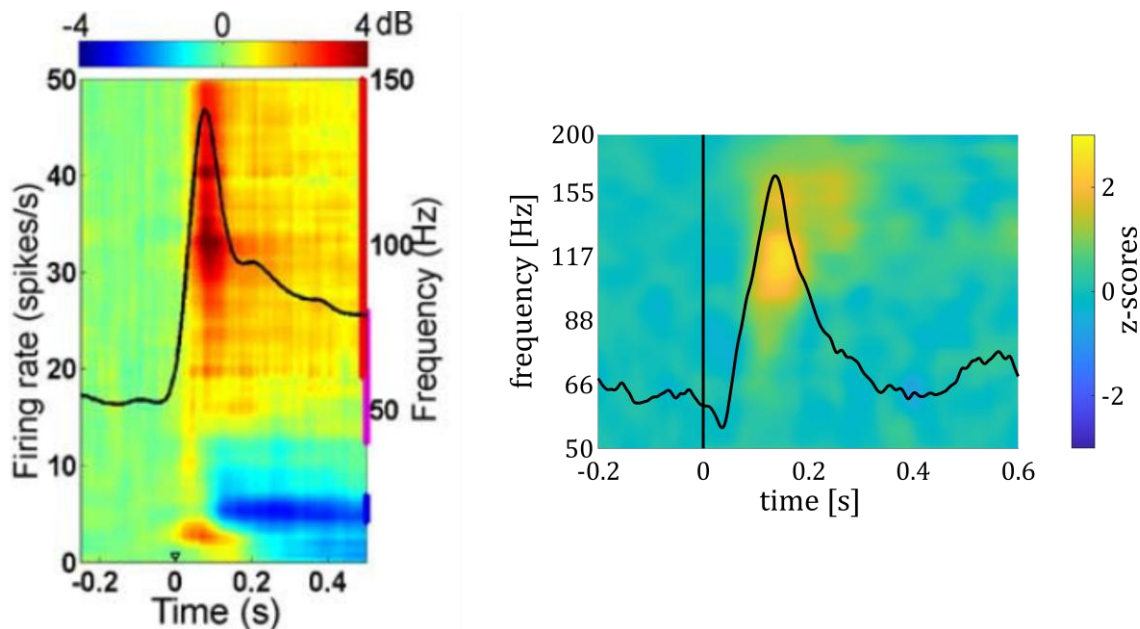


**Figure 1.** Typical HFA response modulation. Time-frequency representation of local field potential power to vibrotactile stimulation in macaque monkeys' secondary somatosensory cortex (left). Black line shows firing rate of an excited neuronal population (Ray et al., 2008). Time-frequency representation of activity in MEG sensors over occipital cortex in healthy human subjects to visual stimulation (right). Black line shows the time course of HFA response modulation.

Given that the HFA signals recorded at the pial surface include feedback projections, it is plausible that these signals can be modulated by attentional processes. In the auditory domain, previous intracranial recordings in epilepsy patients found the HFA to be increased during attentional selection of auditory stimuli (Ray et al., 2008). In the visual domain, there is a lack of studies investigating brain responses in the exact high-frequency range between 80 and 150 Hz, but previous studies investigating attentional modulation of activity primarily focused on broad frequency-bands between 30 and 130 Hz with mixed results (Davidesco et al., 2013; Tallon-Baudry et al., 2005). Tallon-Baudry et al. (2005) found an increase in baseline activity between 30

and 130 Hz and a decrease during stimulus presentation in lateral occipital cortex, but an increase over fusiform gyrus during attentive states. In contrast, Davidesco et al. (2013) presented participants with small and large objects and cued them to attend one of the stimuli. They found activity in the gamma-range (30 – 90 Hz) in visual cortex to be increased during attentive states, while previous studies using a narrower gamma-range (30 – 50 Hz) failed to show such modulations (Chalk et al., 2010). Furthermore, Davidesco et al. (2013) found attentional modulation of gamma activity to occur earlier in early visual cortical areas compared to higher visual areas. High-frequency modulation during selective attention was also found in intracranial recordings (Szczepanski et al., 2014). Participants were instructed to covertly attend either to the left or right visual field and respond to a target. Szczepanski et al. (2014) found an increase in HFA during attentive states over visual areas. Most interestingly, ~20 % of the recorded electrodes exhibited stronger HFA responses contralateral to the attended visual field.

These findings suggest that the HFA is not only involved in general sensory processing but also plays a critical role for attentional processes. To better understand this, it is essential to explore the mechanisms underlying selective attention itself.

### **1.3 Selective Attention**

In our everyday lives, we are confronted with a continuous stream of incoming information from different sensory domains at the same time. To adequately react to important incoming stimuli, we use a process that seems simple at first glance. We need to select a target stimulus in the environment while suppressing distracting information. We might drive towards a red light while a child with a green balloon is crossing the road. The selection of the task-relevant red light enters a competition with the distracting green balloon, of which the properties must also be detected as quickly as possible.

Thus, selective attention is the net result of target selection and distractor suppression (Feldmann-Wüstefeld & Vogel, 2019). Since salient distractors capture attention, it is reasonable that searching for targets amid salient distractors comes with costs due to perceptual load (Gutteling et al., 2022): in behavioral tasks, reaction times increase and performance decreases with proximity between target and distractor, indicating that distractors induce spatial interference (Feldmann-Wüstefeld et al., 2021; Zhao et al., 2023), which is scaled with the proximity to the target (Hickey & Theeuwes, 2011; Mathôt et al., 2010; Mounts, 2000). Furthermore, visual search is facilitated by prior knowledge especially about the distractor characteristics (Arita et al., 2012; Donohue et al., 2018; Müller et al., 1995; Olivers & Humphreys, 2003; Watson & Humphreys, 2000), which seems paradoxical at first glance. The ignoring paradox states that to avoid distraction by an irrelevant item it is necessary to have prior knowledge about

the characteristics of the item (in the case of the visual system i.e. color, shape, position in the visual field; Moher & Egeth, 2012).

On a neural level, the N2pc ERP component is regarded as a reliable marker for visual attention selection and can be recorded using visual search displays containing a target stimulus among distracting nontarget stimuli (Eimer, 1996). It is characterized by an increased negativity at posterior electrodes contralateral to the presentation side of a target stimulus 200 to 300 ms after stimulus presentation (Eimer, 1996; Luck & Hillyard, 1994). Originally, the N2pc was suggested to reflect a filtering process to suppress distracting information stemming from nontarget stimuli surrounding the target (Luck & Hillyard, 1994). However, in a recent study Hickey et al. (2009) showed that the N2pc can be decomposed into two distinct components, one reflecting target processing ( $N_T$ ; Negativity to lateralized target), while the other reflects the suppression of distractor information ( $P_D$ ; Positivity to lateralized distractor). Thus, as a marker for selective attention, the N2pc component reflects the result of target selection and distractor suppression (Hickey et al., 2009).

While neural mechanisms of target enhancement have been studied excessively (Eimer, 1996, Luck & Hillyard 1994, J.-M. Hopf, 2000), the neural mechanisms of distractor suppression we only start to understand. To isolate the brain response to targets and distractors, symmetrical search displays are usually used in which either one of the stimuli is presented centrally while the other is presented laterally. A stimulus array with a lateral distractor and a central target will elicit a  $P_D$  response contralateral to the distractor, while a stimulus array with a lateral target and a central distractor will elicit a  $N_T$  response contralateral to the target (see **Figure 2**). Recent studies found that the  $P_D$  is absent when attentional demands were reduced (target just had to be detected; Hickey et al., 2009), and that  $P_D$  amplitude increases with faster reaction times (Gaspar & McDonald, 2014; Sawaki et al., 2012). These results indicate that the  $P_D$  actually represents active distractor suppression. Furthermore, a previous study found evidence for an initial selection of the lateral distractor preceding the  $P_D$  which is in line with the ignoring paradox (Donohue et al., 2018).

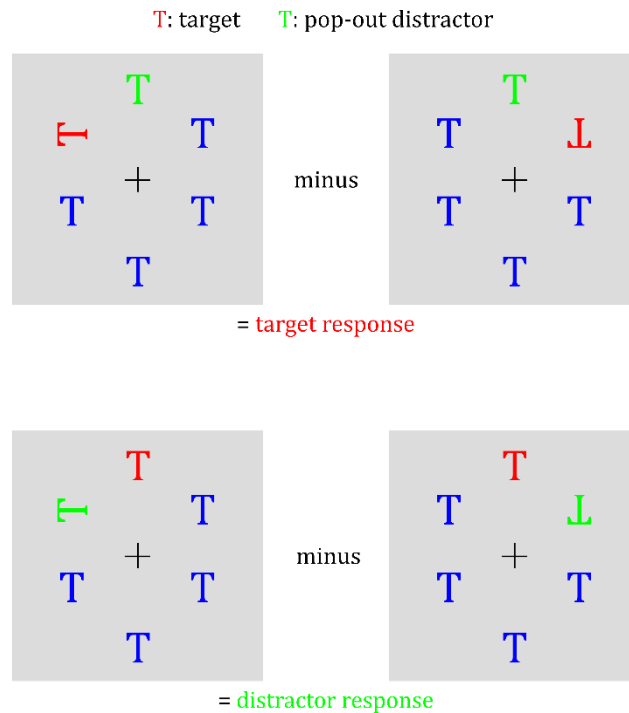


**Figure 2.** Search paradigm separating event-related brain responses to lateral targets (target response) and distractors (distractor response). Adapted from (Donohue et al., 2018).

It has long been known that prior knowledge of distractor properties facilitates visual search on a behavioral level. Recent studies claim to show this also on a neural level: statistical learning of a location at which the distractor is more likely to be presented lead to a reduction in  $P_D$  amplitude when the distractor is presented at this location (Moorselaar & Slagter, 2019; van Moorselaar et al., 2020). Critically, if the  $P_D$  component actually represents distractor suppression one would expect the  $P_D$  to be increased in amplitude after statistical learning due to an enhanced suppression of the learned distractor location. It could be that the process of distractor suppression has been initiated before the start of the  $P_D$  response.

#### 1.4 Statistical Learning in Visual Search

In cognitive science, statistical learning describes the implicit or explicit extraction of regularities in the environment over space and time (de Waard et al., 2023). As a fundamental mechanism underlying various cognitive functions – including vision, semantic memory and language acquisition – it is regarded as a key phenomenon in many theories of information processing (Frost et al., 2019; Schapiro & Turk-Browne, 2015). Statistical learning occurs across the lifespan and has been robustly demonstrated across multiple sensory modalities using different experimental manipulations (Schapiro & Turk-Browne, 2015). Here, I focus on implicit statistical learning of spatial locations in the context of selective attention.

In visual search, unforeseen salient distracting information impairs the perception of targets. However, prior knowledge about the distractor (e.g. the distractor location) can reduce distractor interference (Donohue et al., 2018). In this case, statistical learning establishes an internal model in a way that within the attentional priority map, the location at which a distractor more likely appears is suppressed compared to other locations (Wang & Theeuwes, 2018). Recent research showed that target enhancement, but not distractor suppression can be modulated by trial-by-trial cueing (Noonan et al., 2016). These results indicate, that distractor suppression does not operate under the same top-down control as target enhancement and thus represents a qualitatively different mechanism (Noonan et al., 2016).

## 2 General Methodology

### 2.1 Electroencephalography

Over 100 years ago, Hans Berger recorded the first EEG, discovering oscillatory brain activity in the alpha range (Berger, 1929). EEG established as one of the standard non-invasive methods to measure brain activity via electrodes placed on the scalp (see **Figure 3**). It mainly reflects summarized postsynaptic potentials at the dendrites of tens of thousands of neurons (Cohen, 2014). During the process of an action potential, neurotransmitter dock on ion channels in the dendritic membrane, ions flow in and out of the cell, producing a change of potential inside and outside the neuron. This generates an electrical field that surrounds the neural cell. The summation of the electrical fields of those neuronal populations is strong enough to generate a field at the top layer of the scalp, which then can be picked up by EEG electrodes that are placed on the scalp in combination with an electroconductive gel paste (Biasiucci et al., 2019). EEG, while limited in spatial resolution compared to functional magnetic resonance imaging (fMRI), excels in its ability to provide millisecond-level temporal resolution. This makes EEG particularly advantageous for neurophysiological investigations, as it enables the precise analysis of transient brain responses (Cohen, 2014).

Using ERPs, we can analyze brain activity in response to specific events or stimuli (Blackwood & Muir, 1990; Sur & Sinha, 2009). In an experimental setup participants are presented with the different visual stimuli, the presentation onset of these stimuli is marked in the ongoing EEG signal and the signal is then epoched around these events, resulting in different trials (Karnath & Thier, 2012). With this technique, we are able to compare brain activity between different experimental conditions.

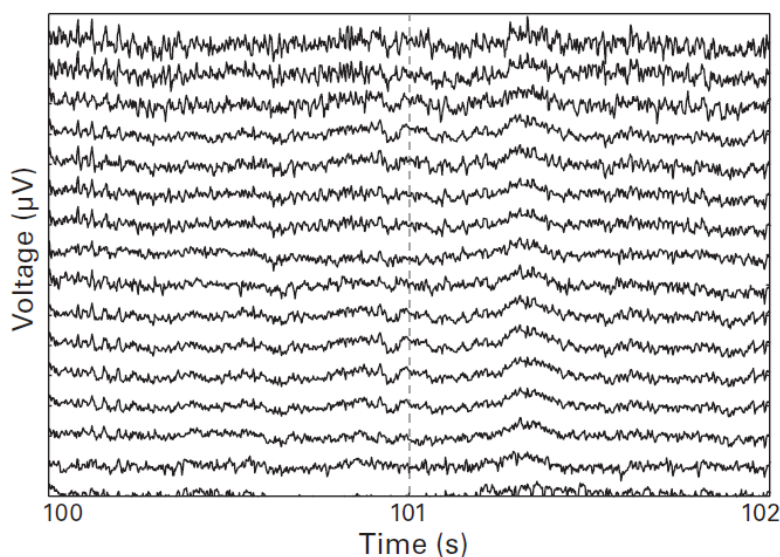


**Figure 3.** Example of a raw EEG data time series after 0.1 Hz high-pass filter. Each line corresponds to an electrode (Cohen, 2014).

## 2.2 Magnetencephalography

Like EEG, MEG is a neurophysiological method with a temporal resolution in the millisecond range (Pollok & Schnitzler, 2010) – hence of processing steps in the human brain. In 1968, David Cohen carried out the first MEG recording, at that time without superconducting quantum interference devices (SQUIDS), using a copper induction coil (Cohen, 1968). Nowadays MEGs contain between 100 and 300 magnetic sensors and are equipped with both magnetometers and gradiometers. Magnetometers consist of one pick-up coil, while gradiometers consist of two oppositely orientated pick-up coils to reduce electromagnetic interference (Pollok & Schnitzler, 2010). The system I used for my recordings contains 306 sensors at 102 measuring points, each comprising two orthogonally orientated planar gradiometers and one magnetometer. MEG measures small magnetic fields in the femtotesla ( $10^{-15}$  Tesla) range. These magnetic fields are generated by cellular electrical ion currents of activated neurons (see *Chapter 2.1 Electroencephalography*) and are aligned orthogonal to them (Pollok & Schnitzler, 2010). As with EEG, the measurement of neuromagnetic fields requires the simultaneous activation of tens of thousands of neurons arranged in parallel. Due to the aforementioned orthogonal alignment of the magnetic fields to the electric fields, magnetometers can only measure tangentially aligned dipoles and thus rather pick up activity that is evoked in the cortical sulci (see *Figure 4*; Hansen et al., 2010).

While magnetic signals pass through the bones and skull without interference, electrical signals are volume conducted through these areas, which reduces the signal-to-noise ratio at higher frequencies. Thus, MEG is better suited for analyzing high-frequency activity compared to EEG (Cohen, 2014).

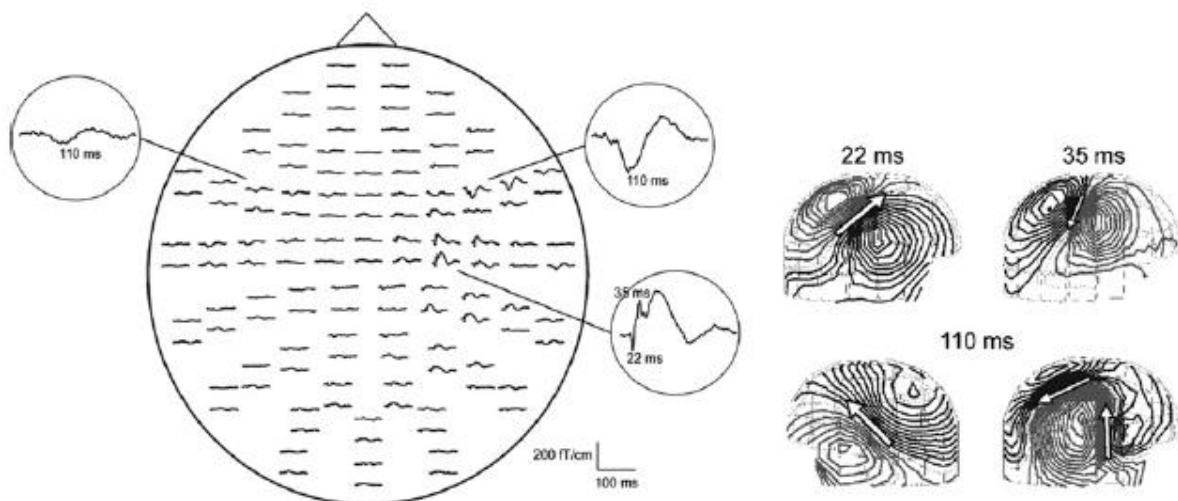


**Figure 4.** Evoked fields after stimulation of the medial nerve. Averaged ERFs for each sensor (left). Depiction of efflux and influx fields (right; Pollok & Schnitzler, 2010).

### **2.3 Participants**

All data presented in this thesis were recorded at the University Department of Neurology in Magdeburg and were approved by the local ethics committee (“Ethical Committee of the Otto-von-Guericke University Magdeburg”). After providing their informed consent, the participants took part in the studies, usually taking two to three hours. Participants ranged from 18 to 40 years of age and all participants reported normal or corrected to normal vision and no history of neurological or psychiatric diseases. Participants were compensated with ~ 30€, depending on experimental time.

### **2.4 Apparatus**

For all studies conducted in this thesis, participants were seated in a dimmed, magnetically shielded recording booth. Stimuli were projected onto a semi-transparent screen (1920 × 1080 px; 53 cm diagonal length) with a viewing distance of 100 cm to the participant with an DLP-LED-projector (ProPixx VPixx Technologies, Saint-Bruno, Canada; refresh rate: 120 Hz). Responses were given with the left and/or right hand via a MEG-compatible VPixx response system (VPixx Technologies, Saint-Bruno, Canada). Acquisition of MEG data was performed in a sitting position using a whole-head Elekta Neuromag TRIUX MEG system (Elekta Oy, Helsinki, Finland), which contains 102 magnetometers and 204 planar gradiometers. For studies in which I also analyzed EEG data, EEG was recorded with 30 passive electrodes simultaneous to the MEG data. The right mastoid was used as a reference electrode and Fpz electrode functioned as a ground electrode. Vertical EOG was recorded bipolar with electrodes placed above and under the right eye. Horizontal EOG was recorded bipolar with electrodes placed on the left and right outer canthus. Sampling rate of MEG, EEG and EOG data was set to 1000 Hz.

In 2 studies, participant’s eye movements and pupil data of the left eye were recorded using an EyeLink 1000 Plus system (SR Research) with a Long-Range Mount configuration and a built-in camera. The Long-Range Mount configuration was attached to the presentation screen, so that all participants were seated in the same distance to the eye tracking camera. Prior to data collection, participants completed an eye tracker calibration with the built-in 9-point grid method. Sampling rate of the Eye Tracker was set to 500 Hz (since brain data were usually downsampled to 500 Hz).

### **2.5 Thought Probe Sampling**

To accurately detect and analyze the neuronal correlates of MW, we need to be able to reliably tell when the subjects' minds wandered. Thus, it is common practice in MW studies to identify MW episodes via thought sampling (Seli, Carriere, et al., 2013). Two approaches exist for thought sampling: the self-caught method and the probe-caught (thought probe) method (Seli, Carriere, et al., 2013). Using the self-caught method, participants indicate whenever during performing a task they recognize that they were mind wandering (Smallwood & Schooler, 2006). This method relies

on meta-awareness, which may be diminished during MW, leading to a lack of correlation between self-caught measures and objective performance metrics (J. Schooler et al., 2004). During thought probes, the given task (usually at the end of a trial) is randomly interrupted and participants are asked to indicate whether they were mind wandering prior to the probe (Christoff et al., 2009; Smallwood et al., 2008). Several studies showed robust correlations between thought probe measures and performance-related objective measures like reaction times and error rates (Cheyne et al., 2006; Christoff et al., 2009).

Over the last decade, researchers applied the thought probe method in different ways (Weinstein, 2018). In some studies, thought probes asked the participants to reflect back on a longer period such as experimental blocks (Farley et al., 2013). Some studies analyzed data of a specific time window before the thought probe rather than including only the last trial before the probe (Compton et al., 2024). Another study asked participants to freely report the content of their thoughts (Baird et al., 2011). However, most studies asked participants to rate their attentional focus on a Likert-scale (Christoff et al., 2009; Thomson et al., 2014; Ye et al., 2014).

In this work, participants were presented with thought probes in 20 % of the trials in a given study, asking them to rate their attentional focus in the trial immediately preceding the thought probe (“Where were your thoughts during the last trial?”) on a 5-point Likert-scale from 1 (“thoughts were anywhere else” – OFF) to 5 (“thoughts were totally at the task” – ON). The thought probes were neutral in a way that the question did not reference any of the states (ON-task / OFF-task) and the order of the response options was counterbalanced (Weinstein, 2018). Thought probes were presented in a pseudo-random order with the restriction that two consecutive probes had to be separated by at least one trial. Due to this approach, only a limited number of trials could be included in the analysis since I assumed that more thought probes would decrease the time between single probes reducing the time for MW (Seli et al., 2013). Furthermore, results of a recently published study indicate that eight to ten thought probes are sufficient to gain reliable and valid information about the MW rates (Welhaf et al., 2022). To increase statistical power, the five MW ratings were grouped in three groups of brain states (OFF: 1 & 2; MID: 3; ON: 4 & 5). I included only the trials immediately preceding the thought probes in the analysis to avoid blurring the distinction between brain states, as the exact timing of the thought probe interrupting the MW episode was unknown.

## **2.6 General Preprocessing of Brain Data**

Generally, MEG, EEG and EOG data of all studies included in this thesis were preprocessed in the following manner. All preprocessing steps were conducted using Matlab 2013b (Mathworks, Natick, USA). First, maxwell filtering was applied to reduce external noise and MEG, EEG and EOG data were down-sampled to 500 Hz. All filtering (see below) was performed using zero phaseshift

infinite impulse response filters (fourth order; `filtfilt.m` in Matlab). EEG and EOG data were filtered between 1 and 40 Hz, while MEG data were filtered between 1 and 200 Hz (to analyze the HFA) using a Butterworth bandpass filter. Following this, the data were notchfiltered to discard line noise (50Hz, 100 Hz, 150 Hz, 200 Hz). Data were epoched from 1s preceding the stimulus presentation to 2 s after the presentation onset – sufficiently long to prevent edge effects during filtering. Each trial was then baseline-corrected relative to the 500 ms interval preceding the stimulus presentation. Activity stemming from eye movement artifacts was excluded from the data, using a linear integration approach (Parra et al., 2005). Trials with a variance that exceeded 4 times the mean variance were excluded since it turned out across studies that this results in a reasonable amount of  $\sim 2\%$  of trials. Furthermore, to discard trials of excessive, nonphysiological amplitude, a threshold of 3pT was used, which the absolute MEG values must not exceed. By finally visually inspecting the data, epochs exhibiting excessive muscle activity, as well as time intervals containing artifactual signal distortions, such as signal steps or pulses, were excluded.

## 2.7 Hilbert Transform

Recording brain data over a longer duration, i.e. using EEG or MEG, comes with several issues that have to be addressed. Continuously recorded brain data are defined by constant switches between inherent brain states of deeper neuronal populations, leading to an ongoing change in the main source of the recorded signal (*nonstationarity*; Dikanev et al., 2005). This also leads to an ongoing change in the power spectrum and amplitude of the recorded signal (*nonlinearity*; Indic et al., 1999; Kunhimangalam et al., 2008). Furthermore, especially brain data in response to external stimulation are *autocorrelated* since activity at time point  $t$  depends on activity at time point  $t - 1$  (Shinn et al., 2023). The Hilbert Transform represents a useful tool to analyze these data. It expresses frequency as a rate of change in phase, allowing the frequency to vary with time and thus enabling us to analyze temporal changes in the activity of a certain frequency band (Huang et al., 1998).

The output of the Hilbert Transform is a time-discrete analytic signal ( $A(t)$ ), which contains a real part ( $f(t)$ ) and an imaginary part ( $Hf(t)$ ).

$$A(t) = f(t) + jHf(t)$$

The real part describes the original data, while the imaginary part, the actual Hilbert Transform, is the (convolution of the) original data shifted by  $90^\circ$  (convolution of original data with the signal  $1/\pi t$ ) (see **Figure 5**; Le Van Quyen et al., 2001).

$$Hf(t) = \frac{1}{\pi} \int_{-\infty}^{\infty} \frac{f(t')}{t - t'} dx$$

The instantaneous amplitude is calculated as  $|A(t)|$  and can be interpreted as a function that smoothly interpolates between the peaks of an oscillatory waveform (Canolty & Knight, 2010).

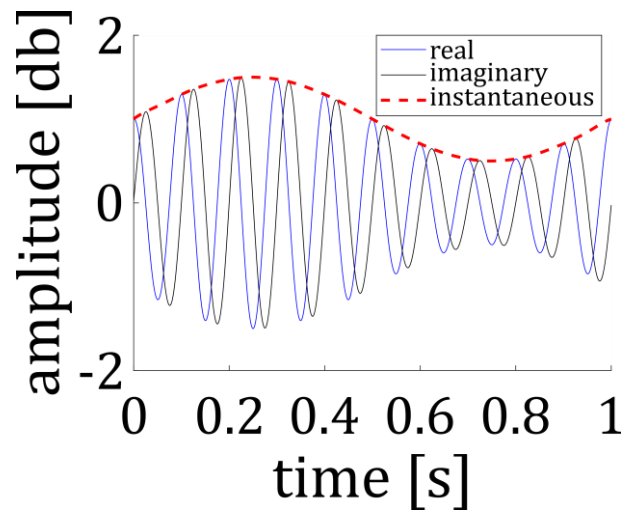


**Figure 5.** Example of Hilbert Transform. A sine wave was created (blue line), and its Hilbert transform (black line) and the instantaneous amplitude (red dashed line) of the analytic signal were calculated. The real part is the original data, while the imaginary part is a cosine wave, since cosine is sine phase-shifted by 90°.

## 2.8 Extracting the Broadband High-Frequency Activity Response

To extract the HFA response out of the ongoing MEG-data, the ongoing signal will first be epoched into several trials ranging from -1s to 2s around stimulus presentation. Next, the time series data for each trial and channel will be band-pass filtered in the broadband high frequency range (80–150 Hz) and Hilbert-transformed to obtain the analytic amplitude  $A(t)$  (see **Chapter 2.7 Hilbert Transform**). To identify MEG sensors showing a significant HFA response, the HFA amplitude values within the first 300 ms will be standardized. This can be done by performing a baseline correction to correct for both zero mean and unit standard deviation in the baseline period, i.e., at each time point the baseline mean will be subtracted from the original signal and the result will be divided by the standard deviation of the baseline. Sensors with z-scores higher than 2 in the interval ranging from 0 to 300 ms were labeled as stimulus responsive and HFA data were averaged across these sensors.

## 2.9 Surrogate Data Testing

In general, surrogate data testing is used to detect non-linearity in time series data and describes a technique similar to permutation tests and parametric bootstrapping (Theiler et al., 1992). The

$H_0$  assumes a linear process and many surrogate data sets are generated according to the  $H_0$ . The surrogate data thus describe a linear process and are compared to the original time series using a discriminating statistic. If the statistical parameter reaches significance, a difference between the surrogate data and the original time series is given, the  $H_0$  is rejected and non-linearity in the time series data is assumed (Galka, 2000).

Due to the nature of brain data as a nonlinear and nonstationary signal, in this work a surrogate data testing technique was used to analyze the temporal evolution of the signals of interest. To identify the time interval of significant brain responses (e.g. time interval of the C1, HFA, N<sub>T</sub> or P<sub>D</sub>), a surrogate distribution of the time series was generated by circularly shifting the time series data of participants in 1000 iterations. Each time point of the original time series data was compared to the surrogate distribution. The cumulative distribution function was calculated and subtracted from 1, resulting in a  $P$  value for each time point, indicating whether there was a significant amplitude modulation compared to the baseline activity.

### 3 Working Hypotheses

The theoretical background and the practical methods outlined in Chapter 1 and 2 build the basis for the different studies and analyses carried out as part of this thesis. In Chapter 4 and 5, the different studies along with the results and a discussion of the findings, will be explained in more detail. This chapter will give an overview of the studies, analyses and the respective hypotheses.

1<sup>st</sup> and 2<sup>nd</sup> study – *The HFA as a Feedforward or Feedback Signal*. As described in Chapter 1, whether the visual HFA solely represents a feedforward signal or includes feedback projections still remains unsolved. To tackle this, participants were presented with a visual detection task and I used the EEG-C1 component, representing the initial visual feedforward sweep to V1, as a reference measure. In the first study I analyzed the response characteristics of the MEG-HFA and the EEG-C1 to systematic contrast modulations of task-irrelevant visual stimulation.

- **Assuming that HFA also measures for visual input, a critical assumption would be that HFA and C1 overlap in latency.**

To test this, I compared participants' HFA and C1 onset times, as well as peak times. Furthermore, I analyzed whether average HFA and C1 amplitudes systematically varied with stimulus contrast. In the second study, I analyzed whether C1 and HFA amplitudes change during episodes of MW compared to focused attention. I used the same experimental paradigm as in the first study but in 20% of the trials participants were asked to rate their attentional focus on a Likert-scale ranging from 1 ("thoughts were anywhere else" – OFF) to 5 ("thoughts were totally at the task" – ON).

- **Following the assumptions of the attentional decoupling theory, the HFA should be reduced in amplitude during episodes of MW.**

To this end, I compared mean HFA and C1 amplitudes during MW and focused attention.

3<sup>rd</sup>, 4<sup>th</sup> and 5<sup>th</sup> study – *The HFA in Selective Attention*. As described in Chapter 1, selective attention, and thus the processes of target selection and distractor suppression, represents a crucial mechanism in our everyday life. Since previous studies showed attentional modulation of the HFA, in my third study I analyzed whether the HFA can serve as a marker for attentional selection. For that, participants were presented with a visual discrimination task used to elicit distinct brain responses to laterally presented targets (target enhancement,  $N_T$ ) and distractors (distractor suppression,  $P_D$ ).

- **If the HFA serves as a marker for selective attention, it should show similar response characteristics as the lower-frequency  $N_T$  and  $P_D$  components and distinguish between lateral targets and distractors.**

To this end, I compared the HFA elicited by lateral targets with the HFA elicited by lateral distractors. Furthermore, I compared the HFA's response characteristics like onset times, peak latency and performance correlation with those of the lower-frequency  $N_T$  and  $P_D$  components. In my fourth study I investigated whether the HFA and  $P_D$  responses could be modified by implicit statistical learning (see *Chapter 1.4 Statistical Learning in Visual Search*). For that, I adapted the paradigm used in my third study to elicit distinct  $N_T$  and  $P_D$  responses, with the modification that half of the experimental blocks functioned as statistical learning blocks. In 65 % of trials in those blocks the distractor was presented on one of the six locations closest to the vertical meridian if the target was presented centrally. This was done to establish statistical learning of the distractor position.

- **If the participants implicitly learned that the distractor is more likely presented close to the central target, the distractor suppression signals ( $P_D$  and HFA to lateral distractors) for these locations should be higher in learning blocks compared to non-learning blocks.**

To test this, I compared the distractor suppression signals ( $P_D$  and HFA) between learning and non-learning blocks. Furthermore, I compared the temporal evolution of microsaccades with the lower-frequency  $N_T$ ,  $P_D$  and HFA response. In a previous study, Wienke et al. (2021) found the N2pc component as a marker for selective attention to be increased during episodes of MW compared to focused attention using MEG recordings. Since the N2pc component represents the net result of target enhancement and distractor suppression, the question arises whether the increased N2pc during MW in Wienke et al. (2021) was due to higher target enhancement or distractor suppression signals. To shed light on this, in my fifth study I analyzed data of a subset of participants from the fourth study. In 20% of trials participants were asked to rate their attentional focus in the trial immediately preceding the thought probe on a 5-point Likert-scale from 1 ("thoughts were anywhere else"—OFF) to 5 ("thoughts were totally at the task"—ON).

- **On the basis of the results in Wienke et al. (2021), the  $N_T$ ,  $P_D$  or both components should be increased during episodes of MW.**

To test this, I compared mean  $N_T$  and  $P_D$  amplitudes during MW and focused attention.

## 4 The HFA as a Feedforward or Feedback Signal

The present chapter is based on the following publications:

Schmid, P., Klein, T., Minakowski, P., Sager, S., Reichert, C., Knight, R. T., & Dürschmid S. (2024). Temporal kinetics of brain state effects on visual perception. bioRxiv 2024.08.02.606289; doi: <https://doi.org/10.1101/2024.08.02.606289>

Schmid, P., Reichert, C., Knight, R. T., & Dürschmid, S. (2025). Differential contributions of the C1 ERP and broadband high-frequency activity to visual processing. *Journal of Neurophysiology*, 133(1), 78-84. doi: <https://doi.org/10.1152/jn.00292.2024>

### 4.1. Introduction

Intracranial recordings in humans suggest that the HFA represents local neuronal population dynamics (Ray et al., 2008, Leonard et al., 2024). This is further supported by investigations showing a modulation of the HFA onset response by differences in the contrast of visual stimuli (Bartoli et al., 2019), supporting its role in input to visual cortex. However, recent investigations indicate, that the HFA signal also includes substantial corticocortical feedback representations, questioning its role as a pure feedforward signal in visual processing (Leszczyński et al., 2020).

During wakefulness, humans undergo rapid brain state changes, frequently transitioning between focused wakefulness (ON state) and inattention to external events (OFF state) (Killingsworth & Gilbert, 2010), referring to a focus on internal thoughts (Warmesley & Summer, 2020), including the concept of MW. As mentioned in *Chapter 1.1*, MW is associated with an increase in perceptual errors (He et al., 2011, Yanko Spalek, 2014) and diminished scalp EEG responses (Braboszcz & Delorme, 2011; Kam et al., 2011; Xu et al., 2018). According to the perceptual decoupling theory, these findings are interpreted to be due to reduced sensory representation (Smallwood & Schooler, 2015). However, how MW affects sensory representation of visual information on a neural basis remains unclear.

It remains untested whether human HFA involves feedback signals or solely represents feedforward information. To address this, I compared the HFA responses with the initial feedforward sweep to V1, indexed by the C1 component. The C1-EEG, peaking before 100 ms at parietal-occipital electrodes, reflects V1 feedforward activity and aligns with sensory MUA (Di Russo et al., 2002; Kraut et al., 1985; Lakatos et al., 2007). If HFA tracks visual input, it should overlap temporally with the C1. Using simultaneous EEG-MEG recordings, I examined HFA-MEG and C1-EEG responses to visual contrast modulations and compared their temporal dynamics across brain states. I found that the C1 precedes the sustained HFA, indicating sensory feedback. HFA was reduced during MW but represented sensory evidence, manifested by intact target discrimination independent of HFA amplitude.

## 4.2. Methods and Material

### 4.2.1 Participants

After obtaining informed consent 19 subjects (12 female, *range*: 20 – 33 years,  $M = 26.53$  years,  $SD = 4.53$ ) participated in study 1 and 23 subjects (17 female, *range*: 18-35 years,  $M = 26.58$ ,  $SD = 4.95$ ) participated in study 2. Sample sizes were comparable with previous studies investigating the C1 and HFA (Gebodh et al., 2017;  $N = 16$ ; Iemi et al., 2019;  $N = 26$ ; Wienke et al., 2021;  $N = 16$ ).

### 4.2.2 Paradigm

#### *Stimuli*

I employed a visual detection paradigm with task-irrelevant high contrast checkerboard wedges (Iemi et al., 2019) to elicit a robust C1. Black arrows presented in the center of the screen functioned as targets and were accompanied by the checkerboard wedges either in the upper (UVF) or lower (LVF) visual field. All stimuli were presented against a grey background. The targets had a size of 1.5 cm x 0.7 cm, covering 0.54 ° of visual angle (va), while the checkerboards had a size of 12 cm x 10 cm, covering 8.02 ° of va. Each checkerboard wedge was part of a ring-like checkerboard with a spatial frequency of 5 cycles per degree. Furthermore, each wedge covered 3.13 % of the area of the checkerboard (Iemi et al., 2019). The checkerboards in the UVF and LVF were located at polar angles of 25 ° above and 45 ° below the meridian to stimulate the lower and upper banks of the calcarine fissure (Aine et al., 1996; Di Russo et al., 2002). In study 1, the checkerboards' contrast levels varied between 60 % and 90 % in steps of 10 % (see **Figure 6A**) across four blocks in a pseudorandom order to test for differences in amplitude modulation of the C1 and HFA by visual stimulation. In study 2, checkerboard contrast level was kept constant at 100%.

#### *Procedure*

Participants were asked to keep their eyes on the center of the screen. Each trial started with the presentation of a fixation cross for 2.1 s ( $\pm 300$  ms). After this period the target arrow appeared at the fixation location for 100 ms pointing either to the left or right side (see **Figure 6B**).

Participants were asked to identify the direction of the arrow and respond as fast as possible via button press with the right index (for left) or middle finger (for right). The study consisted of four blocks of 272 trials each (1088 total). Checkerboards appeared in the UVF or LVF in 50% of trials each, in a pseudorandomized order. Also, the arrow showed to the left and right in half of the trials. The study was programmed and controlled with Psychtoolbox 3 (Brainard, 1997; Kleiner et al., 2007) running on Matlab (R2018b).

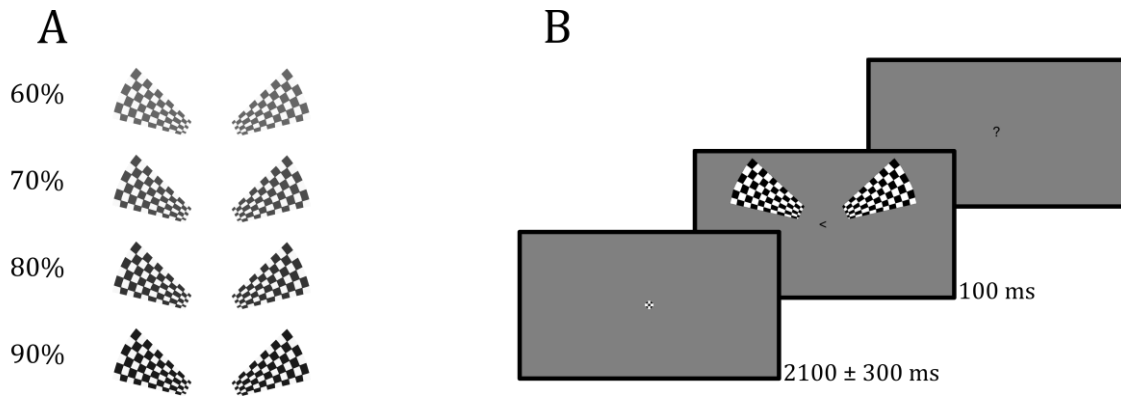


**Figure 6.** Experimental paradigm. **A:** Presentation of the different checkerboard contrast levels. **B:** Visual stimulation with high contrast checkerboards accompanying the visual discrimination task.

#### 4.2.3 Experience Sampling

In 20% of the trials in study 2 the stimulus array was followed by a thought probe in which participants were asked to rate their attentional focus (see *Chapter 2.5 Thought Probe Sampling*).

#### 4.2.4 Simultaneous EEG and MEG Recordings

EEG and MEG activity were recorded simultaneously while participants were seated in a dimmed, magnetically shielded recording booth (see *Chapter 2.4 Apparatus*). Vertical and horizontal EOG data were recorded to extract activity stemming from eye movement artifacts (see *Chapter 2.6 General Preprocessing*). In a subset of participants in study 2, participants' pupil data were recorded using an Eye Tracker (see *Chapter 2.4 Apparatus*). Preparations and recording took about 2.5 hours.

#### 4.2.5 Preprocessing and Artifact Rejection

MEG, EEG and EOG data were preprocessed following the pipeline presented in *Chapter 2.6*. On average, 1.78 % of trials in study 1 and 1.76 % of trials in study 2 were rejected due to artifacts.

#### 4.2.6 Statistical Analysis

For study 1, I conducted the following analysis steps. First, I compared the behavioral measures for different contrast levels (*I – Behavioral Performance*). This included both reaction times and accuracy, defined as the percentage of correct responses. I then analyzed the grand average EEG-C1 response (*II – C1 Component*). Next, I analyzed the grand average MEG-HFA response (*III – Broad Band High Frequency Activity*). In a following step, I compared the latencies of the EEG-C1 and MEG-HFA (*IV – Latency differences between C1 and HFA*) and analyzed whether the components varied with contrast level (*V – Amplitude Modulation with contrast level*).

For study 2, I first compared the behavioral measures for different brain states (*VI – Behavioral Performance*). This included both reaction times and accuracy, and then assessed the distribution

of MW. I analyzed the EEG-C1 component (*VII – C1 Component*) and the MEG-HFA component (*VIII – Broadband High-Frequency Activity*). In the following step, I compared the latencies of the EEG-C1 and MEG-HFA and further analyzed whether C1 peak response predicted participants' HFA amplitude (*IX – Latency differences between C1 and HFA*). Finally, I analyzed whether the EEG-C1 and MEG-HFA varied with brain states (*X – Amplitude Modulation with brain states*). Time intervals of significant grand average responses of C1 and HFA were determined by comparing the observed data against a surrogate distribution (*see Chapter 2.9 Surrogate Data Testing*).

### ***I – Behavioral Performance Study 1***

*Reaction times.* Trials with extreme reaction times < 100 ms or > 2000 ms were marked as outliers and excluded. Trials were then categorized based on the four contrast levels, and reaction times were averaged within subjects across trials corresponding to each contrast level. The averaged reaction times were then compared using a one-way ANOVA with the factor contrast (60%, 70%, 80%, 90%). In addition, I computed reaction time coefficient of variation (RT CV) for every participant for the four contrast levels. RT CV is a measure of RT variability while controlling for RT speed and is computed by dividing the RT's standard deviation by the mean RT and multiplied with the factor 100 (Epstein et al., 2011). The resulting RT CV values were then compared using a one-way ANOVA with the factor contrast (60%, 70%, 80%, 90%).

*Target discrimination performance.* Performance was determined for each subject. The resulting performance values were compared between contrast levels (60%, 70%, 80%, 90%) using a one-way ANOVA.

### ***II – C1 Response Study 1***

To identify the EEG-C1 I first labeled trials regarding the position of the checkerboards presented (LVF vs. UVF), because stimulation in the LVF generates a positive going C1 and stimulation in the UVF generates a negative going C1 (Luck, 2014). Since the C1 component did not differ between UVF and LVF (*see Results II – C1 Response*), responses to UVF stimulation were multiplied by -1 to reverse polarity and then averaged with LVF stimulation in each channel and subject. To identify the C1 window (amplitude modulation over baseline), I compared the C1 activity in posterior EEG channels PO3/4 against a surrogate distribution (*see Statistical Analysis*) and *P* values were corrected for multiple comparisons, using the False Discovery Rate (FDR) method (Benjamini & Hochberg, 1995).

### ***III – Broadband High Frequency Activity Study 1***

The HFA response was identified following the procedure described in *Chapter 2.4*. To determine the time window of significant HFA modulation, each observed time point was compared to a surrogate distribution (see *Chapter 2.9 Surrogate Data Testing*).

### ***IV – C1 and HFA latency comparison Study 1***

To analyze whether individual C1 responses predicted participants' HFA amplitude, C1 and HFA amplitude values were z-scored. Individual C1 and HFA response onset times were defined as the time point amplitude values first exceeded  $z > 3$ , resulting in an onset time point for each subject both for the C1 and HFA. C1 and HFA response onset and peak times were then compared using *t*-tests.

### ***V – Amplitude Modulation with contrast level Study 1***

One-way ANOVAs with the factor contrast comparing C1 and HFA mean amplitudes were carried out separately to test for differences in amplitude modulation as a function of contrast.

### ***VI – Behavioral Performance Study 2***

*Likelihood of brain states.* I tested whether the ratio of brain state reports changed over the experiment to rule out the possibility that changes in cortical dynamics are a result of a change across the experiment and not due to brain state fluctuations throughout the experiment. I averaged participant's brain state ratings for each block and compared the ratio of brain state ratings across the blocks using a 4 x 3 ANOVA with the factors block (I, II, III, IV) and brain state (ON, MID, OFF).

*Reaction times.* Like in study 1, trials with reaction times  $< 100$  ms or  $> 2000$  ms were excluded from the analyses. Reaction times and RT CV were then grouped for the three brain states and compared using a one-way ANOVA with the factor brain state (ON, MID, OFF).

*Target discrimination performance.* Performance was determined for each subject and compared between brain states (ON, MID, OFF) using a one-way ANOVA.

### ***VII – C1 Response Study 2***

I followed the procedure from study 1 to identify the EEG-C1 (see *Statistical Analysis II – C1 Response*). Again, since C1 amplitude did not differ between UVF and LVF (see *Results VII – C1 Response*), I reversed polarity of the C1 generated by UVF stimulation and averaged them in each channel and subject. To find the time window of significant C1 response in EEG channels PO3/4, I compared the C1 activity against a surrogate distribution. *P*-values were then corrected for

multiple comparisons, using the FDR method. To rule out the possibility that possible differences in C1 amplitude occurred due to differences in pupil size (Bombeke et al., 2016), I checked whether pupil dilation differed between brain states in the C1 time interval.

### ***VIII – Broadband High Frequency Activity Study 2***

Like in study 1, the HFA response was identified following the procedure described in *Chapter 2.4*. To determine the time window when the HFA showed a significant modulation, each observed time point was compared to a surrogate distribution (see ***Chapter 2.9 Surrogate Data Testing***) and *P*-values were corrected for multiple comparisons using the FDR method.

### ***IX – C1 and HFA latency comparison Study 2***

Similar to study 1, C1 and HFA amplitude values were first z-scored and onset times were defined as the time point amplitude values first exceeded  $z > 3$ , resulting in an onset time point for each subject both for the C1 and HFA. C1 and HFA response onset times were then compared using a *t*-test and Pearson's correlation coefficient of C1 and HFA onset times was calculated. Individual C1 and HFA peak responses were compared using a *t*-test and by calculating Pearson's correlation coefficient of C1 and HFA peak times. To test whether C1 amplitude magnitude predicts HFA amplitude Pearson correlation coefficients between C1 amplitude at peak time point (at ~ 68ms) and HFA amplitude values at each time point were calculated separately. The correlation coefficients were compared with a surrogate distribution (see ***Chapter 2.9 Surrogate Data Testing***). In 1.000 iterations, the C1 and HFA values of the subjects at the time of the highest observed correlation were taken, C1 and HFA values were randomly reassigned to the subjects and the Pearson correlation coefficient was calculated again. Calculating the 99% Confidence Interval for the correlation coefficient resulted in a critical coefficient value. Correlation coefficients exceeding this critical value were considered as showing a significant correlation between C1 peak response and HFA amplitude.

### ***X – Amplitude Modulation with brain states Study 2***

Differences between brain states in C1 and HFA were analyzed separately using *t*-tests. Since the HFA response is known to have a fast onset and a slowly decreasing flank, mean amplitudes of the increasing HFA flank and the decreasing HFA flank were analyzed separately.

### 4.3 Results

#### Study 1

##### *I – Behavioral Results Study 1*

*Reaction times.* Participants' reaction times did not differ between contrast levels neither with respect to mean values ( $F_{3,54} = 0.12$ ;  $P = .95$ ; see **Figure 7**) nor variance ( $F_{3,54} = 0.42$ ;  $P = .74$ ; see **Figure 7**).

*Target discrimination performance.* Participants' performance did not differ between contrast levels ( $F_{3,54} = 1.84$ ;  $P = .15$ ; see **Figure 7**).

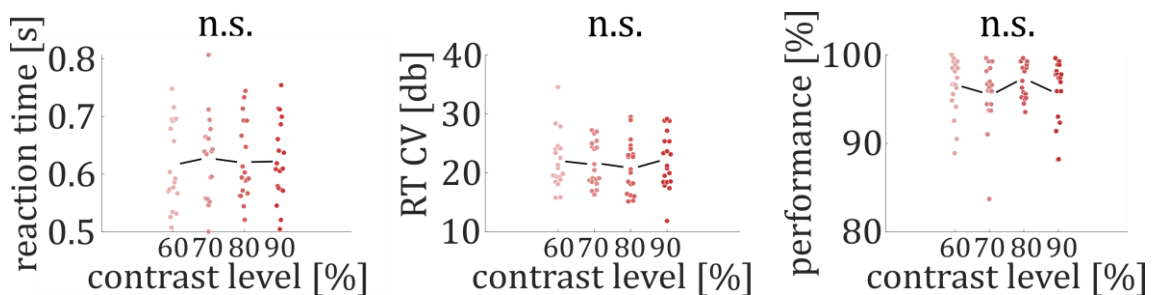


**Figure 7.** Behavioral Results. Neither reaction times (left), reaction time variability (middle), nor performance (right) differed between contrast levels.

##### *II – C1 Response Study 1*

The C1 component peaked at posterior EEG electrodes PO3 and PO4. Time-resolved  $t$ -tests showed no significant differences between the two EEG channels ( $PO3_{max} = 3.52 \mu V$ ;  $PO4_{max} = 3.72 \mu V$ ; all  $P > .07$ ). Thus, the C1 response was averaged across both sensors in the subsequent analysis. Checkerboards in the UVF and LVF elicited a negative and positive C1 response at posterior electrodes, respectively. Since absolute C1 amplitude values did not differ between UVF and LVF ( $M_{UVF} = 4.89 \mu V$ ;  $M_{LVF} = 4.59 \mu V$ ;  $t_{19} = 0.76$ ;  $P = .45$ ; see **Figure 8A**), the negatively trending C1 component for UVF stimulation was converted (see *Statistical Analysis II – C1 Response*) and the resulting time series was averaged across UVF and LVF trials to obtain a single C1 response. The C1 showed a significant amplitude modulation over baseline in the time interval from 44 to 88 ms ( $C1_{crit} = 0.26 \mu V$ ;  $C1_{max} = 3.55 \mu V$  at 66 ms; all  $P$  values  $< .0014$ ; see **Figure 8A**).

##### *III – Broad Band High-Frequency Activity Study 1*

I found a significant HFA amplitude modulation between 76 ms and 266 ms ( $HFA_{crit} = 0.22 fT$ ;  $HFA_{max} = 0.57 fT$  at 198 ms; all  $P$  values  $< .05$ ; see **Figure 8B**).

**IV – C1 and HFA latency comparison Study 1**

The C1 showed an earlier temporal evolution compared to the HFA with both an earlier onset ( $C1_{onset} = 44$  ms;  $HFA_{onset} = 88$  ms;  $t_{18} = 5.03$ ;  $P = .00009$ ) and peak time than the HFA ( $C1_{peak} = 68$  ms;  $HFA_{peak} = 172$  ms;  $t_{18} = 6.38$ ;  $P = .000005$ ; see **Figure 8C**). However, temporal evolutions of C1 and HFA did not correlate ( $P_{onset} = .24$ ;  $P_{peak\ time} = .36$ ;  $P_{peak\ amplitude} = .24$ ).

**V – Amplitude modulation with contrast level Study 1**

Analyzing the C1 amplitude in time interval of 44 to 88 ms, revealed a main effect of contrast ( $F_{3, 54} = 8.72$ ;  $P < .001$ ; see **Figure 8A**). Post-hoc *t*-test revealed a higher C1 response elicited by checkerboards with 90 % contrast compared to checkerboards with 60 % ( $C1_{90\%} = 2.71$   $\mu$ V;  $C1_{60\%} = 2.30$   $\mu$ V;  $t_{18} = 5.58$ ;  $P < .0001$ ) and 80 % contrast ( $C1_{80\%} = 2.38$   $\mu$ V;  $t_{18} = 4.28$ ;  $P < .001$ ). There were no differences comparing C1 peak latencies between contrast levels ( $F_{3, 54} = 0.83$ ;  $P = .48$ ). Neither HFA amplitudes ( $F_{3, 54} = 0.62$ ;  $P = .61$ ; see **Figure 8B**), nor peak latencies differed between contrast levels ( $F_{3, 54} = 1.14$ ;  $P = .34$ ).

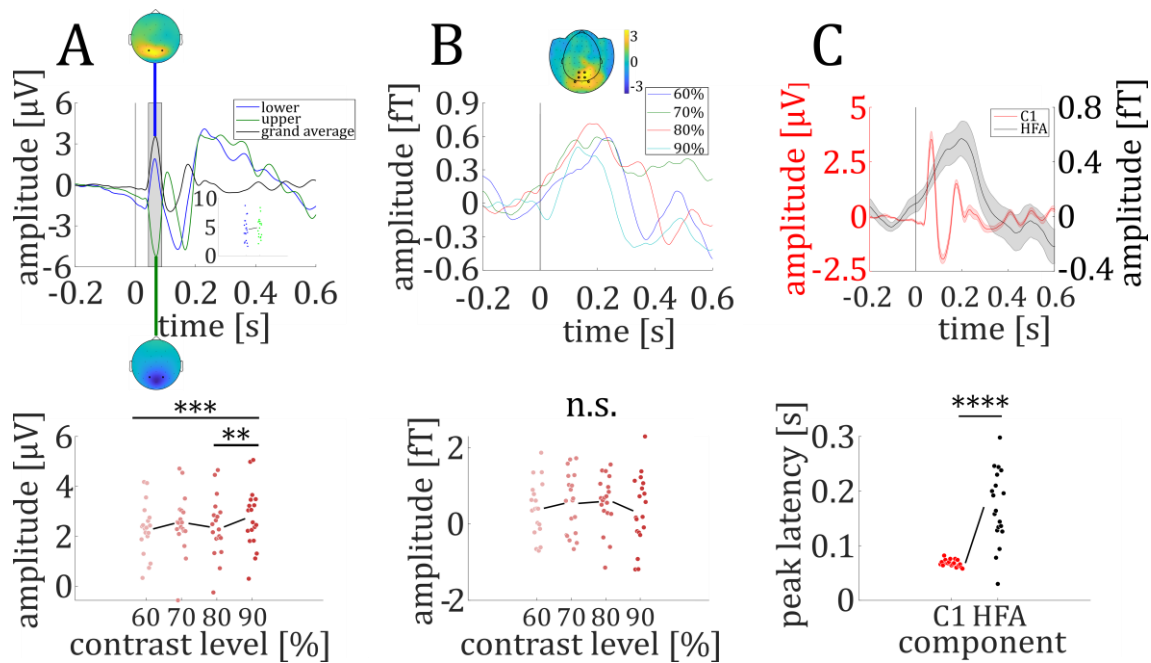


**Figure 8.** Neural Results. **A:** C1 grand average for LVF stimulation (blue line) and UVF stimulation (green line) with topographic plot, with PO3 and PO4 electrodes highlighted. Collapsed C1 grand average response (black line; responses to UVF stimulation were multiplied by -1 to reverse polarity and then averaged with LVF stimulation in each channel and subject), grey shaded area shows time interval of significant C1 response (upper). Absolute maximal C1 amplitude for LVF stimulation and UVF stimulation (small inset). C1 amplitude for different contrast level (lower). C1 amplitude increased with stimulus contrast level. **B:** Colored lines show HFA grand average responses to the different stimulus contrast level (upper). Topographic plot with the six significant MEG channels highlighted (upper inset). Mean HFA amplitude for different contrast level (lower). **C:** Time course of grand average C1 and HFA response (upper). Participant's individual time points at which the C1 and HFA reached their peaks. The C1 component peaked significantly earlier than the HFA (lower). Shaded colored lines represent the standard error of mean (SEM). Colored circles represent single data points. \*\* =  $P < .001$ ; \*\*\* =  $P < .0001$ ; \*\*\*\* =  $P < .00001$ .

## Study 2

### VI – Behavioral Results Study 2

*Likelihood of brain states.* Thought probes were presented on average every 16.51 s ( $SD = 1.35$ s; range: 14.57 s – 20.12 s). The 4 x 3 ANOVA with the factors block (I, II, III, IV) and brain state (ON, MID, OFF) showed no significant main effect of block ( $F_{3, 262} = 0.01$ ;  $P = .998$ ), brain state ( $F_{2, 262} = 0.58$ ;  $P = .56$ ; see **Figure 9**) nor interaction effect ( $F_{6, 262} = 1.01$ ;  $P = .42$ ), indicating that the frequency of the different brain states did not differ across the experiment (see **Figure 9**).

*Reaction times.* Participants' reaction times differed between brain states ( $F_{2, 44} = 12.83$ ;  $P < .0001$ ; see **Figure 9**). Post-hoc  $t$ -tests revealed longer reaction times during OFF than ON ( $M_{OFF} = 628$  ms;  $M_{ON} = 581$  ms;  $t_{22} = 3.91$ ;  $P < .001$ ) and MID trials ( $M_{MID} = 602$  ms;  $t_{22} = 2.94$ ;  $P < .01$ ), as well as longer reaction times during MID than ON trials ( $t_{22} = 3.50$ ;  $P < .01$ ). Similarly, RT CV values differed between brain states ( $F_{2, 44} = 10.54$ ;  $P < .001$ ; see **Figure 9**), with higher RT CV values for OFF trials compared to ON trials ( $M_{OFF} = 24.64$ ;  $M_{ON} = 18.79$ ;  $t_{22} = 3.55$ ;  $P < .01$ ) and MID trials ( $M_{MID} = 20.44$ ;  $t_{22} = 3.60$ ;  $P < .01$ ). No difference was found between ON and MID trials ( $t_{22} = 1.57$ ;  $P = .13$ ).

*Target discrimination performance.* Participants' performance differed between brain states ( $F_{2, 44} = 6.27$ ;  $P < .01$ ; see **Figure 9**). Post-hoc  $t$  tests revealed worse performance in OFF compared to ON trials ( $M_{OFF} = 93.2$  %;  $M_{ON} = 97.5$  %;  $t_{22} = 3.09$ ;  $P < .01$ ), but no performance difference between OFF and MID trials ( $M_{MID} = 95.0$ %;  $t_{22} = 1.72$ ;  $P = .10$ ), nor between ON and MID trials ( $t_{22} = 2.13$ ;  $P = .05$ ). Note, that overall performance was very high across brain states.

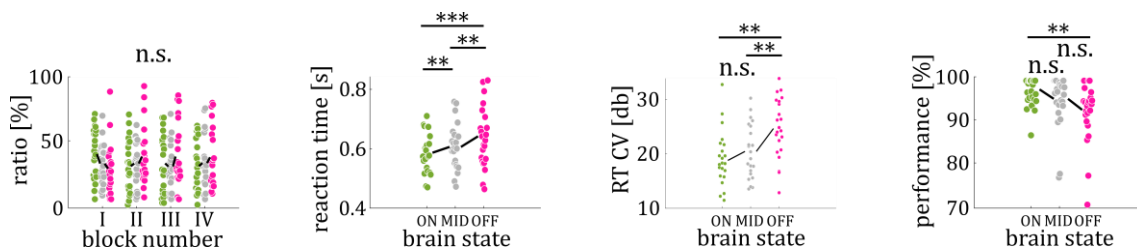


**Figure 9.** Behavioral Results. Likelihood of brain states did not vary across the blocks (left). Reaction times changed with brain states with slowest (second from left) and more variable (second from right) responses during OFF trials. Subjects made most errors during OFF trials (right). Colored circles represent single data points. \*\* =  $P < .01$ ; \*\*\* =  $P < .001$ .

### VII – C1 Response Study 2

Like in study 1, the C1 component peaked at the posterior EEG electrodes PO3/4 and time-resolved  $t$ -tests showed no significant differences between the two EEG channels ( $PO3_{max} = 3.35$   $\mu$ V;  $PO4_{max} = 3.04$   $\mu$ V; all  $P > .13$ ). Thus, the C1 was averaged across both sensors. Absolute C1 amplitude values did not differ between UVF and LVF ( $M_{UVF} = 4.14$   $\mu$ V;  $M_{LVF} = 5.32$   $\mu$ V;  $t_{22} = 1.95$ ;  $P = .06$ ), and the negatively trending C1 component for UVF stimulation was thus converted. I then

averaged the resulting time series across UVF and LVF trials to obtain a single C1 response. The C1 component showed a significant modulation over baseline in the time interval from 46 to 88 ms ( $z_{C1_{crit}} = 1.48$ ;  $z_{C1_{max}} = 22.20$  at 68 ms; all  $P$ -values  $< .00001$ ; see **Figure 10A**). Pupil dilation did not differ between brain states in the C1 time interval (mean  $zPD_{ON} = 2.38$ ; mean  $zPD_{OFF} = 0.72$ ;  $t_{13} = 1.18$ ;  $P = .26$ ).

### VIII – Broadband High Frequency Activity Study 2

Five MEG sensors showed a significant HFA amplitude modulation between 50 ms and 288 ms after stimulus onset ( $z_{crit} = 3.00$ ;  $HFA_{max} = 5.22$  at 122 ms; all  $P$ -values  $< .041$ ; see **Figure 10A**).

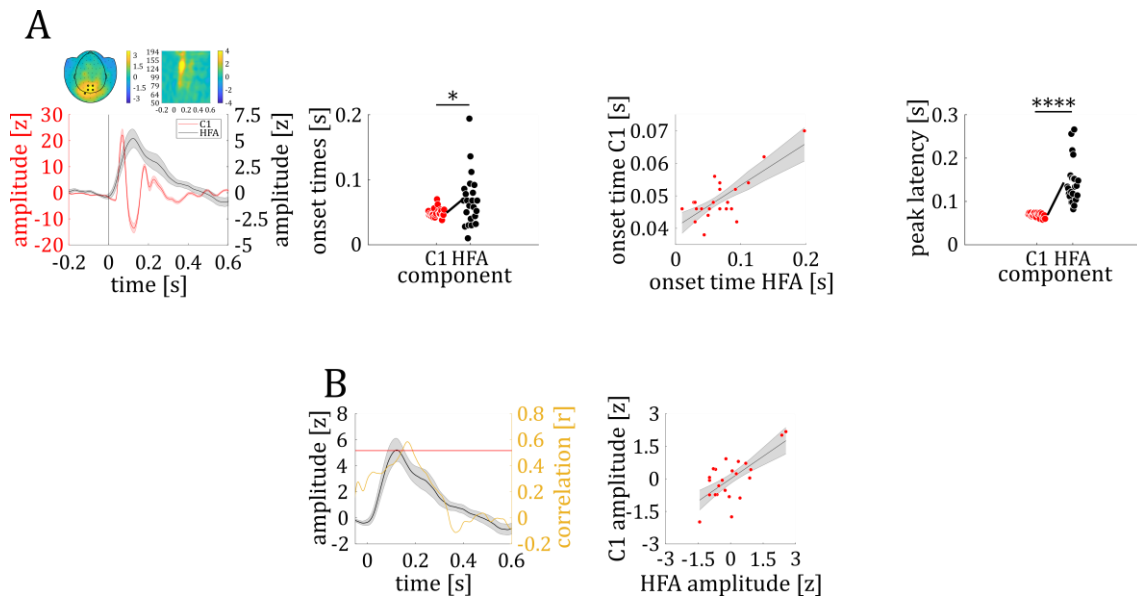


**Figure 10.** Neural grand average results. **A:** Time course of grand average C1 and HFA response (left). Topographic plot and time-frequency representation show spatial and frequency-specificity of the HFA response. Both onset (second from left) and peak (right) of C1 were earlier than onset and peak of HFA. The scatter plot shows the strong correlation of HFA and C1 onset times (second from right). **B:** Prediction of HFA magnitude by C1 peak response. Black line shows HFA and yellow line time-resolved correlation coefficient. Red line shows 99% confidence interval for correlation coefficient value. HFA correlated significantly with peak C1 response in the time range between 140 ms and 192 ms (left). Scatter plot shows maximal correlation between HFA and peak C1 response (right). Colored circles represent single data points. \* =  $P < .05$ ; \*\*\*\* =  $P < .00001$ .

### IX – C1 and HFA latency comparison Study 2

Comparing the temporal evolution of the C1 and HFA showed both a significant earlier onset of C1 ( $C1_{onset} = 49$  ms;  $HFA_{onset} = 69$  ms;  $t_{22} = 2.62$ ;  $P = .02$ ; see **Figure 10A**) and onset times were strongly correlated ( $r = .76$ ;  $P < .0001$ ; see **Figure 10A**) indicating that this effect exists on a single-subject level. Furthermore, the C1 peaked earlier than the HFA ( $C1_{peak} = 68$ ms;  $HFA_{peak} = 144$  ms;  $t_{22} = 7.07$ ;  $P < .00001$ ; see **Figure 10A**), but peak times were not correlated ( $P = .43$ ). The peak C1 amplitude at 68 ms correlated with HFA amplitude between 140 ms and 192 ms ( $r_{crit} = .50$ ,  $r_{max} = .58$  at 166 ms;  $P = .002$ ; see **Figure 10B**).

**X – Amplitude Modulation with brain states Study 2**

C1 amplitude did not differ between brain states ( $t_{22} = 1.02$ ;  $P = .32$ ; see **Figure 11**). However, the increasing flank of the HFA (50 – 122 ms) showed a significant difference between brain states with higher HFA amplitude in ON compared to OFF trials ( $t_{22} = 1.99$ ;  $P = .03$ ; see **Figure 11**). No such difference was found for the decreasing flank (122 – 288 ms;  $t_{22} = 0.57$ ;  $P = .71$ ; see **Figure 11**).

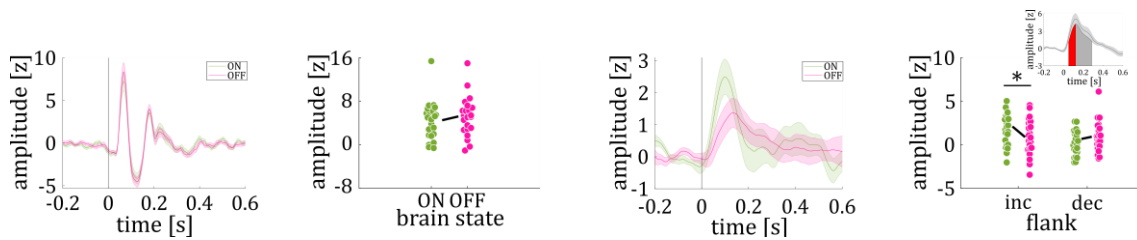


**Figure 11.** Neural correlates modulation with brain states. C1 does not show variation with brain state (ON – green; OFF – magenta; left) Individual mean C1 amplitude for ON and OFF trials (second from left). HFA shows variation with brain states in the time interval of the increasing but not decreasing flank (see inset; second from right and right). Shaded colored lines represent the standard error of mean (SEM). Colored circles represent single data points. \* =  $P < .05$

**4.4 Discussion**

In two studies I used simultaneous EEG-MEG recordings to investigate whether the HFA solely reflects input to visual cortex and is primarily influenced by bottom-up information or by internal brain states. I used the EEG-C1 response as a reference measure, which is recognized as a marker for initial sensory input to the visual cortex. Only the C1 amplitude, but not the HFA, was sensitive to small contrast changes, with the HFA peaking later in time than the C1. Furthermore, the HFA, but not the C1, was reduced during MW.

In both studies, bilateral checkerboards evoked an EEG-C1 response similar to other studies (Di Russo et al., 2003; Iemi et al., 2019; Zhu & Luo, 2012). The C1 is the first visual ERP wave with polarity changes depending on the presentation of stimuli in the visual field. Due to the retinotopic organization of the visual pathway and V1, stimuli in the upper visual field are mainly projected to the lower bank of the calcarine fissure leading to a dipole pointing downward, while lower visual field stimuli are projected to the upper bank of the calcarine fissure leading to a dipole pointing upward, allowing precise localization of C1 generators in V1 without source localization analyses (Luck & Kappenman, 2012). The C1 is primarily driven by external stimulus characteristics, such as stimulus size and contrast (Gebodh et al., 2017). Increasing stimulus contrasts lead to a systematic increase in C1 peak amplitude, further supporting the notion that the C1 component reflects the physical properties of the external stimuli. This is in line with my results of a C1 amplitude modulation by stimulus contrast. Whether the C1 component can be modulated by attentional resources remains a matter of debate. While some studies report

significant attentional modulation of C1 amplitude (Dassanayake et al., 2016; Kelly et al., 2008; Pan et al., 2024; Qin et al., 2023; Wolf et al., 2022), others have failed to find or replicate such effects (Baumgartner et al., 2018; Clark & Hillyard, 1996; Di Russo et al., 2012; Ding et al., 2014). In my study, I did not find any modulation of the C1 by inattention during MW.

The HFA response in my study revealed an onset prior to 100 ms, with a peak response prior to 200 ms and a slowly decreasing amplitude, closely resembling the HFA observed in intracranial studies (Bartoli et al., 2019; Gerber et al., 2017; Golan et al., 2017; Vishne et al., 2023), especially distinct in V1 electrodes (Bartoli et al., 2019; Golan et al., 2017). Furthermore, my stimuli and the low spatial spread of high frequencies indicate that the HFA originates in V1.

Although the MEG-HFA exhibited a similar time course, I did not find contrast modulation as observed in previous studies (Bartoli et al., 2019), which may be attributed to two factors. First, unlike the stimuli in Bartoli et al. (2019), the checkerboard wedges in my study were not behaviorally relevant. Second, Bartoli et al. (2019) used stronger contrast differences. It is possible that the contrast dependent HFA differences, as seen in Bartoli et al. (2019), might be reflected in MEG-HFA. Nonetheless, my findings demonstrate that the C1 is more sensitive to subtle contrast differences, even when they are not task-relevant.

In my study, HFA did not vary systematically with stimulus contrast, challenging the view of the HFA solely representing a feedforward input signal. This is in line with a previous study investigating the HFA response and its relationship to MUA (Leszczyński et al., 2020). The supragranular HFA was found to be a substantial contributor to the recorded surface HFA, suggesting that the surface HFA may include significant cortical feedback representations (Leszczyński et al., 2020). Studies showing that V1 receives more feedback from different regions than feedforward input from thalamic projections (Budd, 1998) support these findings. This may be because feedback signals to V1 have various advantages. Connections between V1 and other cortical areas can drive task-dependent and attentional modulation of V1 activity, enabling the visual system to prioritize relevant information while filtering out irrelevant or distracting information (Muckli & Petro, 2013). Using intracranial recordings in monkeys, Semedo et al. (2022) showed that right after stimulus onset interactions between V1 and higher visual areas are feedforward-dominated and gradually become feedback-dominated (~ 125 ms; Semedo et al., 2022), indicating corticocortical feedback projections to V1 in the time range of MEG-HFA. Furthermore, they found distinct population activity patterns for feedforward and feedback signals, allowing feedback signals to not directly affect feedforward activity (Semedo et al., 2022). The different response characteristics of EEG-C1 and MEG-HFA in my studies further support this notion. In both studies, I found that the HFA onset in the time range of the C1 response but peaked later than the C1 component.

The temporal lag between participants' individual C1 and HFA onset and peak latencies aligns with studies investigating feedback projections to V1. Previous EEG studies exploring the flow of visual information along the dorsal and ventral pathways observed activity in dorsolateral frontal cortical regions approximately 30 ms after C1 onset (Fuxe & Simpson, 2002). This rapid system-wide activation suggests that early feedback processes could be initiated, resulting in early feedback projections to V1 within the time range of N1 and P1, roughly around 100-200 ms (Fuxe & Simpson, 2002). Supporting this, intracranial recordings conducted in macaque monkeys revealed context-dependent modulations in V1 activity unrelated to traditional properties of V1 cell receptive fields, as early as 30 ms after the initial activation of V1 (Lamme, 1995; Zipser et al., 1996). To summarize, these findings suggest that corticocortical feedback projections to V1 can commence as early as 30 ms after the initial activation of V1. Furthermore, in contrast to the C1 component, I observed the HFA amplitude to decrease during periods of MW. Taken together, these findings support the notion that the HFA is not exclusively generated by bottom-up information but also indexes cortical feedback processes.

Previous EEG studies have shown reduced sensory responses, primarily in the low-frequency range (<30 Hz), during MW (Braboszcz & Delorme, 2011; Kam et al., 2011; Smallwood et al., 2008), suggesting decreased sensory input. Studies in animals have primarily focused on brain state changes during locomotion, although inattentive states have also been described (Bezudnaya et al., 2006), contrasting with alert wakefulness. Locomotion, alert wakefulness and inattention differ in arousal levels, with locomotion inducing the highest and inattention the lowest arousal. These behavioral states play a role in the brains' response to visual stimuli, beginning with the thalamus (Bezudnaya et al., 2006) and early processing stages depend on corticothalamic feedback, which is reduced during inattention (Reinhold et al., 2023). Conversely, higher arousal levels lead to increased visual responses (Niell & Stryker, 2010). Previous research has consistently shown that HFA amplitude is modulated by attentional states (Davidesco et al., 2013; Szczepanski et al., 2014; Wienke et al., 2021). Consistent with these results, I demonstrate that the HFA is reduced during periods of MW. However, in line with previous studies reduction in HFA amplitude does not disrupt target discrimination. Vishne et al. (2023) investigated neural correlates of sustained visual perception and found that, despite a reduction in HFA amplitude, performance was maintained. Similarly, I found a reduction in HFA amplitude during moments of MW. Even though target discrimination was reduced during MW, participants were still able to maintain a high level of performance (~ 93%).

In sum, the findings of my first two studies provide evidence for the role of the HFA in feedforward and feedback processing in early visual cortex with feedback processes being modulated by inattentive states like MW.

## 5 The HFA in Selective Attention

This chapter is based on the following manuscript currently under revision:

Schmid, P., Reichert, C., Bartsch M. V., & Dürschmid, S. (2024). Broadband high frequency Activity initializes Distractor Suppression. bioRxiv 2024.08.22.609149; doi: <https://doi.org/10.1101/2024.08.22.609149>

### 5.1 Introduction

As described in *Chapter 1.3*, fast distractor suppression and accurate target selection describe key aspects of selective attention (Wöstmann et al., 2019). While salient distractors complicate visual search (Gutteling et al., 2022; Zhao et al., 2023), prior knowledge about potential distractors can facilitate target detection (Arita et al., 2012; Donohue et al., 2018; Müller et al., 1995; Olivers & Humphreys, 2003; Watson & Humphreys, 2000). Despite extensive literature on target selection (Eimer, 1996; Hopf et al., 2000; Luck & Hillyard, 1994; Woodman et al., 2009), the neural mechanisms underlying distractor suppression are less understood.

To investigate the neural mechanisms underlying target selection ( $N_T$ ) and distractor suppression ( $P_D$ ), stimulus arrays containing a lateral target while the distractor is presented on the vertical meridian and vice versa are used (Hickey et al., 2009; see ***Chapter 1.3 Selective Attention***). Despite the necessity for fast distractor suppression, research usually shows a greater amplitude for the  $N_T$  compared to  $P_D$  (Gaspar & McDonald, 2014; Gaspelin et al., 2023; Gaspelin & Luck, 2018), raising the question of whether there might be another signal reflecting initial target-distractor distinction. Notably, hard-to-control microsaccades peak after 200 ms, in the time range of  $N_T$  and  $P_D$  (Yuval-Greenberg et al., 2008). In contrast, the HFA shows a rapid response modulation (< 200 ms) following stimulus onset (Bartoli et al., 2019; Gerber et al., 2017; Golan et al., 2017.; Vishne et al., 2023), (in part) signaling cortical feedback processes (see ***Chapter 4 The HFA as a Feedforward or Feedback Signal***; Schmid et al., 2025). Furthermore, intracranial studies on attentional selection show a lateralized HFA on attended stimuli (Szczepanski et al., 2014) occurring before the lower-frequency ERPs, rendering the HFA a suitable candidate to initiate early attentional distractor suppression.

As described in *Chapter 1.4*, prior knowledge about distracting information, such as distractor location, can reduce interference (Richter et al., 2024; van Moorselaar & Slagter, 2020). Statistical learning facilitates the establishment of an internal model that suppresses the attentional priority of locations where distractors are more likely to appear (Richter et al., 2024; Wang & Theeuwes, 2018). EEG studies showed  $P_D$  amplitude modulation by implicit learning of a frequent distractor location (Moorselaar & Slagter, 2019; van Moorselaar et al., 2020). If the HFA reflects distractor suppression, one would expect both the HFA and  $P_D$  to be modulated by statistical learning.

The perceptual decoupling theory suggests that attention to external stimuli is reduced during mind wandering, leading to decreased amplitudes of brain responses associated with selective attention, such as the N2pc (Smallwood & Schooler, 2006). However, in a recent study, Wienke et al. (2020) found the N2pc component to be increased in amplitude during periods of MW, indicating heightened selective attention. To elucidate whether this enhancement reflects enhanced target selection or distractor suppression, I analyzed  $N_T$  and  $P_D$  response modulation during MW in a subset of participants.

We used a visual search array, containing target and distractor gratings with different orientation angles, to investigate whether the BHA serves as an early indicator of distractor suppression during target discrimination. In a second experiment we increased the probability of distractors appearing at locations closest to the target to test whether BHA is sensitive to the spatial probability of distractor locations. Our results suggest that indeed, the BHA initiates a distractor suppression mechanism that is trainable by statistical regularities.

In three studies, I employed a visual search task with target and distractor gratings of varying orientation angles to investigate whether the HFA serves as an early indicator of distractor suppression during target discrimination. In a second study I increased the probability of distractors appearing at locations closest to the target to test whether BHA is sensitive to the spatial probability of distractor locations. Additionally, I explored how neural correlates of target enhancement and distractor suppression vary across brain states. My results suggest that indeed, the HFA initiates a distractor suppression mechanism that is trainable by statistical regularities. Moreover, the increased  $P_D$  during MW suggests enhanced distractor suppression.

## 5.2 Methods and Materials

### 5.2.1 Participants

After providing their informed consent, 26 subjects participated in study 3, where nine were excluded from the analysis due to excessive blink and movement artifacts, resulting in a sample size of  $N = 17$  (10 female, *range*: 18 – 38 years,  $M = 26.29$  years,  $SD = 4.92$  years). Thirty subjects participated in study 4 (21 female, *range*: 19 – 39,  $M = 25.47$  years,  $SD = 4.03$  years). Sample sizes are comparable with previous studies investigating the N2pc and its subcomponents (Gaspelin & Luck, 2018; Hilimire et al., 2011; Marturano et al., 2020).

### 5.2.2 Paradigm

#### *Stimuli*

The participants were presented with a visual search array composed of red, green and blue grating patterns, each consisting of three stripes as viewed through a circular aperture, displayed on a gray foreground (see **Figure 12**). Red and green gratings were alternated as targets and

distractors randomly between blocks, while blue gratings served as nontargets. If the red grating was the target, the green grating was the distractor and had to be ignored and vice versa. Search arrays always consisted of 19 nontargets, one pop-out target and one pop-out distractor arranged in 7 columns with 3 gratings each, and were displayed below a fixation cross to ensure a strong N2pc response (Hilimire et al., 2011; Luck et al., 1997). Participants were asked to fixate the cross, which was located at 3.75 ° visual angle (va) above the search array. The size of each grating was 0.54 ° va, and within a column they were spaced 0.01 ° va apart from each other. Target and distractor gratings could be tilted left or right in 10 steps of 1.5 °, ranging from 1.5 ° to 15 °, such that across all trials, there was a continuous distractor-target difference ranging from 0° to 30° in 21 steps. The angle of each individual nontarget was randomly determined, ranging from 0 ° to 90 °. Stimulus generation and experimental control was done using Matlab R2019 (Mathworks, Natick, USA) and the Psychophysics Toolbox (Brainard, 1997). Colors were matched for isoluminance using heterochromatic flicker photometry (Lee et al., 1988).

### ***Procedure***

At the beginning of each of the six blocks, the participants were instructed to either attend the red and ignore the green grating or vice versa in both studies. Participants had to indicate via button press whether the target was tilted to the left or the right side using the right index and middle finger, respectively. Target color varied in a pseudorandom order with 50% of the blocks containing red and the other half containing green as the target color. To distinguish lateral brain responses to target and distractor, only one of them can be presented in a lateralized manner. Thus, if the target was presented on one of the three outer left or right columns, the distractor was presented on the vertical meridian or vice versa. In the MEG, this leads to a lateralized target or distractor response, respectively. Lateral target and distractor trials varied in a pseudorandom order with 50% of the trials containing lateral target and central distractor and vice versa. Eccentricity of lateral target and distractor was counterbalanced, so that the stimuli were presented equally often at the different lateral positions. Each trial started with the presentation of a fixation cross for 1350 ms ( $\pm$  250 ms) followed by the search array was for 100 ms. Participants were asked to respond as fast as possible to the orientation of the target grating. Each of the six blocks contained 252 trials. In study 3, positions of the lateral distractors varied randomly, while in study 4 half of the blocks functioned as implicit learning blocks in a pseudorandomized block order. Previous studies have demonstrated that the interfering effect of distractors increases with their proximity to the target, resulting in slower reaction times, reduced discrimination performance, and increased  $P_D$  amplitude (Feldmann-Wüstefeld et al., 2021; Hickey & Theeuwes, 2011). Thus, to maximize measurable distractor suppression responses in study 4, I chose the lateral positions closest to the central target for the implicit learning account.

Specifically, to induce implicit learning of distractor locations, in 65 % of trials in implicit learning blocks the distractor was presented on one of the six locations closest to the vertical meridian if the target was presented centrally (see red ellipses in **Figure 12**). Since a higher magnitude of the  $P_D$  is thought to index stronger distractor suppression effects (Gaspar & McDonald, 2014; Gaspelin & Luck, 2018), I assumed that amplitudes of distractor suppression signals ( $P_D$  and HFA to lateralized distractors) for these locations should be higher in learning blocks compared to non-learning blocks if participants were able to build up stronger suppression effects at statistically learned locations (see **Chapter 3 Working Hypotheses**).

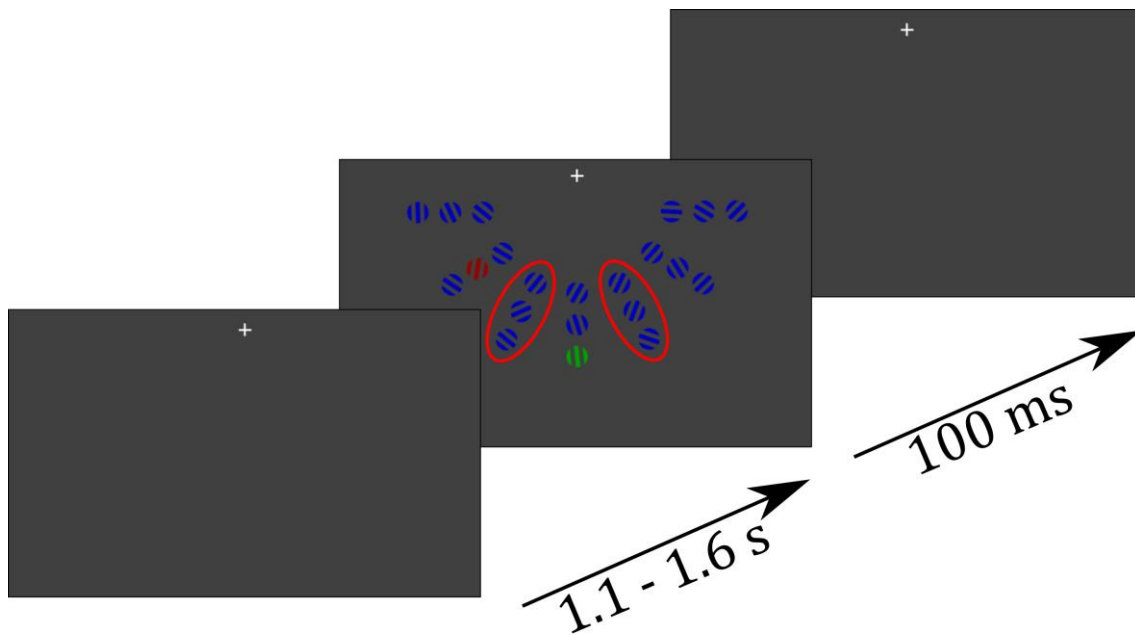


**Figure 12.** Example of a trial. Red ellipses (not visible during the study) mark distractor positions closest to the midline used for statistical learning in study 4. Participants were presented with a fixation cross for 1.1 – 1.6 s, followed by presentation of a search array, containing 19 nontargets, 1 target and one pop-out distractor for 100 ms. In each block the target color was changed between green and red. In blocks with the green grating serving as the target the red grating served as the pop-out distractor and vice versa. After presentation of the search array, participants responded via button press whether the target grating was oriented to the left or right.

### 5.2.3 Experience Sampling

In 20% of the trials in study 4 the stimulus array was followed by a thought probe in which participants were asked to rate their attentional focus (see **Chapter 2.5 Thought Probe Sampling**).

### 5.2.4 MEG Recordings

In both studies, I recorded MEG activity while participants were seated in a dimmed, magnetically shielded recording booth (see **Chapter 2.4 Apparatus**). To extract activity stemming from eye movement artifacts, I further recorded vertical and horizontal EOG data (see **Chapter 2.6 General Preprocessing**). In a subset of 23 participants in study 4, I also recorded participants' pupil data

using an Eye Tracker (see **Chapter 2.4 Apparatus**). Preparations and recording took about 2 hours.

### **5.2.5 Preprocessing and Artifact Rejection**

MEG, EEG and EOG data were preprocessed following the pipeline presented in *Chapter 2.3*. On average, 1.6 % of the trials in study 3 and 1.2 % in study 4 were rejected due to artifacts.

### **5.2.6 Statistical Analysis**

For statistical analysis, I conducted the following analysis steps. In study 3, I compared behavioral measures of reaction times and performance (percentage of correct responses) for lateral targets and distractors as well as for different target orientation angles. Furthermore, I analyzed behavioral responses as a function of the angular difference between target and distractor (*I – Behavioral Performance*). I then tested whether the  $N_T$  and  $P_D$  components varied with behavioral performance (*II –  $N_T$  and  $P_D$  Response*). Next, I identified MEG channels showing stimulus-related MEG-HFA response (*III – Broadband High Frequency Activity*) and tested whether the HFA response differed between lateral targets and distractors (*IV – HFA response to Targets and Distractors*). Following this, I compared the HFA response characteristics to lateral targets and distractors with their respective lower-frequency counterparts (*V – Comparison between HFA Response and  $N_T$  /  $P_D$  Response*). In an exploratory analysis, I finally tested whether lateral targets and distractors elicit a lateralized HFA response (*VI – Lateralized HFA Response*).

In study 4, I first examined the effect of the implicit learning manipulation on participants' performance. I compared performance in trials with lateral distractors between learning and non-learning conditions (*VII – Behavioral Consequences of Implicit Learning*). In a next step, I extracted the  $P_D$  and  $N_T$  components and identified MEG sensors showing a stimulus-related MEG-HFA response (*VIII – Stimulus Response*). I then extracted microsaccades from participants' eye movement data and compared the temporal evolution with the time course of  $P_D$ ,  $N_T$  and HFA responses (*IX – Temporal Evolution of Microsaccades*). In a following analysis, I tested whether the  $P_D$  and HFA to lateral distractors differed between learning and non-learning trials (*X – Amplitude Modulation with Experimental Condition*). In a final step, I investigated whether the HFA and the  $P_D$  and  $N_T$  components were modulated by the eccentricity of lateral target and distractor positions (*XI – Amplitude Modulation with Experimental Condition*).

In a subset of 25 participants from study 4, I tested whether MW impacts behavioral performance and neural correlates of selective attention. Five participants from the original data set had to be excluded since they did not report MW in at least one of the experimental conditions (lateral target, lateral distractor). On a behavioral level, I analyzed whether the ratio of participants' brain state reports changed throughout the experiment and whether reaction times and target

discrimination performance differed between brain states (*XII – Behavioral Consequences of Brain State Changes*). In a next step, I tested whether  $P_D$  and  $N_T$  amplitude differed between brain states (*XIII –  $P_D/N_T$  Amplitude Modulation with Brain States*).

To determine statistical significance of the grand average responses of  $N_T$ ,  $P_D$  and HFA, I compared the observed data against a surrogate distribution (see *Chapter 2.9 Surrogate Data Testing*).

### ***I – Behavioral Performance Study 3***

*Discrimination performance.* I compared performance between lateral and central targets and tested whether greater target orientation angles improved performance. Performance differences across target angles were evaluated using a one-way ANOVA with the factor stimulus angle (1.5° to 15° in 10 steps of 1.5°). To quantify the distractor effect, I assessed changes in target discrimination performance based on the angular difference between target and distractor orientation. I grouped performance for trials with low ( $\leq 7.5^\circ$ ) and high ( $\geq 9^\circ$ ) target angles and compared them using a *t*-test. To anticipate low and high target angles corresponds to subthreshold ( $< 70\%$ ; see *Results*) and suprathreshold performance ( $> 80\%$ ), respectively. Hence, in the following I use subthreshold and suprathreshold performance referring to low and high target angles, respectively. I then tested the distractor effect in high-angle targets since only targets with high angles allow strongest angular differences (e.g., a small target angle of 1.5° to the left would allow only for a maximal angular difference of 16.5° when the distractor is tilted 15° to the right). Angular differences between target and distractor, ranging from 0° to 30°, were divided in two halves (low vs. high, see *Results*). I averaged participants' performance for high target angles and compared them between low and high angular differences using a *t*-test.

*Reaction times.* I carried out the same analysis steps as for the performance comparisons. First, I compared reaction times between lateral targets and distractors using a one-way ANOVA. Post-hoc, I grouped reaction times for trials with subthreshold and suprathreshold performance target angles and compared them using a *t*-test. In a last step I averaged participants' reaction times for suprathreshold stimuli and compared them between low and high angular differences using a *t*-test.

### ***II – $N_T$ and $P_D$ Response Study 3***

The  $N_T/P_D$  response was determined in the following way (Boehler et al., 2011): For each participant, I averaged MEG data separately for trials with targets/distractors presented in the right and left visual field. The  $N_T/P_D$  was quantified in sensors showing strongest mean activity between 200 ms and 300 ms after stimulus presentation in corresponding efflux/influx zones. The signal of the sensor corresponding to the influx was subtracted from the signal of the sensors corresponding to the efflux. I then calculated the difference wave by subtracting MEG activity to

targets in the right visual field from targets in the left visual field. To better compare  $N_T$  and  $P_D$  responses, I presented both  $N_T$  and  $P_D$  data as a positive going responses (by inverting the sign of the  $N_T$  waveform), and for better comparison of the response characteristics of the lower-frequency components with the HFA, I z-standardized the  $N_T$  and  $P_D$  (see **Chapter 2.8 Extracting the Broadband High-Frequency Activity**). To assess the time range of significant  $N_T/P_D$  response, I compared each time point of the observed modulation between 100 and 400 ms with a surrogate distribution (see **Chapter 2.9 Surrogate Data Testing**).  $P$  values were then corrected for multiple comparisons, using the FDR method (Benjamini & Hochberg, 1995). Finally, I analyzed the relationship between participants'  $N_T/P_D$  amplitude and participants' performance using Pearson correlation coefficients, resulting in a time series of correlation coefficients. I also analyzed the relationship between participants'  $P_D$  amplitude and their performance using Pearson correlation coefficients. Finally, I compared mean  $N_T$  and  $P_D$  responses using a  $t$ -test to reveal possible differences in the neuronal response to lateralized targets and distractors in the lower-frequency components.

### **III – Broad Band High Frequency Activity Study 3**

The HFA response was identified following the procedure described in *Chapter 2.4*. To determine the time window of significant HFA modulation, I compared the HFA response at each observed time point to a surrogate distribution (see **Chapter 2.9 Surrogate Data Testing**).

### **IV – HFA Response to Targets and Distractors Study 3**

In a next step I tested whether the HFA distinguishes between lateral targets and distractors. I grouped HFA response for trials with lateral target and distractor. For both conditions (lateral target, lateral distractor), I determined the time interval of significant HFA amplitude modulation over baseline by comparing the HFA response at each observed time point with a surrogate distribution (see **Chapter 2.9 Surrogate Data Testing**). Afterwards, I compared mean HFA responses to lateral targets and distractors using  $t$ -tests. Since the HFA response is known to have a fast onset and a slowly decreasing flank (see **Chapter 1.2 Broadband High-frequency Activity**), I compared mean amplitudes of the increasing and decreasing HFA flank separately. To investigate the relationship between the participants' HFA amplitude and their performance, I calculated Pearson's correlation coefficients, resulting in a time series of correlation coefficients.

### **V – Comparison between HFA Response and $N_T/P_D$ Response Study 3**

To investigate how the HFA response characteristics relate to those of the lower-frequency bandpass counterparts ( $N_T$  and  $P_D$ ), I compared the correlation between HFA amplitude and performance with the correlation between the respective lower-frequency components amplitude and performance. I further analyzed possible latency differences between the HFA

response to lateral targets and the  $N_T$ , as well as between the HFA response to lateral distractors and the  $P_D$  by calculating participants' individual time points of peak response for each component and comparing them using *t*-tests. In a final step I analyzed the direct link between participants' mean HFA and lower-frequency component amplitudes by calculating the Pearson's correlation coefficient. I also tested whether HFA amplitude predicted  $P_D$  and  $N_T$  amplitude and calculated Pearson correlation coefficients between HFA amplitude at peak time point and  $P_D$  and  $N_T$  amplitude values at each time point separately. I compared these correlation coefficients with a surrogate distribution. In 1.000 iterations, I took the HFA and lower-frequency component values of the subjects at the time of the highest observed correlation, randomly reassigned the HFA and lower-frequency component values to the subjects and then calculated the Pearson correlation coefficient. Calculating the 99% Confidence Interval for the correlation coefficient resulted in a critical coefficient value. Correlation coefficients exceeding this critical value were considered as showing a significant correlation between HFA peak response and lower-frequency component amplitude. Finally, I used Williams *t*-test to determine whether the correlation coefficients of the HFA- $P_D$  correlation and the HFA- $N_T$  correlation differed from each other (Williams, 1959).

### ***VI – Lateralized HFA Response Study 3***

In an exploratory analysis, I investigated whether lateral targets and distractors elicit a lateralized HFA response. I first analyzed whether the grand average HFA showed a lateral response. I averaged HFA response over stimulus responsive channels (see *Statistical Analysis III – Broad Band High Frequency Activity*) located in the contralateral and ipsilateral hemispheres to the presented stimulus separately, resulting in a contralateral and ipsilateral time course of HFA response. To investigate whether HFA showed a lateral response like  $N_T$  and  $P_D$ , I separated trials for lateral target and distractor, resulting in separate contralateral and ipsilateral HFA responses for lateral target and distractor. I then compared mean contralateral and ipsilateral HFA responses using *t*-tests.

### ***VII – Behavioral Consequences of Implicit Learning Study 4***

*Discrimination Performance.* I compared performance (percentage of correctly reported target orientation) in trials with lateral distractors between learning and non-learning conditions. I compared performance for all trials and for trials where the distractor was presented at the position with the highest occurrence probability. I averaged participants' performance and compared it between learning and non-learning conditions using a *t*-test.

*Reaction Times.* I carried out the same analysis steps as for the performance comparisons.

**VIII – Stimulus Response Study 4**

The procedure to characterize the  $N_T$  and  $P_D$  response in study 4 followed the analysis steps for the  $N_T$  and  $P_D$  response in study 3 (see *Statistical Analysis II –  $N_T$  and  $P_D$  Response*). Analyzing the HFA response, I followed the steps to extract the HFA response in study 3 (see **Chapter 2.8 Extracting the Broadband High-Frequency Activity Response**).

**IX – Temporal Evolution of Microsaccades Study 4**

In study 4, I used the built-in function of the eye tracker to extract saccadic eye movements. For each participant, I first epoched the ongoing signal from 1 s preceding the stimulus presentation to 2 s after the presentation onset, resulting in a matrix containing information on the temporal evolution of saccadic eye movements for each trial. I then averaged the data across trials for each participant indicating how many saccadic events occurred on average at a given time point during the trials. Since I was interested in microsaccades, I only included saccades with an amplitude  $< 0.5^\circ$  va. In a final step, I compared the temporal evolution of microsaccades with the  $N_T$ ,  $P_D$  and HFA response. I calculated participants' time points of peak  $N_T$ ,  $P_D$  and HFA amplitude as well as the time points at which the most microsaccades occurred and compared peak microsaccade time points with peak  $N_T$ ,  $P_D$  and HFA time points separately using  $t$ -tests. Finally, I analyzed whether microsaccade rates differed between trials with lateral target and distractor by comparing mean microsaccade rates in the time range of the observed lower-frequency components using a  $t$ -test.

**X – Amplitude Modulation with Experimental Condition Study 4**

I then analyzed the effect of implicit learning on the  $P_D$  and  $N_T$  components and the HFA. I averaged  $P_D$ ,  $N_T$  and HFA activity for trials with the distractor (for  $P_D$  and HFA) and target (for  $N_T$ ) being presented on one of the six locations closest to the vertical meridian (see **Figure 12**) for learning and non-learning trials separately and analyzed possible differences between learning and non-learning trials in mean  $P_D$ ,  $N_T$  and HFA response separately using a  $t$ -test. Similar as in study 3 (see *Statistical Analysis IV – HFA Response to Targets and Distractors*), I compared mean amplitudes of the increasing and decreasing HFA flank separately. As I could only include a limited number of trials in the analysis of the implicit learning data due to the nature of my implicit learning approach, I z-standardized the  $P_D$ ,  $N_T$  and HFA time series (see *Statistical Analysis II –  $N_T$  and  $P_D$  Response*).

**XI – Amplitude Modulation with Stimulus Position Study 4**

In an additional analysis, I investigated the influence of the eccentricity of lateral targets and distractors on the lower-frequency  $P_D$  and  $N_T$  and the HFA amplitude. I grouped lateral stimulus positions in three columns (inner, middle, outer), depending on their distance to the vertical

meridian and averaged  $P_D$ ,  $N_T$  and HFA activity for trials with the distractor (for  $P_D$  and  $HFA_{\text{distractor}}$ ) and target (for  $N_T$  and  $HFA_{\text{target}}$ ) being presented on the three columns separately. I then analyzed possible  $P_D$  and  $N_T$  mean amplitude differences between the three columns using one-way ANOVAs with the factor column. For the HFA to lateral targets and distractors I analyzed possible mean amplitude differences between the three columns using 2x3 ANOVAs with the factors flank (increasing, decreasing) and column (inner, middle, outer).

## ***XII – Behavioral Consequences of Brain State Changes Study 5***

*Likelihood of brain states.* I tested whether the ratio of brain state reports changed over the experiment to rule out the possibility that changes in cortical dynamics are a result of a change across the experiment and not due to brain state fluctuations throughout the experiment. I averaged participant's brain state ratings for each block and compared the ratio of brain state ratings across the blocks using a 6 x 3 ANOVA with the factors block (I, II, III, IV, V, VI) and brain state (ON, MID, OFF).

*Target discrimination.* I compared participants' overall target discrimination performance between ON and OFF states using *t*-tests.

*Reaction times.* I ran the same analyses for reaction times as for target discrimination performance.

## ***XIII – $P_D/N_T$ Amplitude Modulation with Brain States Study 5***

Looking at neural correlates of selective attention, I identified time windows of significant grand average  $N_T$  and  $P_D$  response. In a next step, I analyzed whether mean  $N_T$  and  $P_D$  responses differ between ON and OFF states using *t*-tests.

## **5.3 Results**

### **Study 3**

#### ***I – Behavioral Performance Study 3***

*Discrimination performance.* Participants discriminated central targets better than lateral targets ( $M_{\text{central}} = 78.5\%$ ;  $M_{\text{lateral}} = 72.7\%$ ;  $t_{16} = 2.63$ ;  $P = .02$ ; see **Figure 13A**). A one-way ANOVA with the factor target orientation angle ( $1.5^\circ$  to  $15^\circ$  in 10 steps of  $1.5^\circ$ ) showed a significant main effect ( $F_{9,160} = 32.69$ ;  $P < .0001$ ) with higher orientation angles increasing performance (see **Figure 13A**). Post-hoc *t*-tests revealed that performance for trials with subthreshold ( $\leq 7.5^\circ$ ; see **Chapter 5.2.5 Statistical Analysis I – Behavioral Performance**) targets was lower than for suprathreshold ( $\geq 9^\circ$ ) targets ( $M_{\text{sub}} = 68.7\%$ ;  $M_{\text{supra}} = 82.3\%$ ;  $t_{16} = 19.75$ ;  $P < .0001$ ). I next tested whether the target-

distractor orientation angle difference modulated discrimination performance (see **Figure 13A**). I evaluated target discrimination performance by examining angular differences for suprathreshold targets ( $\geq 9^\circ$ ; see **Figure 13A**). I averaged performance for trials with low ( $< 13.5^\circ$ ) and high ( $> 16.5^\circ$ ) target-distractor angular difference, separately. I found a significant difference between low and high angular differences ( $M_{\text{low}} = 83.5\%$ ;  $M_{\text{high}} = 80.4\%$ ;  $t_{16} = 3.17$ ;  $P = .006$ ; see **Figure 13A**), with higher performance in low angular difference trials.

**Reaction times.** Reaction times did not differ between trials with lateral targets vs. lateral distractors ( $M_{\text{Target}} = 553$  ms  $M_{\text{Distractor}} = 566$  ms;  $t_{16} = 1.07$ ;  $P = .30$ ; see **Figure 13B**). A one-way ANOVA with the factor target orientation angle ( $1.5^\circ$  to  $15^\circ$  in 10 steps of  $1.5^\circ$ ) did not show an effect ( $F_{9,160} = 1.13$ ;  $P = .34$ ). In a next step, I averaged reaction times for suprathreshold target trials for low and high angular differences separately. I did not find any differences in reaction times between low and high angular differences ( $M_{\text{low}} = 536$  ms;  $M_{\text{high}} = 564$  ms;  $t_{16} = 1.16$ ;  $P = .26$ ; see **Figure 13B**).

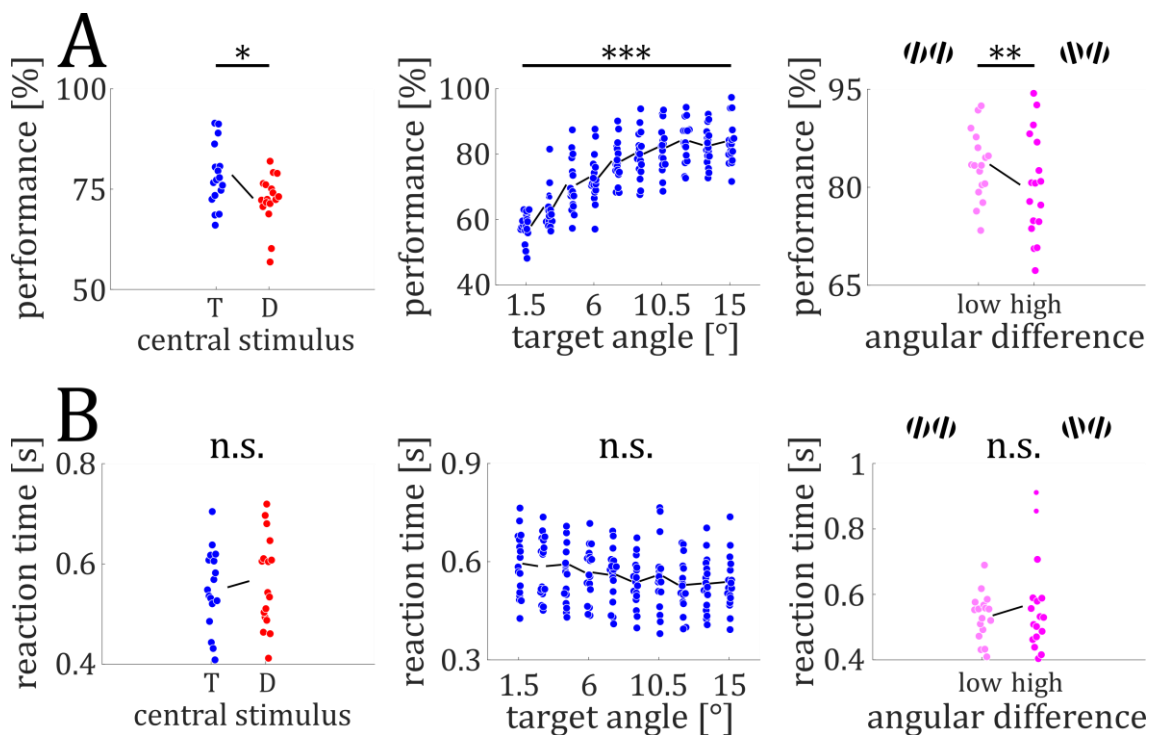


**Figure 13.** Behavioral Results Study 3. **A:** Participants discriminated central targets better than lateral targets (left). Performance increased with target orientation angle (middle). Performance for high target angle stimuli ( $9^\circ$  to  $15^\circ$ ) was higher for lower angular differences between target and distractor ( $0^\circ$  to  $13.5^\circ$ ) compared to higher angular differences ( $16^\circ$  to  $30^\circ$ ) (right). **B:** No differences in reaction times between trials with central target and distractor (left). No differences in reaction times between the different target orientation angles (middle). No differences in reaction times for high target angle stimuli between lower and higher angular differences (right). Colored circles represent single data points. \* =  $P < .05$ . \*\* =  $P < .01$ . \*\*\* =  $P < .0001$ .

### ***II – N<sub>T</sub> and P<sub>D</sub> Response Study 3***

Lateral targets elicited a N<sub>T</sub> response between 166 and 330 ms ( $z_{\text{crit}} = 3.47$ ;  $N_{T\text{max}} = 15.24$  at 258 ms; all  $P < .04$ ; see **Figure 14A**). Participants' performance was not correlated with N<sub>T</sub> amplitude, neither for the time resolved analysis ( $r_{\text{max}} = .40$  at 180 ms; all  $P > .11$ ; see **Figure 14A**), nor for correlation with N<sub>T</sub> averaged across the time interval of significant N<sub>T</sub> ( $r = .24$ ;  $P = .36$ ; see **Figure 14A**). Lateral distractors elicited a P<sub>D</sub> between 260 and 370 ms ( $z_{\text{crit}} = 1.43$ ;  $P_{D\text{max}} = 5.43$  at 320 ms; all  $P < .02$ ; see **Figure 14A**). The P<sub>D</sub> amplitude was not correlated with participants' performance either, neither in a time-resolved manner ( $r_{\text{max}} = .34$  at 324 ms; all  $P > .19$ ; see **Figure 14B**), nor for averaged P<sub>D</sub> response ( $r = .37$ ;  $P = .14$ ; see **Figure 14B**). I found the amplitude of the N<sub>T</sub> twice as large as the P<sub>D</sub> ( $M_{N_T} = 10.80$ ;  $M_{P_D} = 4.22$ ;  $t_{16} = 3.55$ ;  $p = .003$ ; see **Figure 14A**). Furthermore, the N<sub>T</sub> response ( $\sim 246$  ms;  $SD = 27$  ms) peaked significantly earlier compared to the P<sub>D</sub> response ( $\sim 328$  ms;  $SD = 23$  ms;  $t_{16} = 10.44$ ;  $P < .0001$ ).

### ***III – Broad Band High Frequency Activity Study 3***

A total of 18 occipital magnetometers showed a significant HFA response to lateral stimuli between 84 and 204 ms ( $z_{\text{crit}} = 0.85$ ;  $HFA_{\text{max}} = 2.73$  at 136 ms; all  $P$  values  $< .05$ ; see **Figure 14C**).

### ***IV – HFA Response to Targets and Distractors Study 3***

I found a significant HFA response to stimulus arrays containing a lateral target between 96 ms and 180 ms ( $z_{\text{crit}} = 0.57$ ;  $HFA_{\text{max}} = 1.76$  at 134 ms; all  $P < .05$ ; see **Figure 14D**) and a significant HFA response to lateral distractors between 92 and 206 ms ( $z_{\text{crit}} = 0.99$ ;  $HFA_{\text{max}} = 2.43$  at 142 ms; all  $P < .04$ ; see **Figure 14D**). The increasing flank (84 ms – 134 ms, see **Figure 14C**) of the HFA responses did not show differences between lateral targets and distractors ( $M_{\text{Target}} = 1.27$ ;  $M_{\text{Distractor}} = 1.84$ ;  $t_{16} = 1.73$ ;  $P = .10$ ). However, HFA amplitude of the decreasing flank (134 ms – 204 ms) was higher for lateral distractors compared to lateral targets ( $M_{\text{Target}} = 1.10$ ;  $M_{\text{Distractor}} = 1.92$ ;  $t_{16} = 2.31$ ;  $P = .035$ ; see **Figure 14D**).

### ***V – Comparison between HFA Response and N<sub>T</sub> / P<sub>D</sub> Response Study 3***

In a following step, I compared the response characteristics of the N<sub>T</sub> and P<sub>D</sub> with the HFA's response characteristics.

*HFA response to lateralized targets vs. N<sub>T</sub>.* While the N<sub>T</sub> was not correlated with performance, the HFA amplitude to lateral targets was correlated to individual performance both for the time resolved analysis ( $r_{\text{max}} = .67$  at 118 ms; all  $P < .0125$ ; see **Figure 14A**) and the averaged HFA to targets ( $r = .65$ ;  $P = .005$ ; see **Figure 14A**). The HFA<sub>target</sub> ( $\sim 174$  ms;  $SD = 70$  ms) peaked earlier than the N<sub>T</sub> ( $\sim 246$  ms;  $SD = 27$  ms;  $t_{16} = 3.72$ ;  $P = .002$ ; see **Figure 14E**). Neither mean, nor peak

HFA<sub>target</sub> response was correlated to mean ( $r = -.08$ ;  $P = .76$ ) and peak ( $r_{\max} = .33$  at 168 ms;  $P = .19$ ) N<sub>T</sub> response, respectively.

*HFA response to lateralized distractors vs. P<sub>D</sub>*. The HFA to lateral distractors (at ~ 142 ms;  $SD = 64$  ms) peaked earlier than the P<sub>D</sub> (~ 328 ms;  $SD = 23$  ms;  $t_{16} = 7.51$ ;  $P < .0001$ ; see **Figure 14F**). Both mean and peak HFA response were correlated to mean ( $r = .57$ ;  $P = .017$ ) and peak ( $r_{\max} = .64$  at 344 ms;  $P = .006$ ; see **Figure 14B**) P<sub>D</sub> response, respectively. The HFA amplitude to lateralized distractors, but not the P<sub>D</sub>, was correlated to performance (time-resolved analysis:  $r_{\max} = .74$  at 122 ms; all  $P < .0125$ ; average HFA amplitude:  $r = .70$ ;  $P = .002$ ; see **Figure 14B**). Williams *t*-test revealed a significant difference between the correlation coefficients of the HFA-N<sub>T</sub> ( $r = -.08$ ) and the HFA-P<sub>D</sub> ( $r = .57$ ) correlation ( $t_{14} = 2.16$ ;  $P = .049$ ), indicating that the HFA is significantly stronger correlated to the P<sub>D</sub> component compared to the N<sub>T</sub> component.

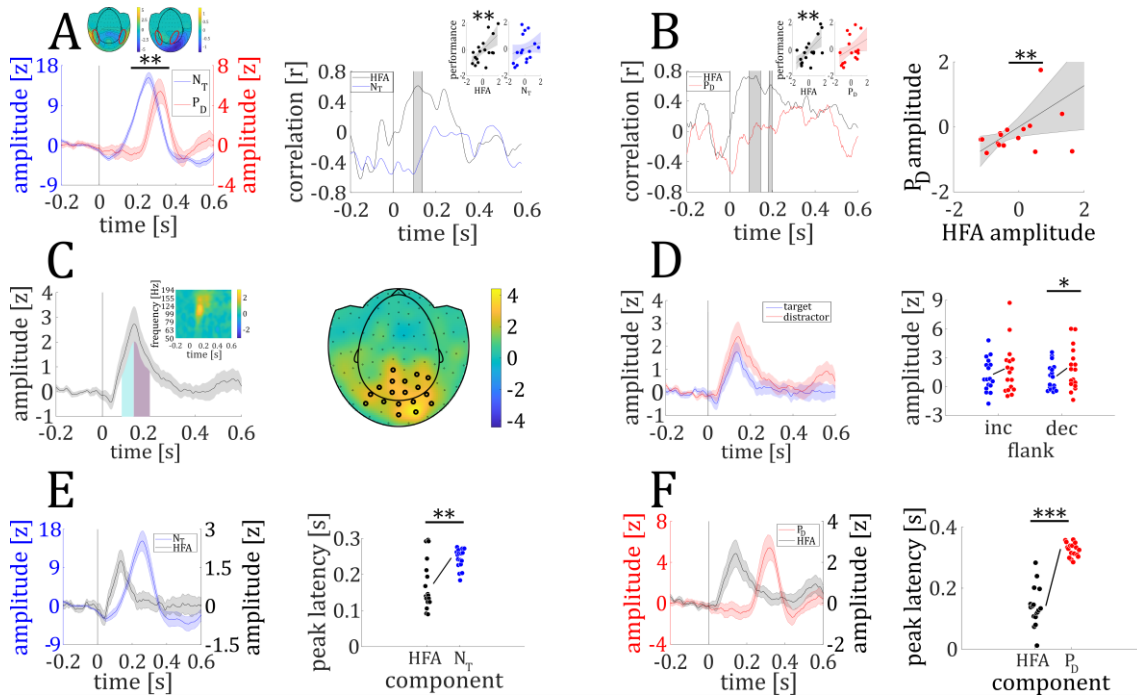


**Figure 14.** MEG Results Study 3. **A:** Time course of the N<sub>T</sub> (blue) and P<sub>D</sub> (red) responses to lateral targets and distractors, respectively (left panel). Mean amplitude of the N<sub>T</sub> response was higher compared to the P<sub>D</sub>. Upper left (N<sub>T</sub>) and right (P<sub>D</sub>) inset show the topographical distribution of MEG activity to lateral targets and distractors, respectively, with corresponding efflux / influx zones. Correlation coefficient at each time point between participants' HFA response to lateral targets (black) and their performance and between participants' N<sub>T</sub> (blue) and their performance (right panel). Insets show correlation coefficient between participants' performance and their mean HFA and N<sub>T</sub>, respectively. **B:** Correlation coefficient at each time point between participants' HFA response to lateral distractors (black) and their performance and between participants' P<sub>D</sub> (red) and their performance (left panel). Insets show the correlation between participants' performance and their mean HFA and P<sub>D</sub>, respectively. Maximal correlation between P<sub>D</sub> (at 344 ms) and peak HFA response (at 122 ms) (right panel). **C:** Time course of overall HFA response, showing time intervals of increasing (cyan) and decreasing (purple) flank (left panel) and its time-frequency representation (small inset). Topographical distribution of overall HFA response with sensors showing a significant response being highlighted (right panel). **D:** Time course of HFA response to lateral targets (blue) and distractors (red) (left panel). Individual mean HFA amplitude for lateral targets and distractors for the increasing and decreasing HFA flank (right panel). HFA amplitude of the decreasing flank was higher for

lateral distractors compared to targets. **E**: Time course for HFA to lateral targets (black) and  $N_T$  (blue) (left panel). Individual time points of peak HFA and  $N_T$  response (right panel). **F**: Time course for HFA to lateral distractors and  $P_D$  (third panel). Individual time points of peak HFA and  $P_D$  response (right panel). Colored circles represent single data points. Shaded colored lines represent the standard errors of the means (SEM). \* =  $P < .05$ . \*\* =  $P < .01$ . \*\*\* =  $P < .001$ .

### VI – Lateralized HFA response Study 3

Seven of the sensors showing a significant HFA modulation were located in the left hemisphere, while nine were located in the right hemisphere (see *Results III – Broadband High Frequency Activity*; see **Figure 15A**). When I compared mean contralateral and ipsilateral grand average HFA responses in the time range of the decreasing flank, I found a higher HFA response contralateral to the presented stimulus compared to ipsilateral ( $M_{\text{contra}} = 2.47$ ;  $M_{\text{ipsi}} = 1.64$ ;  $t_{16} = 2.22$ ;  $P = .04$ ; see **Figure 15B**). HFA response to lateral targets ( $t_{16} = 1.24$ ;  $P = .23$ ; see **Figure 15C**) and distractors ( $t_{16} = 0.61$ ;  $P = .55$ ; see **Figure 15D**) did not differ between contralateral and ipsilateral hemisphere.

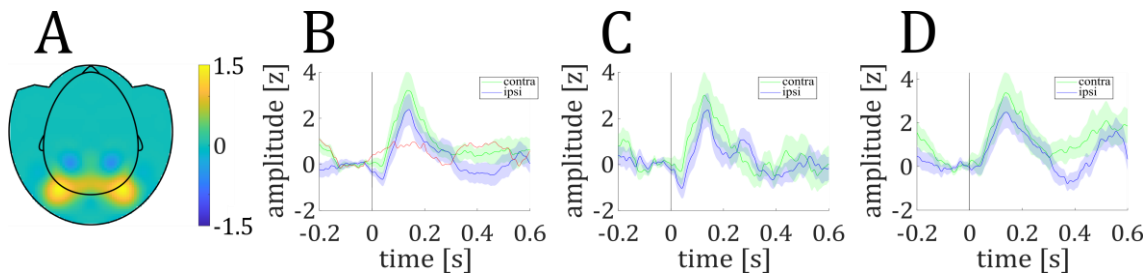


**Figure 15.** Lateralized HFA Response. **A**: Topographical distribution of overall HFA response (contralateral minus ipsilateral). **B**: Contralateral and ipsilateral HFA response to lateral stimuli (target and distractor). Red line shows the difference wave (contralateral minus ipsilateral). **C**: Contralateral and ipsilateral HFA response to lateral targets. **D**: Contralateral and ipsilateral HFA response to lateral distractors. Shaded colored lines represent the standard error of the means (SEM).

In sum, I found participants' behavioral performance to increase with increasing target angle and higher performance for trials with lower angular difference between target and distractor grating. I further found that the HFA response differed between lateral targets and distractors and was correlated to participants' individual performance and  $P_D$  amplitude.

### Study 4

#### VII – Behavioral Consequences of Implicit Learning Study 4

*Discrimination performance.* Performance did not differ between learning and non-learning blocks, neither for all lateral distractor trials ( $M_{\text{learning}} = 80.5\%$ ;  $M_{\text{non-learning}} = 80.2\%$ ;  $t_{29} = 0.19$ ;  $P = .85$ ), nor for trials where the distractor was presented at the position with the highest occurrence probability ( $M_{\text{learning}} = 80.4\%$ ;  $M_{\text{non-learning}} = 79.6\%$ ;  $t_{29} = 0.53$ ;  $P = .60$ ; see **Figure 16A**).

*Reaction times.* Reaction times did not differ between learning and non-learning blocks, neither for all lateral distractor trials ( $M_{\text{learning}} = 659$  ms;  $M_{\text{non-learning}} = 661$  ms;  $t_{29} = 0.55$ ;  $P = .59$ ), nor for trials where the distractor was presented at the position with the highest occurrence probability ( $M_{\text{learning}} = 660$  ms;  $M_{\text{non-learning}} = 663$  ms;  $t_{29} = 0.69$ ;  $P = .50$ ; see **Figure 16A**).

#### VIII – Stimulus Response Study 4

In study 4, lateral targets elicited a  $N_T$  response between 154 and 328 ms ( $z_{\text{crit}} = 1.17$ ;  $N_{T\text{max}} = 7.74$  at 244 ms; all  $P < .05$ ; see **Figure 16B**), while lateral distractors elicited a  $P_D$  response between 234 and 362 ms ( $z_{\text{crit}} = 0.59$ ;  $P_{D\text{max}} = 4.29$  at 298 ms; all  $P < .003$ ; see **Figure 16B**). Furthermore, the  $N_T$  showed a stronger modulation than the  $P_D$  response ( $M_{N_T} = 5.44$ ;  $M_{P_D} = 2.97$ ;  $t_{29} = 4.63$ ;  $P = .00007$ ; see **Figure 16B**) and peaked earlier than the  $P_D$  ( $N_T \sim 215$  ms,  $SD = 22$  ms;  $P_D \sim 301$  ms,  $SD = 27$  ms;  $t_{24} = 12.75$ ;  $P < .000001$ ).

A total of 14 occipital magnetometers showed a significant HFA response between 68 and 210 ms ( $z_{\text{crit}} = 0.60$ ;  $HFA_{\text{max}} = 4.22$  at 122 ms; all  $P$  values  $< .05$ ; see **Figure 16B**).

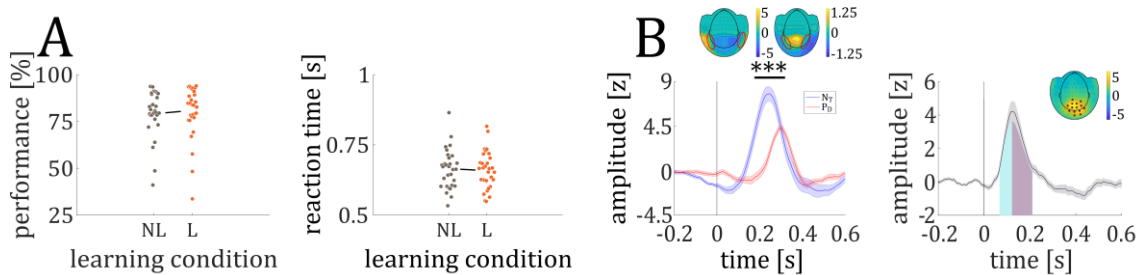


**Figure 16.** Behavioral Results and Grand Average Data. **A:** Performance (left) and reaction times (right) did not differ between learning and non-learning trials. **B:** Time course of the  $N_T$  (blue) and  $P_D$  (red) grand average responses to lateral targets and distractors, respectively (left). The  $N_T$  response was higher compared to the  $P_D$  response. Upper left ( $N_T$ ) and right ( $P_D$ ) inset show the topographical distribution of MEG activity to lateral targets and distractors, respectively, with corresponding efflux / influx zones. Time course of overall HFA response, showing time intervals of increasing (cyan) and decreasing (purple) flank (right). Topographical distribution of overall HFA response with sensors showing a significant response being highlighted (small inset). Colored circles represent single data points. Shaded colored lines represent the standard error of the means (SEM). \*\*\* =  $P < .0001$ .

#### IX – Temporal Evolution of Microsaccades Study 4

Comparing peak latency times between microsaccades, HFA and the lower-frequency bandpass signals, I found no difference in peak times between microsaccades and  $N_T$  ( $\text{microsaccades}_{\text{peak}} = 215$  ms;  $N_{T\text{peak}} = 251$  ms;  $t_{22} = 0.98$ ;  $P = .34$ ), but the  $P_D$  peaked later than microsaccades ( $P_{D\text{peak}} = 304$  ms;  $t_{22} = 2.39$ ;  $P = .026$ ). In contrast I found that HFA precedes microsaccades ( $\text{microsaccades}_{\text{peak}} = 215$  ms;  $HFA_{\text{peak}} = 131$  ms;  $t_{22} = 2.40$ ;  $P = .025$ ; see **Figure 17A**).

I found more microsaccades to lateral targets compared to distractors ( $M_{\text{Target}} = 0.0004$ ;  $M_{\text{Distractor}} = 0.00003$ ;  $t_{22} = 2.20$ ;  $P = .038$ ; see **Figure 17B**), indicating that differences in amplitude

modulation of  $N_T$  ( $M = 5.44$ ) and  $P_D$  ( $M = 2.97$ ) might at least in part be explained by differences in microsaccade rate.

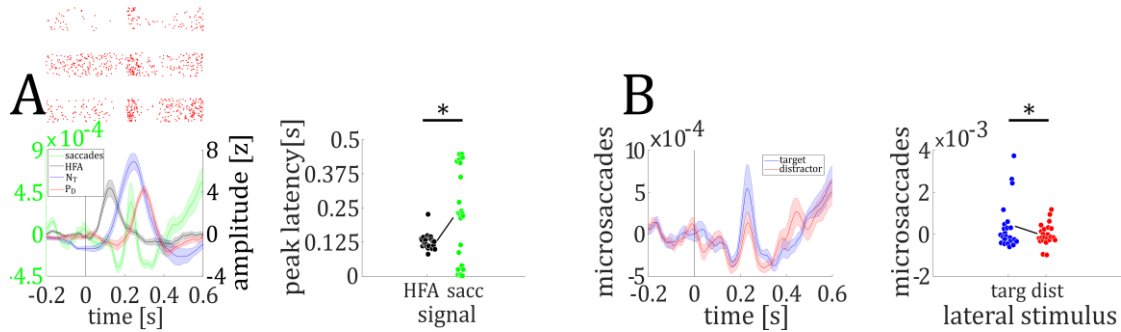


**Figure 17.** Temporal Evolution of Microsaccades. **A:** Time course of microsaccadic eye movements ( $< 0.5^\circ$  va), HFA,  $N_T$  and  $P_D$  response (left). Red dots mark single microsaccadic events of three example participants (upper inset, 3 rows). Individual time points of peak HFA and microsaccade response (right). **B:** Time course of microsaccades to lateral targets and distractors (left). Individual mean microsaccade rate to lateral targets and distractors (right). Colored circles represent single data points. Shaded colored lines represent the standard error of the means (SEM). \* =  $P < .05$ .

#### ***X – Amplitude Modulation with Experimental Condition Study 4***

Comparing mean  $P_D$  responses between learning and non-learning trials for distractors located close to the midline (marked positions in **Figure 12**), I found a higher  $P_D$  response in learning trials compared to non-learning trials ( $M_{\text{learning}} = 1.74$ ;  $M_{\text{non-learning}} = 0.97$ ;  $t_{29} = 2.88$ ;  $P = .007$ ; see **Figure 18A**). The  $N_T$ , showed no difference between learning and non-learning trials ( $M_{\text{learning}} = 2.17$ ;  $M_{\text{non-learning}} = 2.09$ ;  $t_{29} = 0.30$ ;  $P = .77$ ), which was expected since the statistical probability of the target locations was identical for learning and non-learning blocks.

While the increasing flank of the HFA (68 – 122 ms) showed no significant difference between learning and non-learning trials ( $M_{\text{learning}} = 1.08$ ;  $M_{\text{non-learning}} = 0.73$ ;  $t_{29} = 1.44$ ;  $P = .16$ ), I found the decreasing flank of the HFA (122 – 210 ms) in learning trials to be increased in amplitude compared to non-learning trials ( $M_{\text{learning}} = 1.07$ ;  $M_{\text{non-learning}} = 0.61$ ;  $t_{29} = 2.06$ ;  $P = .0485$ ; see **Figure 18B**).

#### ***XI – Amplitude Modulation with Stimulus Position Study 4***

While mean  $N_T$  response did not differ between the three lateral columns ( $F_{2,87} = 0.04$ ;  $P = .96$ ),  $P_D$  amplitude increased with proximity between the lateral distractor and central target ( $F_{2,87} = 3.91$ ;  $P = .02$ ).

Similar to the  $N_T$  component, the HFA to lateral targets was not modulated by lateral target position (main effect column:  $F_{2,174} = 1.43$ ;  $P = .24$ ). A 2x3 ANOVA analyzing the increasing and decreasing flank of the HFA to lateral targets between the three lateral distractor columns

revealed a marginally significant main effect of column ( $F_{2,174} = 2.71$ ;  $P = .07$ ), indicating a trend of increasing HFA with proximity between the lateral distractor and central target.

While I found no behavioral consequences of implicit learning on participants' performance, I found the  $P_D$  and the HFA to lateral distractors to be increased during blocks of implicit learning. Amplitude of  $P_D$  and HFA to lateral distractors increased with closer proximity to the central target, regardless of learning condition. Analyzing eye movement data, we found that microsaccades ( $< 0.5^\circ$ ) occurred after the HFA, but in the time range of  $N_T$  and  $P_D$  components. Additionally, the rate of microsaccades increased in trials with a lateral target compared to lateral distractor.

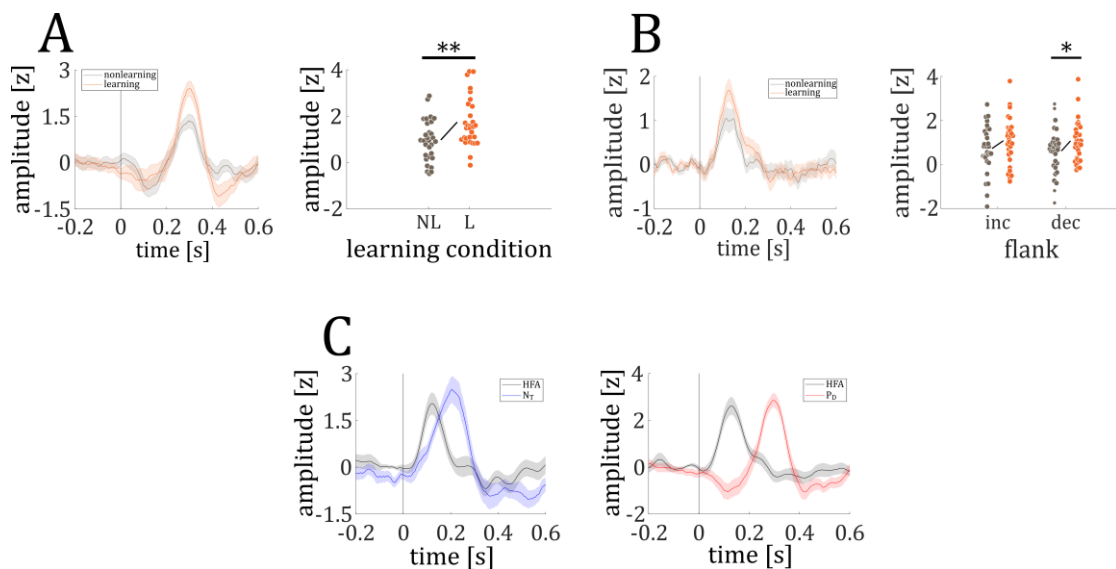


**Figure 18.** Modulation of Neural Response by Implicit Learning. **A:** Time course of  $P_D$  response in learning and non-learning condition (left). Individual mean  $P_D$  amplitude for learning and non-learning trials, for distractors close to the midline. Mean  $P_D$  response was higher in learning compared to non-learning trials (right). **B:** Time course of HFA response in learning and non-learning condition (left). Individual mean HFA amplitude for learning and non-learning trials for the increasing and decreasing HFA flank (right). HFA amplitude of the decreasing flank was higher for learning trials compared to non-learning trials. **C:** Time course of  $N_T$  (blue) and HFA (black) response to lateral targets presented on the inner column (left). Time course of  $P_D$  (red) and HFA (black) response to lateral distractors presented on the inner column (right). Colored circles represent single data points. Shaded colored lines represent the standard error of the means (SEM). \* =  $P < .05$ . \*\* =  $P < .01$ .

## XII – Behavioral Consequences of Brain State Changes Study 5

*Likelihood of brain states.* The  $6 \times 3$  ANOVA with the factors block (I, II, III, IV, V, VI) and brain state (ON, MID, OFF) showed a significant main effect of brain state ( $F_{2, 414} = 39.42$ ;  $P < .00001$ ; see **Figure 19**). However, I found no significant main effect of block ( $F_{5, 414} = 0.38$ ;  $P = .86$ ), nor interaction effect ( $F_{10, 414} = 0.72$ ;  $P = .71$ ). Post-hoc  $t$ -tests revealed that participants reported more often to be ON task ( $M = 45.5\%$ ) compared to OFF task ( $M = 25.1\%$ ;  $t_{24} = 2.86$ ;  $P = .009$ ) and MID

( $M = 29.0\%$ ;  $t_{24} = 2.84$ ;  $P = .009$ ), but no differences were found between MID and OFF reports ( $t_{24} = 0.75$ ;  $P = .46$ ). These results indicate that brain states differed in their frequency, but that this pattern did not change throughout the experiment.

*Target discrimination.* Participants' overall performance differed between brain states with higher performance during ON ( $M = 80.25\%$ ) than OFF trials ( $M = 74.78\%$ ;  $t_{24} = 3.00$ ;  $P = .006$ ; see **Figure 19**).

*Reaction times.* Participants' overall reaction times differed between brain states with longer reaction times during OFF ( $M = 684$  ms) than ON trials ( $M = 662$  ms;  $t_{24} = 2.71$ ;  $P = .01$ ; see **Figure 19**).

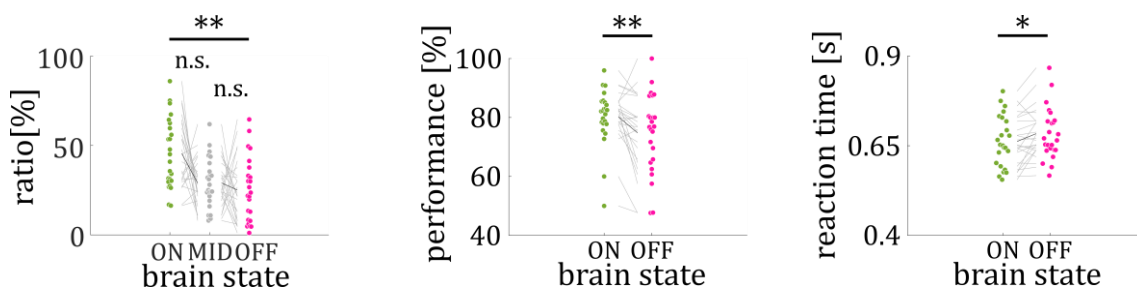


**Figure 19.** Behavioral Results. Brain state reports differed with more ON state than OFF state reports (left). Reaction times changed with brain states with slowest responses during OFF trials (middle). Subjects made most errors during OFF trials (right). Colored circles represent single data points. \* =  $P < .05$ . \*\* =  $P < .01$ .

### XIII – $P_D/N_T$ Amplitude Modulation with Brain States Study 5

*Grand average  $N_T/P_D$  response.* Lateral targets elicited a significant  $N_T$  response between 134 and 288 ms ( $N_{Tcrit} = 11.57$  fT;  $N_{Tmax} = 66.06$  fT at 216 ms; all  $P < .05$ ; see **Figure 20A**), while lateral distractors elicited a  $P_D$  response between 230 and 350 ms ( $P_{Dcrit} = 4.26$  fT;  $P_{Dmax} = 23.62$  fT at 290 ms; all  $P < .05$ ; see **Figure 20A**). In line with the previous results, the  $N_T$  showed a higher amplitude modulation ( $M_{NT} = 44.30$  fT;  $M_{PD} = 17.22$  fT;  $t_{24} = 6.54$ ;  $P < .000001$ ) and peaked earlier than the  $P_D$  ( $N_T \sim 222$  ms,  $SD = 35$  ms;  $P_D \sim 290$  ms,  $SD = 36$  ms;  $t_{24} = 6.27$ ;  $P < .000001$ ).

*$N_T/P_D$  modulation with brain states.* While  $N_T$  amplitude did not vary between brain states ( $M_{ON} = 67.40$  fT;  $M_{OFF} = 87.74$  fT;  $t_{24} = 1.45$ ;  $P = .16$ ; see **Figure 20B**),  $P_D$  amplitude was higher during OFF ( $M = 70.32$  fT) compared to ON trials ( $M = 44.58$  fT;  $t_{24} = 2.43$ ;  $P = .024$ ; see **Figure 20C**).

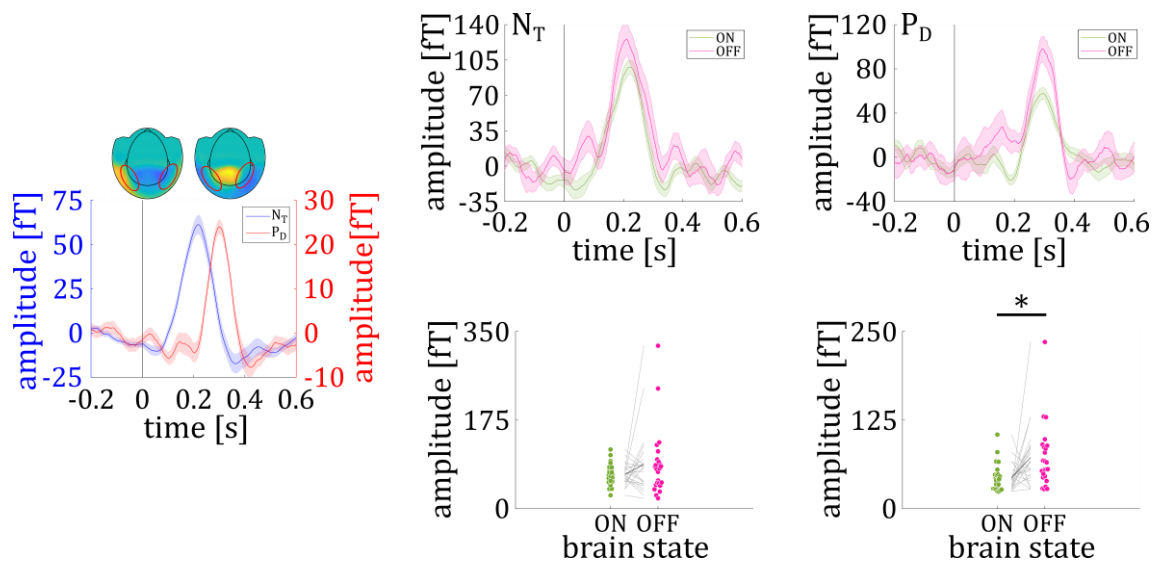


**Figure 20.** Neural Results. **A:** Time course of the  $N_T$  (blue) and  $P_D$  (red) grand average responses to lateral targets and distractors, respectively (left). The  $N_T$  response was higher and peaked earlier than the  $P_D$  response. Upper left ( $N_T$ ) and right ( $P_D$ ) inset show the topographical distribution of MEG activity to lateral targets and distractors, respectively, with corresponding efflux / influx zones. **B:**  $N_T$  time course for ON and OFF states (upper). Mean  $N_T$  amplitude did not differ between brain states (lower). **C:**  $P_D$  time course for ON and OFF states (upper). Mean  $P_D$  amplitude was higher during OFF compared to ON trials. Colored circles represent single data points. Shaded colored lines represent the standard error of the means (SEM). \* =  $P < .05$ .

## 5.4 Discussion

I examined whether broadband high-frequency activity (HFA) represents an early marker of spatial selective attention and distractor suppression by comparing the HFA response in the MEG to lower-frequency  $N_T$  and  $P_D$  components. I found that the HFA recorded at MEG sensors covering the occipital cortex distinguished between lateral targets and distractors with a higher amplitude to lateral distractors. The HFA preceded the lower-frequency components by more than 100 ms and was correlated to individual performance and  $P_D$  (but not  $N_T$ ) response. In a second study, I examined how implicit learning modulated the  $P_D$  and HFA responses and compared the time course of microsaccades to HFA,  $N_T$  and  $P_D$ . Both, the  $P_D$  and HFA to lateral distractors, increased in amplitude during implicit learning indicative of a trainable distractor suppression mechanism. Microsaccades peaked later than the HFA, but in the time range of the lower-frequency components. MW was associated with an enhanced  $P_D$  response, indicating more distractor suppression during MW. Taken together, these results indicate that the early visual HFA reflects the initial instance of effective distractor suppression.

In line with previous literature (Wienke et al., 2021), I found target discrimination to increase with increasing target stimulus angles. Indicative of a location-based effect, participants showed better performance and faster reaction times to central compared to lateral targets. This aligns with a previous study (Hilimire et al., 2011), which used search displays containing 16 letters, including targets (colored horizontal/upright 'T's), distractors (colored horizontal/upright 'L's),

and non-targets (gray horizontal 'T's). However, since target and distractor similarity did not vary systematically in their paradigm, they could not detect a feature-based distractor effect. In my study, performance increased with greater orientation similarity between target and distractor angle. However, reaction times did not change with target-distractor orientation difference, ruling out the interpretation of response interference (Maniscalco et al., 2012). These results indicate a feature-based distractor effect based on the angular difference between targets and distractors.

Both the  $N_T$  and  $P_D$  were elicited by lateral targets and distractors, respectively. In line with previous findings (Donohue et al., 2018; Drisdelle & Eimer, 2021; Hickey et al., 2009), I observed an  $N_T$  onset around 200 ms and a peak response around 250 ms after stimulus presentation. Critically, the  $P_D$  in my studies peaked later than the  $N_T$  (~80 ms), but showed the same topography as found in Donohue et al. (2018), resembling an inverted N2pc field with an efflux component over central occipital areas and an influx component at lateral occipital areas. Despite the differences in stimuli in previous studies, I found a similar relationship between  $N_T$  and  $P_D$  magnitude. Donohue et al. (2018) used a symmetric search array with T letters around a fixation cross, restricting the color-defined target or distractor to lateral positions. In line with their results, I found a stronger neural response to lateral targets ( $N_T$ ) than to lateral distractors ( $P_D$ ). Given that distractor suppression is an essential process, one might expect its neural correlate to be comparable with the target selection response. Previous work also suggests EEG/MEG amplitude modulation by microsaccades (Yuval-Greenberg et al., 2008). Lateral targets require a spatial shift of attention for successful discrimination, explaining the higher microsaccade rate to lateral targets (Rucci et al., 2007). The spikes elicited by the microsaccadic movements could then add to the MEG amplitude (Liu et al., 2023; Lowet et al., 2018). Microsaccades in my study peaked around 200 ms (Yuval-Greenberg et al., 2008), overlapping with lower-frequency components and explaining their field distribution (Carl et al., 2012; Liu et al., 2023). Since I observed more microsaccades to lateral targets than to lateral distractors, the higher  $N_T$  amplitude might partially be explained by microsaccades. These results further indicate that specifically lower-frequency responses might be influenced by microsaccadic eye movements. The late and reduced  $P_D$  in addition to fewer microsaccades compared to lateral target trials indicate that the suppression process has already been initiated earlier.

The HFA showed a stronger modulation to lateral distractors compared to targets. In line with a cortical “selection for rejection” mechanism (Bartsch et al., 2021; Donohue et al., 2018), the peak HFA predicted the strength of individual  $P_D$  (but not  $N_T$ ) responses. In Donohue et al (2018), the authors proposed the N1pc as an early marker for selection for rejection, peaking around the decreasing flank of the HFA in my study. However, in contrast to the HFA, the N1pc did not show differences in amplitude to lateral targets versus distractors and can thus be seen as a general

“attend-to-me” signal to salient items (Sawaki & Luck, 2010). Since the HFA was only correlated to the  $P_D$ , but not the  $N_T$ , the results suggest that the HFA represents a more selective “selection for rejection” mechanism and thus serves as an early marker of distractor suppression.

Aligning with previous findings (Feldmann-Wüstefeld et al., 2021; Hickey & Theeuwes, 2011), I found the  $P_D$  to increase with increasing proximity between target and distractor, while I did not find any modulation of  $N_T$  amplitude. In a modified version of the additional singleton task Feldmann-Wüstefeld et al. (2021) presented participants with a visual search display containing circular (nontargets and salient distractor) and diamond shaped stimuli (target), requiring participants to respond to the orientation of a line inside the target stimulus. Performance increased and  $P_D$  amplitude decreased with distance between target and distractor (Feldmann-Wüstefeld et al., 2021). The HFA to lateral distractors in my study shows a trend towards the same pattern with HFA amplitude numerically increasing with proximity between the central target and lateral distractor. These results further support the conclusion that the HFA is involved in distractor selection for suppression.

HFA has been the focus of studies using human intracranial recordings (Miller et al., 2014) but is only recently described in non-invasive recordings (Wienke et al., 2021). Similar to my first studies, the observed HFA response showed a fast onset prior to 100 ms, a peak response prior to 200 ms and a slowly decreasing flank, closely resembling the HFA observed in intracranial studies (Bartoli et al., 2019; Gerber et al., 2017; Golan et al., 2017; Vishne et al., 2023).

Previous studies investigating attentional modulation of neural activity primarily focused on broad gamma-bands between 30 and 130 Hz with mixed results (Tallon-Baudry et al. 2005; Davidesco et al. 2013; see **Chapter 1.2 High-Frequency Activity**). However, Szczepanski et al. (2014) investigated high-frequency modulation (> 80 Hz) during selective attention using intracranial recordings. Covertly attending to either the left or right visual field led to an increased HFA over visual areas, with ~20 % of electrodes exhibiting stronger HFA responses contralateral to the attended visual field. This is in line with my results of an increased HFA in MEG sensors contralateral to lateral stimuli.

In a recent study, Wienke et al. (2020) found the N2pc component to be increased in amplitude during periods of MW, indicating higher selective attention. This clearly contradicts the assumptions of the perceptual decoupling theory, according to which attention to external stimuli should be reduced during MW (Smallwood & Schooler, 2006). Since it is well known that selective attention and the N2pc can be divided into distinct processes of target enhancement ( $N_T$ ) and distractor suppression ( $P_D$ ), the question arises whether the enhanced N2pc in Wienke et al. (2020) was based on more target enhancement or distractor suppression during MW. My results

of an enhanced  $P_D$ , but not  $N_T$  amplitude during MW indicate that distractor suppression is increased during periods of MW. These results might be explained by an upregulation of attentional resources, particularly distractor suppression, since MW can be seen as a highly disruptive form of internal distraction (Forster, 2013).

A central finding of my study is that HFA is modulated by implicit learning, a relationship not yet demonstrated. Since spatial proximity between targets and distractors increases interference (Hickey & Theeuwes, 2011; Mathôt et al., 2010; Mounts, 2000), I increased the occurrence probability of distractors at positions close to the central targets to test whether the HFA/ $P_D$  responses could be modified by statistical learning. Detecting and learning statistical regularities in the environment does not necessarily always translate into enhanced behavioral performance (Conway & Christiansen, 2006; Fiser & Aslin, 2001; Siegelman et al., 2018). In line with these results, participants in my study showed no performance improvement, which can be attributed to the target orientation angles being too small to discriminate despite successful distractor suppression. However, I found increased amplitude of the HFA to lateral distractors and the later  $P_D$  during implicit statistical learning. In a previous study, van Moorselaar and Slagter (2019) found the  $P_D$  to be reduced during statistical learning. These conflicting results can be explained by several factors. First, in their study, the distractor was consistently presented at one specific location, whereas in my statistical learning blocks, it appeared more frequently at the six lateral locations closest to the vertical target. Consequently, the lateral distractor in my study still induced some interference due to its less predictable position. Second, repeated presentation of the distractor at a fixed location may induce a repetition suppression effect, characterized by reduced low-frequency (Grill-Spector et al., 2006) and high-frequency neural responses (Eckert et al., 2022). This is unlikely in my study, as HFA increased in the learning condition. Additionally, differences between learning and non-learning conditions cannot be attributed to closer proximity between target and distractor in the learning condition. These findings support the idea that HFA is a selection-for-rejection mechanism that is reinforced by statistical learning.

The findings of these studies extend prior work on the human HFA and spatial attention. The HFA distinguished between lateral targets and distractors and preceded the lower-frequency components by more than 100 ms. The HFA further predicted participants' performance and  $P_D$  response. These results indicate that the HFA is best suited to test the temporal evolution of stimulus discrimination as a key marker of successful subsequent distractor suppression.

## 6 General Discussion

This thesis encompasses five combined EEG/MEG studies, which investigated the neurophysiological basis of MW and its impact on visual attention in the human brain. For this purpose, I analyzed different ERP/ERF components (C1, HFA, N<sub>T</sub>, P<sub>D</sub>) while participants were engaged in visual attention tasks. MW is a common everyday phenomenon, occurring in 30 to 40% of waking hours, highlighting the need to investigate its underlying mechanisms and behavioral impact (Killingsworth & Gilbert, 2010). The perceptual decoupling theory predicts that during MW attention is shifted to the internal stream of thoughts and the brain is perceptually decoupled from the external environment (Schooler et al., 2011). To examine this, I investigated how MW affects different stages of visual processing using EEG and MEG recordings. Identifying the stages of visual processing affected by MW will enhance our understanding of its neural mechanisms and contribute to strategies for mitigating its negative effects.

### 6.1 Summary of Experimental Results

In the first two studies (see *Chapter 4 The HFA as a Feedforward or Feedback Signal*), I investigated whether the HFA in human visual cortex solely represents a feedforward mechanism and how it is modulated by MW. This investigation was motivated by two key findings: First, rodent research and intracranial recordings in epilepsy patients suggest that the visual HFA represents MUA (Bartoli et al., 2019; Ray et al., 2008), underpinning its role in input to visual cortex. Second, recent research emphasized the HFA's role in feedback loops to V1 (Leszczyński et al., 2020). The first study aimed to unravel the role of MEG-HFA in feedforward and feedback processing in V1. The second study focused on how the HFA is modulated with internal brain state changes.

**Hypothesis 1** proposed that **if HFA also measures for visual input, a critical assumption would be that HFA and C1 overlap in latency**. In the first study, I observed that the MEG-HFA onset and peak occurred later than the EEG-C1 response. Furthermore, only the C1 response – an established marker for initial sensory input to V1 – but not the HFA was modulated by small changes in the contrast level of visual stimuli. My results of an increasing C1 amplitude with increasing stimulus contrast support the notion that the C1 component reflects the physical properties of the external stimuli and reflects input to visual cortex (Gebodh et al., 2017). While the MEG-HFA in my study showed a similar time course as in previous intracranial investigations (Bartoli et al., 2019; Gerber et al., 2017; Golan et al., 2017; Vishne et al., 2023), I did not find contrast modulation of HFA amplitude (Bartoli et al., 2019). In line with a previous study investigating the HFA response and its relationship to MUA (Leszczyński et al., 2020), my results rather underpin the role of surface HFA in cortical feedback projections. Interactions between V1 and other cortical areas facilitate task-dependent and attentional modulation of V1 activity,

allowing the visual system to enhance relevant information while suppressing distractions (Muckli & Petro, 2013). Furthermore, a recent study found interactions between V1 and higher visual areas to be feedforward-dominated right after stimulus onset and gradually becoming feedback-dominated (~ 125 ms; Semedo et al., 2022), indicating corticocortical feedback projections to V1 in the time range of MEG-HFA. My results indicate that at least the decreasing flank of the HFA includes substantial feedback projections necessary for visual processing.

**Hypothesis 2** stated that **following the assumptions of the attentional decoupling theory, the HFA should be reduced in amplitude during episodes of MW**. Results of my second study showed that behavioral performance during MW was reduced compared to periods of focused attention with worse target discrimination accuracy and higher reaction times variation. While C1 amplitude remained unaffected by brain state changes, the HFA was reduced during periods of MW. While previous EEG studies have shown reduced sensory responses in the low-frequency range (< 30 Hz) during MW (Braboszcz & Delorme, 2011; Kam et al., 2011; Smallwood et al., 2008), to date no studies in humans or animals have demonstrated how the HFA response is modulated by MW. Here, I demonstrated that the decreasing flank of the HFA is reduced during MW, indicating that feedback processes are impaired during MW. Critically, in line with previous studies, reduction in HFA amplitude does not disrupt target discrimination (Vishne et al., 2023). Even though target discrimination was reduced during MW, participants were still able to maintain a high level of performance (~ 93%).

In sum, the findings of the first two studies provide novel evidence supporting the role of the HFA in feedforward and feedback processing in early visual cortex with feedback processes being modulated by inattentive states like MW.

In the subsequent three studies (see **Chapter 5 The HFA in Selective Attention**), I examined whether HFA serves as an early marker of spatial selective attention and distractor suppression and how these processes are modulated by implicit learning and MW. For this purpose, I compared response characteristics of lower-frequency target selection ( $N_T$ ) and distractor suppression ( $P_D$ ) components with the HFA.

**Hypothesis 3** predicted that **if the HFA serves as a marker for selective attention, it should show similar response characteristics as the lower-frequency  $N_T$  and  $P_D$  components and distinguish between lateral targets and distractors**. In the third study, HFA over occipital cortex distinguished between lateral targets and distractors and preceded the lower-frequency components. Furthermore, HFA was positively correlated with behavioral performance and  $P_D$ , but not  $N_T$  amplitude. These results indicate, that the HFA represents a selection for rejection mechanism (Bartsch et al., 2021; Donohue et al., 2018).

**Hypothesis 4** stated: **If the participants implicitly learned that the distractor is more likely presented close to the central target, the distractor suppression signals ( $P_D$  and HFA to lateral distractors) for these locations should be higher in learning blocks compared to non-learning blocks.** In the fourth study, implicit learning was associated with enhanced  $P_D$  and HFA responses. These findings support the idea that HFA is a selection-for-rejection mechanism that is reinforced by statistical learning. Furthermore, microsaccades peaked later than the HFA, in the time range of  $N_T$  and  $P_D$ . These findings suggest that low-frequency responses may be affected by microsaccadic eye movements. The delayed and attenuated  $P_D$ , along with fewer microsaccades compared to lateral target trials, indicate that the suppression process has likely been initiated earlier.

**Hypothesis 5** was based on findings of **Wienke et al. (2021)**, predicting that either  $N_T$ ,  $P_D$  or both would be enhanced during episodes of MW. In my final study, I found that periods of MW led to an enhanced  $P_D$  response, indicating more distractor suppression during MW. This is in line with a previous investigation, finding the  $N2pc$  component to be increased in amplitude during periods of MW (Wienke et al., 2021). These results clearly contradict the perceptual decoupling theory and indicate an adaptive reallocation of attentional resources during MW. The results might be explained by an upregulation of attentional resources to still be able to adequately perform on the task, since MW can be seen as a highly disruptive form of internal distraction.

Taken together, in this project I was able to establish the HFA in non-invasive MEG measurements as an important component of visual information processing, representing feedback information and distractor suppression, among others. Furthermore, my findings reveal that MW has no influence on the initial visual input, but impairs feedback processes like the HFA. Collectively, these results contribute to a more nuanced understanding of how internal brain states influence perceptual and attentional dynamics.

## **6.2 Limitations**

In this work I showed how MW affects different stages of visual information processing. However, it is important to note that investigating such a broad topic comes with certain limitations. Hence, in the following critical evaluation, I will discuss the limitations, serving to guide future research.

*Thought Probe Sampling.* Throughout this thesis, thought probes were used to assess whether participants were mind wandering or focused on the task at hand. Thought probes were presented to participants in 20% of the trials in a pseudorandom order. Thus, only a limited number of trials was included in the analyses, since I assumed that more thought probes would reduce the time for MW due to the sensitive nature of fluctuations of brain states (Seli et al., 2013). This critically leads to a reduction in statistical power since not all trials could be included in the analyses. I tried

to compensate for this and increased statistical power by grouping the five MW ratings in three groups of brain states (see *Chapter 2.5 Thought Probe Sampling*). Furthermore, results of a recently published study indicate that eight to ten thought probes are sufficient to gain reliable and valid information about the MW rates (Welhaf et al., 2022). Another issue that comes with the nature of thought probes is its subjective nature. When using thought probes researchers rely on the introspection of participants, which may lack from time to time. I don't use objective measurements of MW to categorize trials as MW-trials or focused attention trials. However, several studies showed robust correlations between thought probe measures and performance-related measures of MW (Cheyne et al., 2006; Christoff et al., 2009), as well as neural measures of MW like DMN activation (Christoff et al., 2009; Mittner et al., 2016). One could argue that these objective measures of MW again rely on subjective reports of participants about their brain state, making it a circular argument. However, these objective measures have been robustly shown over several studies and experimental paradigms.

*Mind Wandering Dimensions.* MW describes a brain state that occurs when an individual's thoughts become detached from a task at hand (Preiss et al., 2020). This broad definition includes various different dimensions of MW. For example, a MW episode can be deliberate or spontaneous, its' content can be future- or past-oriented. Deliberate and spontaneous MW can serve different goals, activate different brain regions (Golchert et al., 2017; Seli et al., 2015) and have different impacts on behavioral performance. Similarly, thought valence of a MW episode is a predictor for different mood states during MW (Gross et al., 2024; Sina & Plourde, 2020) and thus also affects brain activity and behavioral performance (Banks & Welhaf, 2022; Goller et al., 2020). This leads to the possibility, that different dimensions of MW got mixed together in this study. It would be desirable to split up MW episodes in those different detailed dimensions, but this is in conflict with the limited number of trials included in the MW analyses since it would lead to a further reduction in statistical power.

*Neural Generators.* It is widely accepted that the DMN is activated during periods of MW (Christoff et al., 2009). However, the DMN is also active during a wide range of different activities (Koshino et al., 2014; Smallwood et al., 2021) and there are also other brain regions active during MW (Christoff et al., 2009). Thus, it would be interesting to investigate which neural generators underlie the EEG and MEG-activity during MW recorded in my studies. While EEG and MEG provide a high temporal resolution, they lack in their spatial resolution, limiting the results of source analysis approaches. Recording fMRI activity while participants perform our experimental paradigms would provide us with a high temporal resolution, probably enabling us to pinpoint brain areas active during MW. However, fMRI has a temporal resolution of several seconds and in

a recent study we could show that participants' brain states transition within the time range of 2s. This rapid transition could potentially smear fMRI results.

*MW in daily life.* While researchers see the laboratory as a neutral and controlled place, it may feel unfamiliar or uncomfortable for participants, potentially inducing irregularities in their behavior and cognition (Rubin, 1989). This raises concerns about the extent to which laboratory findings can be generalized to real-world settings, particularly for subjective every day phenomena like MW. For instance, while working memory capacity (WMC) reliably predicts MW in the laboratory, this relationship turns out to be more nuanced in daily life (Kane et al., 2017). Specifically, WMC only predicts MW in situations when people have to control attention, such as when individuals are actively trying to concentrate (Kane et al., 2017). Similarly, while neuroticism predicts MW in the laboratory, openness is a stronger predictor of MW in daily life (Kane et al., 2017). Recent research suggests that MW in the laboratory describes a specific type of MW, more related to unintentional MW (Seli et al., 2016; Unsworth & McMillan, 2017). Consequently, the findings of this project can only be generalized to real-world experiences with caution.

### **6.3 Future Perspectives**

The intention of this project was to disentangle the neurophysiological signature of MW and its impact on different cognitive mechanisms. However, since the studies in this project cannot address all relevant aspects and consequences of MW, there remain questions important to answer in future investigations.

*Mind Wandering Dimensions.* Most studies investigating the impact of MW content on behavioral performance rely on retrospective reports of participants about how often certain contents appeared during MW episodes. This makes it hard to compare performance and neural correlates during different MW types on a within-subject level, since one can only compare participants that e.g. predominantly experience deliberate MW with those who engage in more spontaneous MW. To overcome this limitation, future studies should ask participants about their mind wandering during thought probes. A possible scenario would be to ask participants, after they indicated that they mind wandered, whether this MW episode was deliberate or spontaneous. This would require an enhanced number of trials per participant, since MW trials would further be divided into two conditions. However, with such an experimental design one would be able to compare neural correlates of for example distractor suppression between deliberate and spontaneous MW episodes. A similar approach could also be applied to examine the neural correlates of thought valence during MW.

*Neural Generators.* As previously discussed (see **Chapter 6.2 Limitations**), this study did not investigate the neural generators of the recorded brain responses. While fMRI has limited

temporal resolution for analyzing rapid neural dynamics, intracranial EEG (iEEG) in epilepsy patients offers both high temporal and spatial resolution. This approach could help determine whether the  $P_D$  component and HFA in distractor suppression originate from the same brain regions, further clarifying their relationship. Additionally, iEEG could provide insights into the neural generators of different types of MW during cognitive tasks. Activation of the DMN has been consistently associated with subjective reports of MW, highlighting its central role in the generation of task-unrelated thought (Christoff et al., 2009; Mittner et al., 2016). The DMN comprises brain regions like the posterior cingulate cortex, precuneus and angular gyrus (Broyd et al., 2009; Smallwood et al., 2021), which are predominantly located in posterior cortical areas. Notably these regions correspond spatially to the MEG sensors exhibiting a significant HFA response in my studies. It is therefore plausible that DMN activation in those regions during MW may affect the HFA response. Future investigations analyzing the HFA in those regions using iEEG recordings would shed light on the interplay between the DMN and HFA dynamics during MW. However, a key limitation of iEEG is that electrode placement must be predetermined based on a specific region of interest, as only a limited number of electrodes can be implanted per patient.

*MW in daily life.* Researchers must be careful when generalizing laboratory findings to real-world contexts, particularly for a subjective phenomenon like MW. Investigating neuronal dynamics of MW in real-life settings would provide valuable insights into its real-life manifestations and improve comparability with in-lab studies. However, current methods for acquiring high-quality EEG and MEG data outside the lab remain limited. A promising approach is the use of virtual reality, which can create immersive, ecologically valid environments while maintaining high-quality neural recordings. For instances, presenting participants with a virtual scenario that simulates everyday situations requiring selective attention – like focusing on a target stimulus while ignoring distracting stimuli – could offer a more realistic yet controlled framework for studying the neural correlates of MW in a context closely resembling daily life.

#### **6.4 General Conclusion**

Overall, this project provides critical insights into neurophysiological mechanisms underlying visual processing and selective attention, particularly in relation to HFA and MW. The findings establish the HFA in non-invasive MEG recordings as a key marker of both corticocortical feedback projections and distractor suppression, further highlighting its role in visual processing beyond feedforward mechanisms. While MW did not affect the initial sensory input to V1, it impaired feedback processing. However, MW was also associated with increased distractor suppression, challenging the perceptual decoupling hypothesis and suggesting an adaptive reallocation of attentional resources. Taken together, these studies contribute to a deeper understanding of how

MW and attentional dynamics affect visual perception, offering new insights on the functional role of HFA in cognitive neuroscience.

Despite these advances, several key questions remain for future research, like the differentiation of MW dimensions and their distinct neural correlates. Incorporating thought probes that directly ask participants to classify MW episodes in real-time, future research can characterize the relationship between MW dimensions and neural dynamics more precisely. Additionally, the neural generators of MW-related activity remain an open question, iEEG recordings could shed a light on.

By refining methodological approaches and leveraging advanced neuroimaging techniques, future research can further unravel the complex interplay between MW, attentional control, and neural processing, ultimately improving our understanding of how brain states influence perception and behavior.

**References**

- Abhang, P. A., Gawali, B. W., & Mehrotra, S. C. (2016). Chapter 2—Technological Basics of EEG Recording and Operation of Apparatus. In P. A. Abhang, B. W. Gawali, & S. C. Mehrotra (Hrsg.), *Introduction to EEG- and Speech-Based Emotion Recognition* (S. 19–50). Academic Press. <https://doi.org/10.1016/B978-0-12-804490-2.00002-6>
- Aine, C. J., Supek, S., George, J. S., Ranken, D., Lewine, J., Sanders, J., Best, E., Tjee, W., Flynn, E. R., & Wood, C. C. (1996). Retinotopic Organization of Human Visual Cortex: Departures from the Classical Model. *Cerebral Cortex*, *6*(3), 354–361. <https://doi.org/10.1093/cercor/6.3.354>
- Arita, J. T., Carlisle, N. B., & Woodman, G. F. (2012). Templates for rejection: Configuring attention to ignore task-irrelevant features. *Journal of Experimental Psychology: Human Perception and Performance*, *38*(3), 580–584. <https://doi.org/10.1037/a0027885>
- Baird, B., Smallwood, J., & Schooler, J. W. (2011). Back to the future: Autobiographical planning and the functionality of mind-wandering. *Consciousness and Cognition*, *20*(4), 1604–1611. <https://doi.org/10.1016/j.concog.2011.08.007>
- Banks, J. B., & Welhaf, M. S. (2022). Individual differences in dimensions of mind wandering: The mediating role of emotional valence and intentionality. *Psychological Research*, *86*(5), 1495–1517. <https://doi.org/10.1007/s00426-021-01579-2>
- Bartoli, E., Bosking, W., Chen, Y., Li, Y., Sheth, S. A., Beauchamp, M. S., Yoshor, D., & Foster, B. L. (2019). Functionally Distinct Gamma Range Activity Revealed by Stimulus Tuning in Human Visual Cortex. *Current Biology: CB*, *29*(20), 3345-3358.e7. <https://doi.org/10.1016/j.cub.2019.08.004>
- Bartsch, M. V., Merkel, C., Schoenfeld, M. A., & Hopf, J.-M. (2021). Attention expedites target selection by prioritizing the neural processing of distractor features. *Communications Biology*, *4*(1), 1–15. <https://doi.org/10.1038/s42003-021-02305-9>
- Baumgartner, H. M., Grauly, C. J., Hillyard, S. A., & Pitts, M. A. (2018). Does spatial attention modulate the earliest component of the visual evoked potential? *Cognitive Neuroscience*, *9*(1–2), 4–19. <https://doi.org/10.1080/17588928.2017.1333490>
- Benjamini, Y., & Hochberg, Y. (1995). Controlling the False Discovery Rate: A Practical and Powerful Approach to Multiple Testing. *Journal of the Royal Statistical Society: Series B (Methodological)*, *57*(1), 289–300. <https://doi.org/10.1111/j.2517-6161.1995.tb02031.x>
- Berger, H. (1929). Über das Elektrenkephalogramm des Menschen. *Archiv für Psychiatrie und Nervenkrankheiten*, *87*(1), 527–570. <https://doi.org/10.1007/BF01797193>

## REFERENCES

---

- Bertossi, E., Tesini, C., Cappelli, A., & Ciaramelli, E. (2016). Ventromedial prefrontal damage causes a pervasive impairment of episodic memory and future thinking. *Neuropsychologia*, *90*, 12–24. <https://doi.org/10.1016/j.neuropsychologia.2016.01.034>
- Bezudnaya, T., Cano, M., Bereshpolova, Y., Stoelzel, C. R., Alonso, J.-M., & Swadlow, H. A. (2006). Thalamic burst mode and inattention in the awake LGNd. *Neuron*, *49*(3), 421–432. <https://doi.org/10.1016/j.neuron.2006.01.010>
- Biasiucci, A., Franceschiello, B., & Murray, M. M. (2019). Electroencephalography. *Current Biology*, *29*(3), R80–R85. <https://doi.org/10.1016/j.cub.2018.11.052>
- Binder, J. R., Rao, S. M., Hammeke, T. A., Frost, J. A., Bandettini, P. A., & Hyde, J. S. (1994). Effects of stimulus rate on signal response during functional magnetic resonance imaging of auditory cortex. *Cognitive Brain Research*, *2*(1), 31–38. [https://doi.org/10.1016/0926-6410\(94\)90018-3](https://doi.org/10.1016/0926-6410(94)90018-3)
- Blackwood, D. H., & Muir, W. J. (1990). Cognitive brain potentials and their application. *The British Journal of Psychiatry*, *157*(Suppl 9), 96–101.
- Boehler, C. N., Tsotsos, J. K., Schoenfeld, M. A., Heinze, H.-J., & Hopf, J.-M. (2011). Neural mechanisms of surround attenuation and distractor competition in visual search. *The Journal of Neuroscience*, *31*(14), 5213–5224. <https://doi.org/10.1523/JNEUROSCI.6406-10.2011>
- Bombeke, K., Duthoo, W., Mueller, S. C., Hopf, J.-M., & Boehler, C. N. (2016). Pupil size directly modulates the feedforward response in human primary visual cortex independently of attention. *NeuroImage*, *127*, 67–73. <https://doi.org/10.1016/j.neuroimage.2015.11.072>
- Braboszcz, C., & Delorme, A. (2011). Lost in thoughts: Neural markers of low alertness during mind wandering. *NeuroImage*, *54*(4), 3040–3047. <https://doi.org/10.1016/j.neuroimage.2010.10.008>
- Brainard, D. H. (1997). The Psychophysics Toolbox. *Spatial Vision*, *10*(4), 433–436. <https://doi.org/10.1163/156856897X00357>
- Broyd, S. J., Demanuele, C., Debener, S., Helps, S. K., James, C. J., & Sonuga-Barke, E. J. S. (2009). Default-mode brain dysfunction in mental disorders: A systematic review. *Neuroscience and Biobehavioral Reviews*, *33*(3), 279–296. <https://doi.org/10.1016/j.neubiorev.2008.09.002>
- Brugge, J. F., Volkov, I. O., Oya, H., Kawasaki, H., Reale, R. A., Fenoy, A., Steinschneider, M., & Howard, M. A. (2008). Functional localization of auditory cortical fields of human: Click-train stimulation. *Hearing Research*, *238*(1), 12–24. <https://doi.org/10.1016/j.heares.2007.11.012>

- Budd, J. M. (1998). Extrastriate feedback to primary visual cortex in primates: A quantitative analysis of connectivity. *Proceedings of the Royal Society B: Biological Sciences*, 265(1400), 1037–1044.
- Buzsáki, G., & Draguhn, A. (2004). Neuronal oscillations in cortical networks. *Science (New York, N.Y.)*, 304(5679), 1926–1929. <https://doi.org/10.1126/science.1099745>
- Canolty, R. T., & Knight, R. T. (2010). The functional role of cross-frequency coupling. *Trends in Cognitive Sciences*, 14(11), 506–515. <https://doi.org/10.1016/j.tics.2010.09.001>
- Carl, C., Açıık, A., König, P., Engel, A. K., & Hipp, J. F. (2012). The saccadic spike artifact in MEG. *NeuroImage*, 59(2), 1657–1667. <https://doi.org/10.1016/j.neuroimage.2011.09.020>
- Chalk, M., Herrero, J. L., Gieselmann, M. A., Delicato, L. S., Gotthardt, S., & Thiele, A. (2010). Attention reduces stimulus-driven gamma frequency oscillations and spike field coherence in V1. *Neuron*, 66(1), 114–125. <https://doi.org/10.1016/j.neuron.2010.03.013>
- Cheyne, J. A., Carriere, J. S. A., & Smilek, D. (2006). Absent-mindedness: Lapses of conscious awareness and everyday cognitive failures. *Consciousness and Cognition*, 15(3), 578–592. <https://doi.org/10.1016/j.concog.2005.11.009>
- Cheyne, J. A., Solman, G. J. F., Carriere, J. S. A., & Smilek, D. (2009). Anatomy of an error: A bidirectional state model of task engagement/disengagement and attention-related errors. *Cognition*, 111(1), 98–113. <https://doi.org/10.1016/j.cognition.2008.12.009>
- Christoff, K., Gordon, A. M., Smallwood, J., Smith, R., & Schooler, J. W. (2009). Experience sampling during fMRI reveals default network and executive system contributions to mind wandering. *Proceedings of the National Academy of Sciences of the United States of America*, 106(21), 8719–8724. <https://doi.org/10.1073/pnas.0900234106>
- Clark, V. P., & Hillyard, S. A. (1996). Spatial Selective Attention Affects Early Extrastriate But Not Striate Components of the Visual Evoked Potential. *Journal of Cognitive Neuroscience*, 8(5), 387–402. <https://doi.org/10.1162/jocn.1996.8.5.387>
- Cohen, D. (1968). Magnetoencephalography: Evidence of Magnetic Fields Produced by Alpha-Rhythm Currents. *Science*, 161(3843), 784–786. <https://doi.org/10.1126/science.161.3843.784>
- Cohen, M. X. (2014). *Analyzing Neural Time Series Data: Theory and Practice*. The MIT Press. <https://doi.org/10.7551/mitpress/9609.001.0001>

- Compton, R. J., Shudrenko, D., Mann, K., Turdukulov, E., Ng, E., & Miller, L. (2024). Effects of task context on EEG correlates of mind-wandering. *Cognitive, Affective, & Behavioral Neuroscience*, *24*(1), 72–86. <https://doi.org/10.3758/s13415-023-01138-9>
- Conway, C. M., & Christiansen, M. H. (2006). Statistical Learning Within and Between Modalities: Pitting Abstract Against Stimulus-Specific Representations. *Psychological Science*, *17*(10), 905–912. <https://doi.org/10.1111/j.1467-9280.2006.01801.x>
- Dassanayake, T. L., Michie, P. T., & Fulham, R. (2016). Effect of temporal predictability on exogenous attentional modulation of feedforward processing in the striate cortex. *International Journal of Psychophysiology: Official Journal of the International Organization of Psychophysiology*, *105*, 9–16. <https://doi.org/10.1016/j.ijpsycho.2016.04.007>
- Davidesco, I., Harel, M., Ramot, M., Kramer, U., Kipervasser, S., Andelman, F., Neufeld, M. Y., Goelman, G., Fried, I., & Malach, R. (2013). Spatial and Object-Based Attention Modulates Broadband High-Frequency Responses across the Human Visual Cortical Hierarchy. *The Journal of Neuroscience*, *33*(3), 1228–1240. <https://doi.org/10.1523/JNEUROSCI.3181-12.2013>
- de Waard, J., van Moorselaar, D., Bogaerts, L., & Theeuwes, J. (2023). Statistical learning of distractor locations is dependent on task context. *Scientific Reports*, *13*(1), 11234. <https://doi.org/10.1038/s41598-023-38261-z>
- Di Russo, F., Martínez, A., & Hillyard, S. A. (2003). Source analysis of event-related cortical activity during visuo-spatial attention. *Cerebral Cortex (New York, N.Y.: 1991)*, *13*(5), 486–499. <https://doi.org/10.1093/cercor/13.5.486>
- Di Russo, F., Martínez, A., Sereno, M. I., Pitzalis, S., & Hillyard, S. A. (2002). Cortical sources of the early components of the visual evoked potential. *Human Brain Mapping*, *15*(2), 95–111. <https://doi.org/10.1002/hbm.10010>
- Di Russo, F., Stella, A., Spitoni, G., Strappini, F., Sdoia, S., Galati, G., Hillyard, S. A., Spinelli, D., & Pitzalis, S. (2012). Spatiotemporal brain mapping of spatial attention effects on pattern-reversal ERPs. *Human Brain Mapping*, *33*(6), 1334–1351. <https://doi.org/10.1002/hbm.21285>
- Dikanev, T., Smirnov, D., Wennberg, R., Velazquez, J. L. P., & Bezruchko, B. (2005). EEG nonstationarity during intracranially recorded seizures: Statistical and dynamical analysis. *Clinical Neurophysiology*, *116*(8), 1796–1807. <https://doi.org/10.1016/j.clinph.2005.04.013>
- Ding, Y., Martinez, A., Qu, Z., & Hillyard, S. A. (2014). Earliest stages of visual cortical processing are not modified by attentional load. *Human Brain Mapping*, *35*(7), 3008–3024. <https://doi.org/10.1002/hbm.22381>

- Donohue, S. E., Bartsch, M. V., Heinze, H.-J., Schoenfeld, M. A., & Hopf, J.-M. (2018). Cortical Mechanisms of Prioritizing Selection for Rejection in Visual Search. *The Journal of Neuroscience*, *38*(20), 4738–4748. <https://doi.org/10.1523/JNEUROSCI.2407-17.2018>
- Drisdelle, B. L., & Eimer, M. (2021). P<sub>D</sub> components and distractor inhibition in visual search: New evidence for the signal suppression hypothesis. *Psychophysiology*, *58*(9), e13878. <https://doi.org/10.1111/psyp.13878>
- Eckert, D., Reichert, C., Bien, C. G., Heinze, H.-J., Knight, R. T., Deouell, L. Y., & Dürschmid, S. (2022). Distinct interacting cortical networks for stimulus-response and repetition-suppression. *Communications Biology*, *5*(1), Article 1. <https://doi.org/10.1038/s42003-022-03861-4>
- Eimer, M. (1996). The N2pc component as an indicator of attentional selectivity. *Electroencephalography and Clinical Neurophysiology*, *99*(3), 225–234. [https://doi.org/10.1016/0013-4694\(96\)95711-9](https://doi.org/10.1016/0013-4694(96)95711-9)
- Epstein, J. N., Langberg, J. M., Rosen, P. J., Graham, A., Narad, M. E., Antonini, T. N., Brinkman, W. B., Froehlich, T., Simon, J. O., & Altaye, M. (2011). Evidence for higher reaction time variability for children with ADHD on a range of cognitive tasks including reward and event rate manipulations. *Neuropsychology*, *25*(4), 427–441. <https://doi.org/10.1037/a0022155>
- Farley, J., Risko, E., & Kingstone, A. (2013). Everyday attention and lecture retention: The effects of time, fidgeting, and mind wandering. *Frontiers in Psychology*, *4*. <https://doi.org/10.3389/fpsyg.2013.00619>
- Feldmann-Wüstefeld, T., & Vogel, E. K. (2019). Neural Evidence for the Contribution of Active Suppression During Working Memory Filtering. *Cerebral Cortex*, *29*(2), 529–543. <https://doi.org/10.1093/cercor/bhx336>
- Feldmann-Wüstefeld, T., Weinberger, M., & Awh, E. (2021). Spatially Guided Distractor Suppression during Visual Search. *The Journal of Neuroscience*, *41*(14), 3180–3191. <https://doi.org/10.1523/JNEUROSCI.2418-20.2021>
- Fiser, J., & Aslin, R. N. (2001). Unsupervised statistical learning of higher-order spatial structures from visual scenes. *Psychological Science*, *12*(6), 499–504. <https://doi.org/10.1111/1467-9280.00392>
- Forster, S. (2013). Distraction and Mind-Wandering Under Load. *Frontiers in Psychology*, *4*. <https://doi.org/10.3389/fpsyg.2013.00283>
- Foxe, J., & Simpson, G. (2002). Flow of activation from V1 to frontal cortex in humans. *Experimental Brain Research*, *142*(1), 139–150. <https://doi.org/10.1007/s00221-001-0906-7>

- Frost, R., Armstrong, B. C., & Christiansen, M. H. (2019). Statistical learning research: A critical review and possible new directions. *Psychological Bulletin*, *145*(12), 1128–1153. <https://doi.org/10.1037/bul0000210>
- Galka, A. (2000). *Topics in Nonlinear Time Series Analysis: With Implications for EEG Analysis* (Bd. 14). WORLD SCIENTIFIC. <https://doi.org/10.1142/4286>
- Gaspar, J. M., & McDonald, J. J. (2014). Suppression of Salient Objects Prevents Distraction in Visual Search. *Journal of Neuroscience*, *34*(16), 5658–5666. <https://doi.org/10.1523/JNEUROSCI.4161-13.2014>
- Gaspelin, N., Lamy, D., Egeth, H. E., Liesefeld, H. R., Kerzel, D., Mandal, A., Müller, M. M., Schall, J. D., Schubö, A., Slagter, H. A., Stilwell, B. T., & van Moorselaar, D. (2023). The Distractor Positivity Component and the Inhibition of Distracting Stimuli. *Journal of Cognitive Neuroscience*, *35*(11), 1693–1715. [https://doi.org/10.1162/jocn\\_a\\_02051](https://doi.org/10.1162/jocn_a_02051)
- Gaspelin, N., & Luck, S. J. (2018). Distinguishing among potential mechanisms of singleton suppression. *Journal of Experimental Psychology: Human Perception and Performance*, *44*(4), 626–644. <https://doi.org/10.1037/xhp0000484>
- Gebodh, N., Vanegas, M. I., & Kelly, S. P. (2017). Effects of Stimulus Size and Contrast on the Initial Primary Visual Cortical Response in Humans. *Brain Topography*, *30*(4), 450–460. <https://doi.org/10.1007/s10548-016-0530-2>
- Gerber, E. M., Golan, T., Knight, R. T., & Deouell, L. Y. (2017). Cortical representation of persistent visual stimuli. *NeuroImage*, *161*, 67–79. <https://doi.org/10.1016/j.neuroimage.2017.08.028>
- Golan, T., Davidesco, I., Meshulam, M., Groppe, D. M., Mégevand, P., Yeagle, E. M., Goldfinger, M. S., Harel, M., Melloni, L., Schroeder, C. E., Deouell, L. Y., Mehta, A. D., & Malach, R. (o. J.). Increasing suppression of saccade-related transients along the human visual hierarchy. *eLife*, *6*, e27819. <https://doi.org/10.7554/eLife.27819>
- Golchert, J., Smallwood, J., Jefferies, E., Seli, P., Huntenburg, J. M., Liem, F., Lauckner, M. E., Oligschläger, S., Bernhardt, B. C., Villringer, A., & Margulies, D. S. (2017). Individual variation in intentionality in the mind-wandering state is reflected in the integration of the default-mode, fronto-parietal, and limbic networks. *NeuroImage*, *146*, 226–235. <https://doi.org/10.1016/j.neuroimage.2016.11.025>
- Goller, H., Banks, J. B., & Meier, M. E. (2020). An individual differences investigation of the relations among life event stress, working memory capacity, and mind wandering: A preregistered

## REFERENCES

---

- replication-extension study. *Memory & Cognition*, 48(5), 759–771.  
<https://doi.org/10.3758/s13421-020-01014-8>
- Grill-Spector, K., Henson, R., & Martin, A. (2006). Repetition and the brain: Neural models of stimulus-specific effects. *Trends in Cognitive Sciences*, 10(1), 14–23.  
<https://doi.org/10.1016/j.tics.2005.11.006>
- Gross, M., Raynes, S., Schooler, J. W., Guo, E., & Dobkins, K. (2024). When is a wandering mind unhappy? The role of thought valence. *Emotion*. <https://doi.org/10.1037/emo0001434>
- Gutteling, T. P., Sillekens, L., Lavie, N., & Jensen, O. (2022). Alpha oscillations reflect suppression of distractors with increased perceptual load. *Progress in Neurobiology*, 214, 102285.  
<https://doi.org/10.1016/j.pneurobio.2022.102285>
- Hansen, P., Kringelbach, M., & Salmelin, R. (Hrsg.). (2010). *MEG: An Introduction to Methods*. Oxford University Press. <https://doi.org/10.1093/acprof:oso/9780195307238.001.0001>
- He, H., Li, Y., Chen, Q., Wei, D., Shi, L., Wu, X., & Qiu, J. (2021). Tracking resting-state functional connectivity changes and mind wandering: A longitudinal neuroimaging study. *Neuropsychologia*, 150, 107674. <https://doi.org/10.1016/j.neuropsychologia.2020.107674>
- Head, J., & Helton, W. S. (2013). Perceptual decoupling or motor decoupling? *Consciousness and Cognition*, 22(3), 913–919. <https://doi.org/10.1016/j.concog.2013.06.003>
- Helton, W. S. (2009). Impulsive responding and the sustained attention to response task. *Journal of Clinical and Experimental Neuropsychology*, 31(1), 39–47.  
<https://doi.org/10.1080/13803390801978856>
- Helton, W. S., Kern, R. P., & Walker, D. R. (2009). Conscious thought and the sustained attention to response task. *Consciousness and Cognition*, 18(3), 600–607.  
<https://doi.org/10.1016/j.concog.2009.06.002>
- Henze, D. A., Borhegyi, Z., Csicsvari, J., Mamiya, A., Harris, K. D., & Buzsáki, G. (2000). Intracellular Features Predicted by Extracellular Recordings in the Hippocampus In Vivo. *Journal of Neurophysiology*, 84(1), 390–400. <https://doi.org/10.1152/jn.2000.84.1.390>
- Hickey, C., Di Lollo, V., & McDonald, J. J. (2009). Electrophysiological indices of target and distractor processing in visual search. *Journal of Cognitive Neuroscience*, 21(4), 760–775.  
<https://doi.org/10.1162/jocn.2009.21039>

## REFERENCES

---

- Hickey, C., & Theeuwes, J. (2011). Context and competition in the capture of visual attention. *Attention, Perception, & Psychophysics*, *73*(7), 2053–2064. <https://doi.org/10.3758/s13414-011-0168-9>
- Hilimire, M. R., Mounts, J. R. W., Parks, N. A., & Corballis, P. M. (2011). Dynamics of target and distractor processing in visual search: Evidence from event-related brain potentials. *Neuroscience Letters*, *495*(3), 196–200. <https://doi.org/10.1016/j.neulet.2011.03.064>
- Hopf, J.-M., Luck, S. J., Girelli, M., Hagner, T., Mangun, G. R., Scheich, H., & Heinze, H.-J. (2000). Neural Sources of Focused Attention in Visual Search. *Cerebral Cortex*, *10*(12), 1233–1241. <https://doi.org/10.1093/cercor/10.12.1233>
- Huang, N. E., Shen, Z., Long, S. R., Wu, M. C., Shih, H. H., Zheng, Q., Yen, N.-C., Tung, C. C., & Liu, H. H. (1998). The empirical mode decomposition and the Hilbert spectrum for nonlinear and non-stationary time series analysis. *Proceedings of the Royal Society of London. Series A: Mathematical, Physical and Engineering Sciences*, *454*(1971), 903–995. <https://doi.org/10.1098/rspa.1998.0193>
- Iemi, L., Busch, N. A., Laudini, A., Haegens, S., Samaha, J., Villringer, A., & Nikulin, V. V. (2019). Multiple mechanisms link prestimulus neural oscillations to sensory responses. *eLife*, *8*, e43620. <https://doi.org/10.7554/eLife.43620>
- Indic, P., Pratap, R., Nampoore, V. P. N., & Pradhan, N. (1999). Significance of Time Scales in Nonlinear Dynamical Analysis of Electroencephalogram Signals. *International Journal of Neuroscience*, *99*(1–4), 181–194. <https://doi.org/10.3109/00207459908994323>
- Kam, J. W. Y., Dao, E., Farley, J., Fitzpatrick, K., Smallwood, J., Schooler, J. W., & Handy, T. C. (2011). Slow Fluctuations in Attentional Control of Sensory Cortex. *Journal of Cognitive Neuroscience*, *23*(2), 460–470. <https://doi.org/10.1162/jocn.2010.21443>
- Kane, M. J., Gross, G. M., Chun, C. A., Smeekens, B. A., Meier, M. E., Silvia, P. J., & Kwapil, T. R. (2017). For Whom the Mind Wanders, and When, Varies Across Laboratory and Daily-Life Settings. *Psychological Science*, *28*(9), 1271–1289. <https://doi.org/10.1177/0956797617706086>
- Karnath, H.-O., & Thier, P. (Hrsg.). (2012). *Kognitive Neurowissenschaften*. Springer. <https://doi.org/10.1007/978-3-642-25527-4>
- Kelly, S. P., Gomez-Ramirez, M., & Foxe, J. J. (2008). Spatial attention modulates initial afferent activity in human primary visual cortex. *Cerebral Cortex (New York, N.Y.: 1991)*, *18*(11), 2629–2636. <https://doi.org/10.1093/cercor/bhn022>

- Killingsworth, M. A., & Gilbert, D. T. (2010). A Wandering Mind Is an Unhappy Mind. *Science*, *330*(6006), 932–932. <https://doi.org/10.1126/science.1192439>
- Kleiner, M. (o. J.). *What's new in Psychtoolbox-3?* 89.
- Koshino, H., Minamoto, T., Yaoi, K., Osaka, M., & Osaka, N. (2014). Coactivation of the Default Mode Network regions and Working Memory Network regions during task preparation. *Scientific Reports*, *4*(1), 5954. <https://doi.org/10.1038/srep05954>
- Kraut, M. A., Arezzo, J. C., & Vaughan, H. G. (1985). Intracortical generators of the flash VEP in monkeys. *Electroencephalography and Clinical Neurophysiology/Evoked Potentials Section*, *62*(4), 300–312. [https://doi.org/10.1016/0168-5597\(85\)90007-3](https://doi.org/10.1016/0168-5597(85)90007-3)
- Kunhimangalam, R., Joseph, P. K., & Sujith, O. K. (2008). Nonlinear analysis of EEG signals: Surrogate data analysis. *IRBM*, *29*(4), 239–244. <https://doi.org/10.1016/j.rbmret.2007.09.006>
- Lachaux, J.-P., Axmacher, N., Mormann, F., Halgren, E., & Crone, N. E. (2012). High-frequency neural activity and human cognition: Past, present and possible future of intracranial EEG research. *Progress in neurobiology*, *98*(3), 279–301. <https://doi.org/10.1016/j.pneurobio.2012.06.008>
- Lakatos, P., Chen, C.-M., O'Connell, M. N., Mills, A., & Schroeder, C. E. (2007). Neuronal Oscillations and Multisensory Interaction in Primary Auditory Cortex. *Neuron*, *53*(2), 279–292. <https://doi.org/10.1016/j.neuron.2006.12.011>
- Lamme, V. A. (1995). The neurophysiology of figure-ground segregation in primary visual cortex. *The Journal of Neuroscience: The Official Journal of the Society for Neuroscience*, *15*(2), 1605–1615. <https://doi.org/10.1523/JNEUROSCI.15-02-01605.1995>
- Le Van Quyen, M., Foucher, J., Lachaux, J.-P., Rodriguez, E., Lutz, A., Martinerie, J., & Varela, F. J. (2001). Comparison of Hilbert transform and wavelet methods for the analysis of neuronal synchrony. *Journal of Neuroscience Methods*, *111*(2), 83–98. [https://doi.org/10.1016/S0165-0270\(01\)00372-7](https://doi.org/10.1016/S0165-0270(01)00372-7)
- Lee, B. B., Martin, P. R., & Valberg, A. (1988). The physiological basis of heterochromatic flicker photometry demonstrated in the ganglion cells of the macaque retina. *The Journal of Physiology*, *404*, 323–347.
- Leonard, M. K., Gwilliams, L., Sellers, K. K., Chung, J. E., Xu, D., Mischler, G., Mesgarani, N., Welkenhuysen, M., Dutta, B., & Chang, E. F. (2024). Large-scale single-neuron speech sound encoding across the depth of human cortex. *Nature*, *626*(7999), 593–602. <https://doi.org/10.1038/s41586-023-06839-2>

## REFERENCES

---

- Leszczyński, M., Barczak, A., Kajikawa, Y., Ulbert, I., Falchier, A. Y., Tal, I., Haegens, S., Melloni, L., Knight, R. T., & Schroeder, C. E. (2020). Dissociation of broadband high-frequency activity and neuronal firing in the neocortex. *Science Advances*, 6(33), eabb0977. <https://doi.org/10.1126/sciadv.abb0977>
- Liu, B., Nobre, A. C., & van Ede, F. (2023). Microsaccades transiently lateralise EEG alpha activity. *Progress in Neurobiology*, 224, 102433. <https://doi.org/10.1016/j.pneurobio.2023.102433>
- Lowet, E., Gomes, B., Srinivasan, K., Zhou, H., Schafer, R. J., & Desimone, R. (2018). Enhanced Neural Processing by Covert Attention only during Microsaccades Directed toward the Attended Stimulus. *Neuron*, 99(1), 207-214.e3. <https://doi.org/10.1016/j.neuron.2018.05.041>
- Luck, S. J. (2014). *An Introduction to the Event-Related Potential Technique* (2. Aufl.). A Bradford Book.
- Luck, S. J., Girelli, M., McDermott, M. T., & Ford, M. A. (1997). Bridging the gap between monkey neurophysiology and human perception: An ambiguity resolution theory of visual selective attention. *Cognitive Psychology*, 33(1), 64–87. <https://doi.org/10.1006/cogp.1997.0660>
- Luck, S. J., & Hillyard, S. A. (1994). Spatial filtering during visual search: Evidence from human electrophysiology. *Journal of Experimental Psychology. Human Perception and Performance*, 20(5), 1000–1014. <https://doi.org/10.1037//0096-1523.20.5.1000>
- Luck, S. J., & Kappenman, E. S. (Hrsg.). (2012). *The Oxford handbook of event-related potential components*. Oxford University Press. <https://doi.org/10.1093/oxfordhb/9780195374148.001.0001>
- Maniscalco, B., Bang, J. W., Irvani, L., Camps-Febrer, F., & Lau, H. (2012). Does response interference depend on the subjective visibility of flanker distractors? *Attention, Perception, & Psychophysics*, 74(5), 841–851. <https://doi.org/10.3758/s13414-012-0291-2>
- Marturano, F., Brigadoi, S., Doro, M., Dell'Acqua, R., & Sparacino, G. (2020). A Time-Frequency Analysis for the Online Detection of the N2pc Event-Related Potential (ERP) Component in Individual EEG Datasets. *2020 42nd Annual International Conference of the IEEE Engineering in Medicine & Biology Society (EMBC)*, 1019–1022. <https://doi.org/10.1109/EMBC44109.2020.9175462>
- Mathôt, S., Hickey, C., & Theeuwes, J. (2010). From reorienting of attention to biased competition: Evidence from hemifield effects. *Attention, Perception, & Psychophysics*, 72(3), 651–657. <https://doi.org/10.3758/APP.72.3.651>

## REFERENCES

---

- Miller, K. J., Honey, C. J., Hermes, D., Rao, R. P. N., denNijs, M., & Ojemann, J. G. (2014). Broadband changes in the cortical surface potential track activation of functionally diverse neuronal populations. *NeuroImage*, *85 Pt 2*(0 2), 711–720. <https://doi.org/10.1016/j.neuroimage.2013.08.070>
- Mittner, M., Hawkins, G. E., Boekel, W., & Forstmann, B. U. (2016). A Neural Model of Mind Wandering. *Trends in Cognitive Sciences*, *20*(8), 570–578. <https://doi.org/10.1016/j.tics.2016.06.004>
- Moher, J., & Egeth, H. E. (2012). The ignoring paradox: Cueing distractor features leads first to selection, then to inhibition of to-be-ignored items. *Attention, Perception, & Psychophysics*, *74*(8), 1590–1605. <https://doi.org/10.3758/s13414-012-0358-0>
- Moorselaar, D. van, & Slagter, H. A. (2019). Learning What Is Irrelevant or Relevant: Expectations Facilitate Distractor Inhibition and Target Facilitation through Distinct Neural Mechanisms. *Journal of Neuroscience*, *39*(35), 6953–6967. <https://doi.org/10.1523/JNEUROSCI.0593-19.2019>
- Mounts, J. R. W. (2000). Attentional capture by abrupt onsets and feature singletons produces inhibitory surrounds. *Perception & Psychophysics*, *62*(7), 1485–1493. <https://doi.org/10.3758/BF03212148>
- Muckli, L., & Petro, L. S. (2013). Network interactions: Non-geniculate input to V1. *Current Opinion in Neurobiology*, *23*(2), 195–201. <https://doi.org/10.1016/j.conb.2013.01.020>
- Müller, H. J., Heller, D., & Ziegler, J. (1995). Visual search for singleton feature targets within and across feature dimensions. *Perception & Psychophysics*, *57*(1), 1–17. <https://doi.org/10.3758/BF03211845>
- Niell, C. M., & Stryker, M. P. (2010). Modulation of Visual Responses by Behavioral State in Mouse Visual Cortex. *Neuron*, *65*(4), 472–479. <https://doi.org/10.1016/j.neuron.2010.01.033>
- Noonan, M. P., Adamian, N., Pike, A., Printzlau, F., Crittenden, B. M., & Stokes, M. G. (2016). Distinct Mechanisms for Distractor Suppression and Target Facilitation. *Journal of Neuroscience*, *36*(6), 1797–1807. <https://doi.org/10.1523/JNEUROSCI.2133-15.2016>
- Olivers, C. N. L., & Humphreys, G. W. (2003). Visual marking inhibits singleton capture. *Cognitive Psychology*, *47*(1), 1–42. [https://doi.org/10.1016/S0010-0285\(03\)00003-3](https://doi.org/10.1016/S0010-0285(03)00003-3)
- Pan, W.-N., Zhao, Y.-W., Luo, Z.-X., Chen, Y., & Cai, Y.-C. (2024). Attention modulates early visual processing: An association between subjective contrast perception and early C1 ERP component. *Psychophysiology*, *61*(5), e14507. <https://doi.org/10.1111/psyp.14507>

- Parra, L. C., Spence, C. D., Gerson, A. D., & Sajda, P. (2005). Recipes for the linear analysis of EEG. *NeuroImage*, *28*(2), 326–341. <https://doi.org/10.1016/j.neuroimage.2005.05.032>
- Peelle, J. E., McMillan, C., Moore, P., Grossman, M., & Wingfield, A. (2004). Dissociable patterns of brain activity during comprehension of rapid and syntactically complex speech: Evidence from fMRI. *Brain and Language*, *91*(3), 315–325. <https://doi.org/10.1016/j.bandl.2004.05.007>
- Pollok, B., & Schnitzler, A. (2010). Grundlagen und Anwendung der Magnetenzephalographie. *Das Neurophysiologie-Labor*, *32*(2), 109–121. <https://doi.org/10.1016/j.neulab.2010.04.003>
- Preiss, D. D., Cosmelli, D., & Kaufman, J. C. (2020). *Creativity and the wandering mind: Spontaneous and controlled cognition*. Academic press, imprint of Elsevier.
- Qin, N., Crespi, F., Proverbio, A. M., & Pourtois, G. (2023). A systematic exploration of attentional load effects on the C1 ERP component. *Psychophysiology*, *60*(6), e14301. <https://doi.org/10.1111/psyp.14301>
- Ray, S., Niebur, E., Hsiao, S. S., Sinai, A., & Crone, N. E. (2008). High-frequency gamma activity (80–150Hz) is increased in human cortex during selective attention. *Clinical Neurophysiology: Official Journal of the International Federation of Clinical Neurophysiology*, *119*(1), 116–133. <https://doi.org/10.1016/j.clinph.2007.09.136>
- Reinhold, K., Resulaj, A., & Scanziani, M. (2023). Brain State-Dependent Modulation of Thalamic Visual Processing by Cortico-Thalamic Feedback. *Journal of Neuroscience*, *43*(9), 1540–1554. <https://doi.org/10.1523/JNEUROSCI.2124-21.2022>
- Richter, D., Moorselaar, D. van, & Theeuwes, J. (2024). Proactive distractor suppression in early visual cortex. *eLife*, *13*. <https://doi.org/10.7554/eLife.101733.1>
- Robertson, I. H., Manly, T., Andrade, J., Baddeley, B. T., & Yiend, J. (1997). ‘Oops!’: Performance correlates of everyday attentional failures in traumatic brain injured and normal subjects. *Neuropsychologia*, *35*(6), 747–758. [https://doi.org/10.1016/S0028-3932\(97\)00015-8](https://doi.org/10.1016/S0028-3932(97)00015-8)
- Rubin, D. C. (1989). Issues of regularity and control: Confessions of a regularity freak. In *Everyday cognition in adulthood and late life* (S. 84–103). Cambridge University Press.
- Rucci, M., Iovin, R., Poletti, M., & Santini, F. (2007). Miniature eye movements enhance fine spatial detail. *Nature*, *447*(7146), 852–855. <https://doi.org/10.1038/nature05866>
- Sawaki, R., Geng, J. J., & Luck, S. J. (2012). A Common Neural Mechanism for Preventing and Terminating the Allocation of Attention. *Journal of Neuroscience*, *32*(31), 10725–10736. <https://doi.org/10.1523/JNEUROSCI.1864-12.2012>

- Sawaki, R., & Luck, S. J. (2010). Capture versus suppression of attention by salient singletons: Electrophysiological evidence for an automatic attend-to-me signal. *Attention, Perception, & Psychophysics*, 72(6), 1455–1470. <https://doi.org/10.3758/APP.72.6.1455>
- Schapiro, A., & Turk-Browne, N. (2015). Statistical Learning. In A. W. Toga (Hrsg.), *Brain Mapping* (S. 501–506). Academic Press. <https://doi.org/10.1016/B978-0-12-397025-1.00276-1>
- Schmid, P., Reichert, C., Knight, R. T., & Dürschmid, S. (2025). Differential contributions of the C1 ERP and broadband high-frequency activity to visual processing. *Journal of Neurophysiology*, 133(1), 78–84. <https://doi.org/10.1152/jn.00292.2024>
- Schooler, J., Reichle, E. D., & Halpern, D. V. (2004). Zoning-out during reading: Evidence for dissociations between experience and meta-consciousness. *Thinking and seeing: Visual metacognition in adults and children*, 204–226.
- Schooler, J. W., Smallwood, J., Christoff, K., Handy, T. C., Reichle, E. D., & Sayette, M. A. (2011). Meta-awareness, perceptual decoupling and the wandering mind. *Trends in Cognitive Sciences*, 15(7), 319–326. <https://doi.org/10.1016/j.tics.2011.05.006>
- Seli, P., Carriere, J. S. A., & Smilek, D. (2015). Not all mind wandering is created equal: Dissociating deliberate from spontaneous mind wandering. *Psychological Research*, 79(5), 750–758. <https://doi.org/10.1007/s00426-014-0617-x>
- Seli, P., Carriere, J. S., Levene, M., & Smilek, D. (2013). How few and far between? Examining the effects of probe rate on self-reported mind wandering. *Frontiers in Psychology*, 4. <https://doi.org/10.3389/fpsyg.2013.00430>
- Seli, P., Jonker, T. R., Solman, G. J. F., Cheyne, J. A., & Smilek, D. (2013). A methodological note on evaluating performance in a sustained-attention-to-response task. *Behavior Research Methods*, 45(2), 355–363. <https://doi.org/10.3758/s13428-012-0266-1>
- Seli, P., Risko, E. F., & Smilek, D. (2016). On the Necessity of Distinguishing Between Unintentional and Intentional Mind Wandering. *Psychological Science*, 27(5), 685–691. <https://doi.org/10.1177/0956797616634068>
- Semedo, J. D., Jasper, A. I., Zandvakili, A., Krishna, A., Aschner, A., Machens, C. K., Kohn, A., & Yu, B. M. (2022). Feedforward and feedback interactions between visual cortical areas use different population activity patterns. *Nature Communications*, 13(1), 1099. <https://doi.org/10.1038/s41467-022-28552-w>
- Shinn, M., Hu, A., Turner, L., Noble, S., Preller, K. H., Ji, J. L., Moujaes, F., Achard, S., Scheinost, D., Constable, R. T., Krystal, J. H., Vollenweider, F. X., Lee, D., Anticevic, A., Bullmore, E. T., & Murray, J.

- D. (2023). Functional brain networks reflect spatial and temporal autocorrelation. *Nature Neuroscience*, 26(5), 867–878. <https://doi.org/10.1038/s41593-023-01299-3>
- Siegelman, N., Bogaerts, L., Kronenfeld, O., & Frost, R. (2018). Redefining “Learning” in Statistical Learning: What Does an Online Measure Reveal About the Assimilation of Visual Regularities? *Cognitive Science*, 42(S3), 692–727. <https://doi.org/10.1111/cogs.12556>
- Sina, G., & Plourde, V. (2020). Does Mind-Wandering Relate to Mood and Stress in Young Adults? A Narrative Review. *Spectrum*, 6. <https://doi.org/10.29173/spectrum103>
- Singer, J. L. (1975). Navigating the stream of consciousness: Research in daydreaming and related inner experience. *American Psychologist*, 30(7), 727–738. <https://doi.org/10.1037/h0076928>
- Singer, J. L., & Antrobus, J. S. (1965). EYE MOVEMENTS DURING FANTASIES. IMAGINING AND SUPPRESSING FANTASIES. *Archives of General Psychiatry*, 12, 71–76. <https://doi.org/10.1001/archpsyc.1965.01720310073009>
- Smallwood, J., Beach, E., Schooler, J. W., & Handy, T. C. (2008). Going AWOL in the Brain: Mind Wandering Reduces Cortical Analysis of External Events. *Journal of Cognitive Neuroscience*, 20(3), 458–469. <https://doi.org/10.1162/jocn.2008.20037>
- Smallwood, J., Bernhardt, B. C., Leech, R., Bzdok, D., Jefferies, E., & Margulies, D. S. (2021). The default mode network in cognition: A topographical perspective. *Nature Reviews Neuroscience*, 22(8), 503–513. <https://doi.org/10.1038/s41583-021-00474-4>
- Smallwood, J., & Schooler, J. (2014). The Science of Mind Wandering: Empirically Navigating the Stream of Consciousness. *Annual review of psychology*, 66. <https://doi.org/10.1146/annurev-psych-010814-015331>
- Smallwood, J., & Schooler, J. W. (2006). The restless mind. *Psychological Bulletin*, 132(6), 946–958. <https://doi.org/10.1037/0033-2909.132.6.946>
- Smilek, D., Carriere, J. S. A., & Cheyne, J. A. (2010). Out of mind, out of sight: Eye blinking as indicator and embodiment of mind wandering. *Psychological Science*, 21(6), 786–789. <https://doi.org/10.1177/0956797610368063>
- Spreng, R. N., Mar, R. A., & Kim, A. S. N. (2009). The common neural basis of autobiographical memory, prospection, navigation, theory of mind, and the default mode: A quantitative meta-analysis. *Journal of Cognitive Neuroscience*, 21(3), 489–510. <https://doi.org/10.1162/jocn.2008.21029>

## REFERENCES

---

- Sur, S., & Sinha, V. K. (2009). Event-related potential: An overview. *Industrial Psychiatry Journal, 18*(1), 70–73. <https://doi.org/10.4103/0972-6748.57865>
- Szczepanski, S. M., Crone, N. E., Kuperman, R. A., Auguste, K. I., Parvizi, J., & Knight, R. T. (2014). Dynamic Changes in Phase-Amplitude Coupling Facilitate Spatial Attention Control in Fronto-Parietal Cortex. *PLOS Biology, 12*(8), e1001936. <https://doi.org/10.1371/journal.pbio.1001936>
- Tallon-Baudry, C., Bertrand, O., Hénaff, M.-A., Isnard, J., & Fischer, C. (2005). Attention Modulates Gamma-band Oscillations Differently in the Human Lateral Occipital Cortex and Fusiform Gyrus. *Cerebral Cortex, 15*(5), 654–662. <https://doi.org/10.1093/cercor/bhh167>
- Theiler, J., Eubank, S., Longtin, A., Galdrikian, B., & Doynne Farmer, J. (1992). Testing for nonlinearity in time series: The method of surrogate data. *Physica D: Nonlinear Phenomena, 58*(1), 77–94. [https://doi.org/10.1016/0167-2789\(92\)90102-S](https://doi.org/10.1016/0167-2789(92)90102-S)
- Thomson, D. R., Seli, P., Besner, D., & Smilek, D. (2014). On the link between mind wandering and task performance over time. *Consciousness and Cognition, 27*, 14–26. <https://doi.org/10.1016/j.concog.2014.04.001>
- Unsworth, N., & McMillan, B. D. (2017). Attentional disengagements in educational contexts: A diary investigation of everyday mind-wandering and distraction. *Cognitive Research: Principles and Implications, 2*(1), 32. <https://doi.org/10.1186/s41235-017-0070-7>
- van Moorselaar, D., Lampers, E., Cordesius, E., & Slagter, H. A. (2020). Neural mechanisms underlying expectation-dependent inhibition of distracting information. *eLife, 9*, e61048. <https://doi.org/10.7554/eLife.61048>
- van Moorselaar, D., & Slagter, H. A. (2020). Inhibition in selective attention. *Annals of the New York Academy of Sciences, 1464*(1), 204–221. <https://doi.org/10.1111/nyas.14304>
- Vishne, G., Gerber, E. M., Knight, R. T., & Deouell, L. Y. (2023). Distinct ventral stream and prefrontal cortex representational dynamics during sustained conscious visual perception. *Cell Reports, 42*(7), 112752. <https://doi.org/10.1016/j.celrep.2023.112752>
- Wang, B., & Theeuwes, J. (2018). How to inhibit a distractor location? Statistical learning versus active, top-down suppression. *Attention, Perception, & Psychophysics, 80*(4), 860–870. <https://doi.org/10.3758/s13414-018-1493-z>
- Watson, D. G., & Humphreys, G. W. (2000). Visual marking: Evidence for inhibition using a probe-dot detection paradigm. *Perception & Psychophysics, 62*(3), 471–481. <https://doi.org/10.3758/BF03212099>

## REFERENCES

---

- Weinstein, Y. (2018). Mind-wandering, how do I measure thee with probes? Let me count the ways. *Behavior Research Methods*, *50*(2), 642–661. <https://doi.org/10.3758/s13428-017-0891-9>
- Welhaf, M. S., Meier, M. E., Smeekens, B. A., Silvia, P. J., Kwapil, T. R., & Kane, M. J. (2022). A “Goldilocks zone” for mind-wandering reports? A secondary data analysis of how few thought probes are enough for reliable and valid measurement. *Behavior Research Methods*. <https://doi.org/10.3758/s13428-021-01766-4>
- Wienke, C., Bartsch, M. V., Vogelgesang, L., Reichert, C., Hinrichs, H., Heinze, H.-J., & Dürschmid, S. (2021). Mind-wandering Is Accompanied by Both Local Sleep and Enhanced Processes of Spatial Attention Allocation. *Cerebral Cortex Communications*, *2*(1), tgab001. <https://doi.org/10.1093/texcom/tgab001>
- Williams, E. J. (1959). The Comparison of Regression Variables. *Journal of the Royal Statistical Society Series B: Statistical Methodology*, *21*(2), 396–399. <https://doi.org/10.1111/j.2517-6161.1959.tb00346.x>
- Wolf, M.-I., Bruchmann, M., Pourtois, G., Schindler, S., & Straube, T. (2022). Top-Down Modulation of Early Visual Processing in V1: Dissociable Neurophysiological Effects of Spatial Attention, Attentional Load and Task-Relevance. *Cerebral Cortex*, *32*(10), 2112–2128. <https://doi.org/10.1093/cercor/bhab342>
- Woodman, G. F., Arita, J. T., & Luck, S. J. (2009). A cuing study of the N2pc component: An index of attentional deployment to objects rather than spatial locations. *Brain Research*, *1297*, 101–111. <https://doi.org/10.1016/j.brainres.2009.08.011>
- Wöstmann, M., Alavash, M., & Obleser, J. (2019). Alpha Oscillations in the Human Brain Implement Distractor Suppression Independent of Target Selection. *The Journal of Neuroscience*, *39*(49), 9797–9805. <https://doi.org/10.1523/JNEUROSCI.1954-19.2019>
- Xu, J., Friedman, D., & Metcalfe, J. (2018). Attenuation of deep semantic processing during mind wandering: An event-related potential study. *NeuroReport*, *29*(5), 380–384. <https://doi.org/10.1097/WNR.0000000000000978>
- Yanko, M. R., & Spalek, T. M. (2014). Driving With the Wandering Mind: The Effect That Mind-Wandering Has on Driving Performance. *Human Factors*, *56*(2), 260–269. <https://doi.org/10.1177/0018720813495280>
- Ye, Q., Song, X., Zhang, Y., & Wang, Q. (2014). Children’s mental time travel during mind wandering. *Frontiers in Psychology*, *5*. <https://doi.org/10.3389/fpsyg.2014.00927>

## REFERENCES

---

- Yuval-Greenberg, S., Tomer, O., Keren, A. S., Nelken, I., & Deouell, L. Y. (2008). Transient Induced Gamma-Band Response in EEG as a Manifestation of Miniature Saccades. *Neuron*, *58*(3), 429–441. <https://doi.org/10.1016/j.neuron.2008.03.027>
- Zhao, C., Kong, Y., Li, D., Huang, J., Kong, L., Li, X., Jensen, O., & Song, Y. (2023). Suppression of distracting inputs by visual-spatial cues is driven by anticipatory alpha activity. *PLOS Biology*, *21*(3), e3002014. <https://doi.org/10.1371/journal.pbio.3002014>
- Zhu, X., & Luo, Y. (2012). Fearful faces evoke a larger C1 than happy faces in executive attention task: An event-related potential study. *Neuroscience Letters*, *526*(2), 118–121. <https://doi.org/10.1016/j.neulet.2012.08.011>
- Zipser, K., Lamme, V. A. F., & Schiller, P. H. (1996). Contextual Modulation in Primary Visual Cortex. *The Journal of Neuroscience*, *16*(22), 7376–7389. <https://doi.org/10.1523/JNEUROSCI.16-22-07376.1996>

**List of Figures**

**Figure 1.** Typical HFA response modulation .....4

**Figure 2.** Visual Paradigm for lateral Target and Distractor Response.....7

**Figure 3.** Example of raw EEG data. ....9

**Figure 4.** Example of evoked magnetic fields ..... 10

**Figure 5.** Example of Hilbert Transform ..... 14

**Figure 6.** Experimental Paradigm study 1 and 2.....20

**Figure 7.** Behavioral Results study 1 .....24

**Figure 8.** Neural Results study 1.....25

**Figure 9.** Behavioral Results study 2 .....26

**Figure 10.** Neural Grand Average Results study 2 .....27

**Figure 11.** Neural Brain State Results study 2 .....28

**Figure 12.** Experimental Paradigm study 3, 4, and 5 .....34

**Figure 13.** Behavioral Results study 3 .....41

**Figure 14.** Neural Results study 3.....43

**Figure 15.** Lateralized HFA Response study 3 .....44

**Figure 16.** Behavioral Results and Grand Average study 4 .....45

**Figure 17.** Temporal Evolution of Microsaccades study 4.....46

**Figure 18.** Response Modulation by Implicit Learning study 4.....47

**Figure 19.** Behavioral Brain State Results study 5.....48

**Figure 20.** Neural Brain State Results study 5 .....49

### **Declaration of Honor**

I hereby declare that I prepared this thesis without impermissible help of third parties and that none other than the indicated tools have been used; all sources of information are clearly marked, including my own publications.

In particular I have not consciously:

- Fabricated data or rejected undesired results
- Misused statistical methods with the aim of drawing other conclusions than those warranted by the available data
- Plagiarized external data or publications
- Presented the results of other researchers in a distorted way

I am aware that violations of copyright may lead to injunction and damage claims of the author and also to prosecution by the law enforcement authorities.

I hereby agree that the thesis may be reviewed for plagiarism by mean of electronic data processing.

This work has not yet been submitted as a doctoral thesis in the same or a similar form in Germany or in any other country. It has not yet been published as a whole.

Magdeburg, 11.06.2025

Paul Schmid